Safety in Mines Research Advisory Committee

Final Report

Deterioration mechanisms of drum winder ropes

Mike van Zyl

Research agency: MIKE VAN ZYL INCORPORATED
Project number: GAP 501
Date: December 2000

Executive summary

Deep shaft drum winder operations will be allowed if such winder installations comply with the requirements of a code of practice (SABS0294). The specifications of the winder code of practice were largely based on experience, but some uncertainty existed regarding the effectiveness of some of the specifications in the code. These were drum and headsheave sizes, rope layers, and the maximum dynamic rope load range allowed. The objectives of the investigations described in this report were to determine the effectiveness of the specifications regarding the mentioned uncertainties. The investigations of this report generally only considered triangular strand ropes.

Rope fatigue studies and tests were carried out, bending stresses in wire ropes were analysed and measured, contact stresses on ropes were investigated, and drum winders in service were observed to meet the objectives of the project.

The more prominent findings of this report are:

> Future deep shaft drum winders will operate at rope load ranges of close to 15% of the breaking strengths of the ropes. Under such circumstances broken wires will be generated by the tension-tension fatigue loading of the ropes. However, rope service lives of 100 000 winding cycles will be achievable for triangular strand ropes if the lubrication of a rope is maintained to minimise the effects of fretting fatigue.
>
> The most surprising result is that surface degradation (or the plastic deformation) of the crown wires of the strands of triangular strand ropes does not increase the susceptibility of wires to fatigue crack initiation.
>
> A contact stress experienced during multi-layer coiling on a winder drum is the primary cause for the plastic deformation or degradation of the crown wires of the rope strands. Although it has been found that this surface degradation will not increase the susceptibility of wires to fatigue crack initiation, it is postulated that high contact stresses will generate their own problems (like split wires) if left unchecked. An alternative approach to the pulling in of back ends is proposed in the section on contact stresses to minimise the adverse effects of contact stresses: Pull in back ends much more frequent in the beginning of the service life of a rope.
>
> The analysis and measurement of bending stresses in triangular strand ropes show that the bending of ropes is still not entirely comprehended, but that the bending stresses for drum to rope diameter ratios currently employed will be considerably lower than the stresses generated by the tensile loading of a rope.

Although the findings of this report were different from what was expected or believed earlier, they were not alarming to any extent to warrant immediate changes to the specifications of SABS0294. However, the current specifications in SABS0294 were arrived at after working group discussions over quite a lengthy period, and by giving due consideration to operational and manufacturing constraints and possible impacts on the economics of winding. It is therefore recommended that a working group should consider the recommendations included in this report for possible modifications to the regulations and SABS0294.

The different parts of the project are quite diverse. For that reason, each part is discussed in detail in separate appendices. The main part of this report is a summary of the findings of the different parts of the investigation.

Table of contents

page

List of tables

List of figures

Terminology

New rope strength: The strength of a rope when new, and as determined by a tensile test.

Front end: The section of rope at and near the conveyance end of the rope.

Back end: The section of rope at and near the drum of the winder when the conveyance is at its lowest point in the shaft.

D/d ratio: The ratio between the diameter of a winder drum and the rope diameter, or between the diameter of a headsheave and the rope.

1 Introduction

At the time that the investigation of this report was planned, the statutory regulations for drum winders allowed for shaft operations of 3 000 m and deeper. The regulations allowed ropes to be selected with a static rope load factor at the back end of 25 000/(4 000 + *L*), with *L* the maximum suspended rope length in metres. Such winders and their ropes were required to comply with the requirements of a code of practice, SABS0294.[1]

Winder rope service lives have to be predictable and rates of rope deterioration have to be gradual to ensure that winding ropes will operate safely from one major rope inspection to the next. The current specifications of the winder code of practice (SABS0294) are largely based on experience, and should guard against rapid deterioration of the winder ropes.

However, some uncertainty existed regarding the effectiveness of some of the specifications in the winder code of practice, namely drum and headsheave sizes, rope layers, and the maximum dynamic rope load range allowed. These areas were therefore the focus of the investigations.

A brief description of the actions of a drum winder rope during one winding cycle for hoisting rock is described to enable the reader to have an appreciation of past investigations and the investigations described in this report.

During a typical rock winding cycle on a drum winder, the following occurs:

> When the conveyance is loaded, the load in the whole length of rope is increased. Accelerating the winder during hoisting will temporarily increase the rope loads with some dynamics in addition. The rope will be wound onto the winder drum at the loaded conveyance tension. During descending after off-loading, the rope is wound off the drum at the empty conveyance tension. As a rope section nears the point at which it departs from the drum, it slips on the drum (a total length of 5 mm to 10 mm) to adjust from the winding-on rope tension to the winding-off tension. During deceleration of the winder near shaft bottom, the rope load is temporarily increased again during deceleration, and some rope dynamics will be present during and after the deceleration of the conveyance. The winding cycle will then be complete.

The rope is subjected to the following actions during a winding cycle:

- The change in attached load plus the winding dynamics causes a variation in rope load, i.e. load range.
- Nearly the complete length of rope runs over the headsheave. The rope bends over the headsheave, which will generate additional stresses in the wires of the rope.
- The rope again experiences bending when wound unto the drum. Multi-layer coiling on the drum adds contact stresses at the crown wires of the strand where they make contact with under-lying rope layers. (Multi-layer coiling is required for all deeper shafts, which means that up to five rope layers could be wound on top of one another.)
- During unwinding after off-loading, rope slip-back on the drum is experienced.

- Excessive catenary dynamics could also cause (abnormal) rope damage, by the rope impacting with winder drum flanges or the headsheave, or damage as a result of miscoiling of the rope on the drum. SABS0294 appropriate drum coiling sleeves to be installed. Such sleeves have (virtually) eliminated catenary dynamics problems experienced in the past. Catenary dynamics are not discussed in this report.

After some time in use, a rock winder rope shows a flattening of the crown wires of the strands. This flattening is generally more prominent towards the back end of the rope and the flats

increase with usage of the rope. Apart from the contact of rope layer upon rope layer for multi-layered drum coiling, the "slip-back" action during unwinding of the rope has been perceived as possibly the major contributor towards the flattening of the crown wires of the strands. The perception was that man/material winders and counterweight ropes did not exhibit the same degree and severeness of wire flattening as a rock winder.

The rope of a man winder will experience the same actions as a rock winder rope when hoisting load and descending with an empty conveyance. The "slip-back" of the rope on the drum will be in the opposite direction when load is taken down and empty skips are hoisted. Man winders do not convey full loads every winding trip, and perform fewer winding cycles per day than rock winders. Man-cages are generally 50% heavier than rock hoisting skips for the same payload, which means that, for the same rope and total attached load, the load range of a man winder rope will be lower than that of a rock winder. The degradation of a man winder rope was considered to be less per winding cycle than of a rope of a comparably sized rock winder. Therefore investigations into the degradation or deterioration of drum winder ropes generally focused on rock winders and rock hoisting.

Since the research into establishing new rope factors was started in 1985, various investigations have been carried out in attempts to establish and quantify the degradation or deterioration mechanisms and to determine the factors that contribute to the generation of broken wires.[2,3,4,5,6,7,8,9,10,11] The success of these investigations varied. All possible degradation mechanisms were identified, but in none of the investigations could these mechanisms be quantified.

Excluding environmental influences such as corrosion and accidental damage, the majority of the ropes, used for rock hoisting on drum winders, are discarded because of broken wires.[2,3] A small fraction of ropes are discarded because of plastic deformation and wear. On vertical drum winders, very little material removal (abrasive wear) takes place during the flattening of the wires.[8] Although surfaces of the crown wires of a rope may appear worn, the flattening of wires is primarily the result of plastic deformation. The phrase "plastic wear" is sometimes used to describe the flattening of the wires.

At the start of this investigation, it was generally accepted that the pure tensile load variations that occur on drum winders (up to 15% load range) are too small to result in the generation of fatigue failures (broken wires). Because drum winder ropes develop broken wires in service, it was believed that there had to be some "fatiguing" mechanism present in drum winder systems. It was therefore reasoned that, excluding environmental and accidental damage, fatiguing of drum winder ropes could be the result of one or a combination of the following (in order of perceived importance):

- The plastic wear that flattens the outer wires of all drum winder ropes with usage could make the rope wires more susceptible to crack initiation. Broken wires would therefore be produced at lower load ranges.
- The bending of a rope over a headsheave and on the drum could result in stresses that lead to broken wires.
- The repeated contact stresses experienced by the rope when coiled onto a winder drum could produce broken wires.

The primary objectives of the project described in this report were the investigation of the above deterioration mechanisms. The planned scopes of the different investigations were as follows:

Fatigue performance of triangular strand ropes:

- Obtain the results from fatigue tests done on unused (new) triangular strand ropes from literature.

- Obtain sections from the front, middle and back of ropes discarded from a drum winder. These sections must have normal wear but no singular points of damage (such as corrosion, broken wires etc.). Subject these rope sections to fluctuating tensile loads. On selected rope samples, the fatigue tests would be carried out for an extended number of cycles to determine whether the rate of generation of broken wires increases.

- Compare the onset of wire breaks during the fatigue tests with that of unused ropes to determine to what extent load range, surface damage and the degree of surface damage influence the generation of broken wires.

Bending stresses generated in drum winder ropes:

- The calculation of the bending stress in the wires of triangular strand ropes will be based on information that can be obtained from literature and by using normal analytical methods.

- Determine the influence of winding speed on the rope bending stresses experimentally by carrying out strain gauge measurements on a winder rope while the ropes is wound on and off a winder drum at different speeds. Winding speeds of as much as 10 m/s would be attempted.

- Compare bending stresses with the stresses generated by normal rope loading during a winding cycle to verify by what percentage load range will be increased by bending stresses.

Contact stresses:

- The contact stress investigation was planned as an initial study into the contact stresses experienced by the surface wires of drum winder ropes, because it was reasoned that the large number of unknowns and variables of drum winder systems make it difficult to predict the outcome of this part of the investigation.

Field observations

As part of SIMRAC GAP054 (1995), the requirements for a field study on drum winder rope deterioration were formulated. A number of winders with distinctly different rope service lives were identified for possible future field studies. It was envisaged that studies of the rope deterioration on these winders could be correlated to the operating conditions of the ropes, and so quantify rope deterioration mechanisms and refine the requirements of the winder code of practice.

The recommended field studies were commenced as part of SIMRAC project GAP324 (1996). The investigation included the re-working of the statistical rope life model,[4] and the observation of the rates of deterioration on selected drum winders together with the operating conditions and rope and winder maintenance procedures. No conclusions were reached or recommendations made in the first year of the field observations.

The field studies were continued as part of SIMRAC project GAP439 (1997). The original scope of GAP439 included the investigations of GAP501, but for 1997 SIMRAC could only provide funding for the continuation of the field observations. The GAP439 report describes details of the rope service lives for the selected winders, as well as the observations and measurements made on the winders. Because a winder rope life could be a number of years, the rate at which rope deterioration data accumulate is slow, and no conclusion could be reached after two years of field observations. It was therefore recommended that the field observations should be continued. The field observations were continued as part of the project described in this report (GAP501). A total of six winders were under observation.

The four sections of this report that follow summarise the results obtained from the four different parts of the investigation, namely fatigue performance, bending stresses, contact stresses, and the field observations.

2 Fatigue performance of triangular strand ropes

The formula in the proposed regulations[12] for the strength of drum winder ropes was based on limiting the (dynamic) load range of the rope to 15% of the strength of the rope. The 15% load range limit originated from performance data of Koepe winder ropes. It was therefore not known how critical the prescribed load range limit would be for triangular strand ropes, and especially for ropes with surface degradation as experienced on drum winders. Furthermore, there was a belief that new triangular strand ropes would not develop broken wires during pure tension-tension fatigue tests at a 15% load range.

This part of the investigation required the verification of the influence of surface deterioration of triangular strand ropes on the resistance to the generation of broken wires in service. To be able to compare the performance of used triangular strand ropes to new ropes, tests either had to be carried out on new ropes or information of past tests on new ropes had to be obtained.

As a starting point to the investigation, information was obtained on past fatigue tests carried out on new (as manufactured) triangular strand ropes. Information on fatigue tests on 85 triangular strand rope samples was supplied by Haggie Rand.[13] These tests were carried out in the period from 1957 to 1962 on 38,1 mm diameter (1½") 6x28 triangular strand ropes. The purpose of the Haggie tests was to determine the effect of various base steels and manufacturing methods on the fatigue resistance of the ropes and not specifically to examine the behaviour of the ropes under different cyclic loads.

The Haggie tests are described in detail in Appendix A. Sixteen of the 85 fatigue tests were carried out at a load range of 20% and the rest of the tests were done at a 15% load range. During the fatigue tests described in Appendix A, the load cycles completed when broken wires occurred were noted. For each test a graph of "number of broken wires" against "load cycles completed" were obtained. Although some of the rope "types" had slightly different breaking strengths, the fatigue performance (and scatter of results) of the different rope "types" were much the same. The scatter of the results of all the tests carried out on rope sample lengths of 685 mm are shown in Fig. 2.

Figure 2 shows that, contrary to an earlier stated belief, broken wires did develop at a 15% load range on new triangular strand ropes. The figure further shows that at 20% load range, broken wires started to occur earlier during a fatigue test, and subsequent wire fractures were generated more rapidly. Although more tests were carried out at the 15% load range, the scatter in the results at 15% load range was surprisingly large. (Explanations are given later in this section.)

Appendix A also shows that during the fatigue tests broken wires were generated at stresses lower than the fatigue resistance of a single roping wire. Amongst possible reasons for this increased susceptibility to fatigue are residual stresses in the wires from the rope manufacturing process, and possible secondary bending of outer strand wires. (When a rope has been in use for some time, the gaps between the wire layers in a strand close up and so reduce secondary bending effects.)

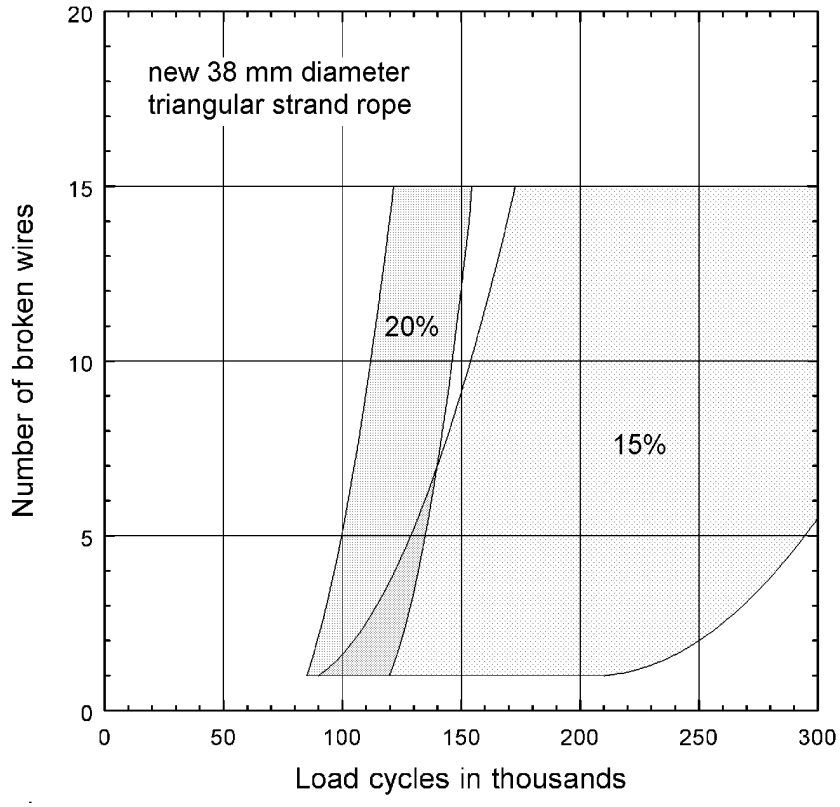

Figure 2: Scatter plots of the new-rope fatigue tests at 15% and 20% load ranges.

For the second part of the rope fatigue investigation, sections of ropes discarded from a drum winder at the end of the service life of the ropes were obtained for fatigue tests on "used ropes". The objectives of these tests were to show whether surface degradation or surface deterioration of the ropes increased susceptibility to fatigue crack initiation and the generation of broken wires, and to show the influence of load range on the rate of generation of broken wires.

The rope sections obtained were from the two underlay ropes of a Blair multi-rope winder (BMR), of a 2 400 m deep shaft. The ropes were 44 mm diameter triangular strand ropes, and the winder on which the rope operated was exclusively used for hoisting rock. The one rope was a left hand lay rope and the other a right hand lay. The lengths of rope obtained were from the front ends of the ropes (conveyance end), from around midshaft, and from near the back ends (drum ends). After some time in service, rock winder ropes exhibit significant degrees of plastic deformation (and some wear) of surface wires. This degradation of the ropes was more significant towards the back ends of the ropes, which is generally the case for drum winder ropes. The crown wires of the rope strands exhibited the most noticeable degradation.

One of the two overlay side ropes reached "discard" in a localised section. The rope set (all four ropes) was discarded because an acceptable service life was obtained. The two underlay ropes had relatively few broken wires (as determined by non-destructive magnetic testing of the ropes).

Stock samples of this rope set were also obtained from Haggie. Stock samples are sections cut from the ropes after manufacture. The stock samples were also subjected to fatigue tests to obtain a direct comparison between the fatigue performance of the new (unused) ropes and the used ropes.

The fatigue tests on the used ropes were carried out at three different load ranges, namely 10%, 15% and 20% of the new breaking strength of the ropes. The fatigue tests on the stock samples were only done at a 15% load range. The mean rope load during all the fatigue tests was 30% of new rope breaking strength, e.g. in the 20% load range case, the rope load was varied from 20% to 40% of the new rope breaking strength.

The fatigue tests on the used ropes and their stock samples are discussed in detail in Appendix B. The more significant findings of Appendix B are repeated in this section of the report.

Tensile-tensile fatigue tests at a 10% load range for 300 000 load cycles did not produce any wire fractures or partially fatigued wires in the "used rope" samples tested.

During the other fatigue tests, the number of load cycles completed when wire fractures occurred were recorded. Scatter bands of the results of the 15% load range and 20% load range tests on the used ropes are shown in Fig. 2.1. The figure shows that, at a load range of 15%, wire fractures occurred as early as 120 000 load cycles, but that at a 20% load range, wire fractures occurred much earlier and that the rate at which fractures accumulated were significantly greater at the 20% load range.

One of the rope samples that was subjected to a 15% load range test was cleaned thoroughly before the start of the fatigue test, i.e. all visible traces of rope lubricant or "grease" was removed from the rope. The results of the fatigue tests at 15% load range on the cleaned rope sample, as well as the four tests carried out on the stock samples (also at 15% load range), lay perfectly between the two scatter bands shown in Fig. 2.1.

The fatigue tests on the stock samples were carried out approximately eight years after the ropes were manufactured. The most probable reason for the relatively poor fatigue performance of the stock samples was poor lubrication. The rope ends from which stock samples are obtained are generally only lubricated internally. The lubricant that was present in the rope could also have dried out during the eight years in storage. The stock samples behaved in a manner similar to the cleaned used rope sample. It was evident that poorly lubricated or "dry" ropes have significantly inferior fatigue performance compared to well lubricated ropes. It was reasoned that the lack of lubricant leads to increased fretting at the inter strand contact points during the fatigue tests. Crack initiation therefore occurred earlier during a fatigue test.

The used rope samples showed visible indentations at the inter strand contact points (generally referred to as nicking). Crack initiation during the fatigue tests started at the nicks in most cases. The stock samples, which were of course never in operation on a winder, had no visible nicking at the inter strand contact point. However, the cracks in the wires of the stock samples also originated at the inter strand contact points during the fatigue tests. The one front end sample that was cleaned before the fatigue test was identical to the other front end samples in all other respects, including the visible nicking. However, the lack of lubricant resulted in earlier crack initiation during the fatigue tests. All of the above therefore suggests that crack initiation in the ropes during the fatigue tests were more a result of fretting than simply a result of the presence of nicks on the wires.

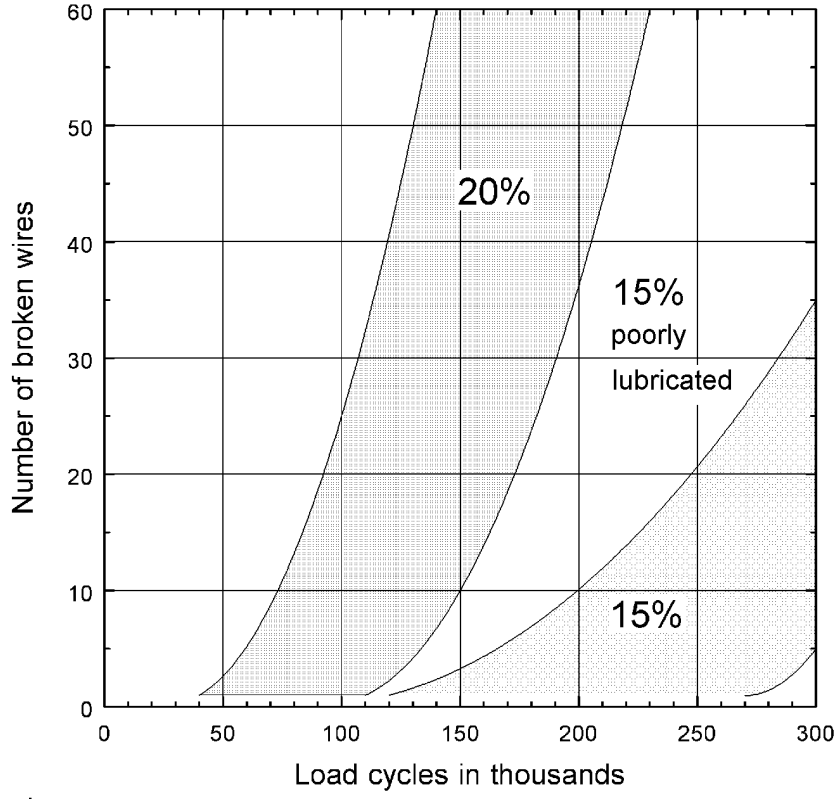

Figure 2.1: Scatter plots of rope fatigue tests on used ropes carried out at 15% and 20% load ranges.

The results of the fatigue tests on "new" rope samples, discussed in Appendix A (Fig. 2) and earlier in this section, showed surprisingly large scatter at a 15% load range, and also an overlapping with the results of the new rope tests at 20% load range. At the time that the fatigue tests of Appendix A were carried out (Fig. 2) the researchers were most probably not aware of the effect of lubrication on inter strand fretting, and consequently did not pay much attention to the lubricated state of the rope samples when subjected to the fatigue tests. The poor results were therefore most probably a result of inadequate lubrication of the ropes, and the results of the tests should therefore be ignored as being representative of actual rope behaviour.

The results of the fatigue tests on used rope samples of Appendix B showed that very few crown wires fractured during the fatigue tests. Less than 2% of the fractured wires were crown wires; the rest of the fractures all originated at the inter strand contact points in the valleys between the strands of the ropes. The fatigue tests showed no differences between the rope sections with different degrees of surface degradation (front, midshaft and back end samples). It was therefore concluded that the degradation visible on the crown wires of the strands of drum winder ropes do not increase the susceptibility to fatigue crack initiation. (If the majority of the wires that fractured during the fatigue tests were crown wires, there would most probably have been a difference between rope samples with different degrees of surface degradation.)

Drum winders, currently used for rock hoisting in South Africa, generate maximum rope load ranges of not more than 12% of the breaking strength of the ropes.[14] The fatigue tests on the used ropes showed that, for load cycles up to 300 000, a 10% load range did not produce wire fractures while a 15% load range did produce fractured wires from after around 120 000 load cycles. The threshold for generating wire fractures in tension-tension fatigue tests for load cycles up to 300 000 therefore lies somewhere between 10% and 15% load range.

Future deep shaft winders will generate rope load ranges between 12% and 15%, and a rapid increase in the generation of broken wires could be expected anytime after 100 000 winding cycles. However, 100 000 winding cycles is greater than the average service life of rock winder ropes.[2,3] Through proper rope maintenance, rope service lives of 100 000 cycles will be achievable for triangular strand ropes. From the above it can be concluded that the 15% rope load range limit of the winder code of practice[1] was a well-chosen value.

Operating drum winder ropes closer to 20% load range will most probably result in uneconomical rope service lives, and a rate of broken wire generation that will be too high for continued safe operation of a winder.

One point of interest: The winder code of practice[1] allows an absolute maximum rope load of 40% of breaking strength (envisaged to occur infrequent and produced by emergency braking near bottom of the shaft while descending with a full load). During the fatigue tests on the used rope samples at a 20% load range, the rope loads varied between 20% and 40% of the rope breaking strength, and broken wires were not generated for at least the first 25 000 load cycles. This indicates that very little damage will be done by infrequently loading a rope to 40% of its strength. The 40% rope load limit may be somewhat onerous for shafts 3 500 m and deeper. The maximum rope load limit of the winder code of practice could be increased to, say, 45% without increasing the rope deterioration rate. However, such a change could compromise safety (risk of rope failure) if corrosion and abnormal damage of the ropes are not well controlled.

Another point of interest: In Both Appendix A and B it was postulated that every length of an outer strand wire that is visible (from where it appears between strands till it disappears again) is a potential fatigue testing sample with one crown section and fretting points at the two inter strand contact points. Different triangular rope constructions and sizes will have a different number of these potential fatigue samples per given length of rope. The number of points at which fatigue cracks could initiate during a fatigue tests should therefore be taken into account when the fatigue performance of different triangular strand rope constructions and different rope lengths are compared. There is no reason why a 2 m long fatigue specimen will not accumulate wire fractures at double the rate than a 1 m long specimen of the same size and construction.

3 Bending stresses in triangular strand ropes

The requirements for winder drum and headsheave diameter to rope diameter ratios (commonly referred to as *D/d* ratios) that were included in the winder code of practice[1] were based on past experience. Calculation of bending stresses that could be generated when a rope is bent, and strain gauge measurements on rope wires when the rope was wound on and off a winder drum are described in Appendix C. The more relevant findings are repeated in this section.

D/d ratios for drum winders are generally of the order of 100, and the trend for future deep winders are to have larger values. With regard to *D/d* ratios generally selected for drum winders, the following quote from a paper by Chaplin:[19]

> "Bending fatigue: the bending ratios (sheave diameter to rope diameter) are so high that the endurance for 'bending over sheaves' fatigue is orders of magnitude greater than actual service life. However, though small, the superimposition of these bending stresses on the stresses associated with tensile load will cause some increase in the tensile fatigue stress range."

However, some uncertainty existed regarding the actual stress levels generated by bending winding ropes around sheaves and onto drums, and especially whether increased winding speed could lead to increased bending stresses. The objectives of the bending stress investigation were to compare bending stresses with the stresses from tensile loading, and to try to establish

whether winding speed had any influence on bending stresses.

In Appendix C it is shown that relative movement between the strands of a rope and relative movement between the wires in a strand have to take place when a rope is bent, otherwise the bending stresses will be significantly greater than the stresses produced by tensile loading of a rope. This makes sense because the flexibility of a rope in bending is one of its greater attributes.

The strain gauge measurements had two objectives: To compare measured stresses with calculated stresses, and to determine the effect of winding speed on the generated bending stresses.

The measurements were carried on one of the ropes of a rock winder. The 48 mm diameter rope had 3,1 mm diameter outer wires, and the *D/d* ratio was just more than 100. The middle crown wire of a rope strand was strain gauged such that the strain gauge would be right on the outside of the bend when the rope was wound onto the drum. The strains on five different strands were measured in this way. All strain gauges were installed on the straight rope section approximately 4 m off the drum with the conveyance at midshaft.

The strain measured on a wire of one of the strands is shown in Fig. 3. This result was most surprising: Instead of an expected tensile strain of the order of 500 µm/m, the strain gauge showed compression of 100 µm/m after being wound onto the drum. The measurements also shows some transient response while the bending onto the drum took place.

The strain measured on the wire of another strand is shown in Fig. 3.1. Although the strain in this wire was tensile after the rope was bent onto the drum, the strain was still far less than expected. Transient response during bending is also evident.

The mechanics and geometry of rope bending is therefore far more complicated than originally anticipated. The same conclusion was reached after an investigation of the rope behaviour at conveyance mounted compensating sheaves of Blair multi-rope winders.[20]

A plausible explanation of the observed rope behaviour in bending is given in Appendix C: The path length of an outer strand wire in a straight rope is different to the path length in a bent rope. The difference varies further with the arc length of the bend. During bending of a rope, a wire will have to continuously adjust is position to maintain some degree of load equilibrium along its length. Restrictions to the free movement of the wire, imposed by friction and the shape of the wire, will lead to unpredictable behaviour.

The analysis of bending of a rope and the calculation of the unequal outer strand wire lengths for bending a rope over a sheave or onto a drum will require a substantial analysis of the spatial geometry of a rope and its strands and wires. With such an analysis is may be possible to predict the condition of a wire after it is bent, but the calculation of the transient response during bending will not be possible.

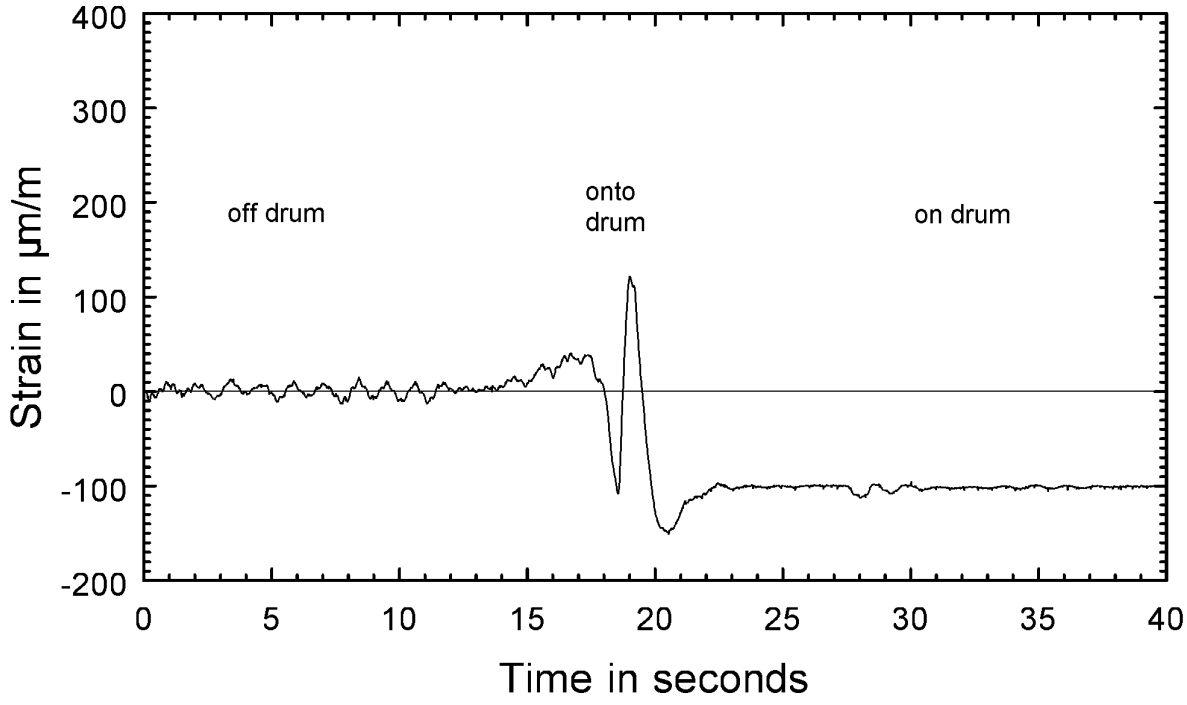

Figure 3: ***Strain measured on the middle crown wire of a strand when wound onto the drum.***

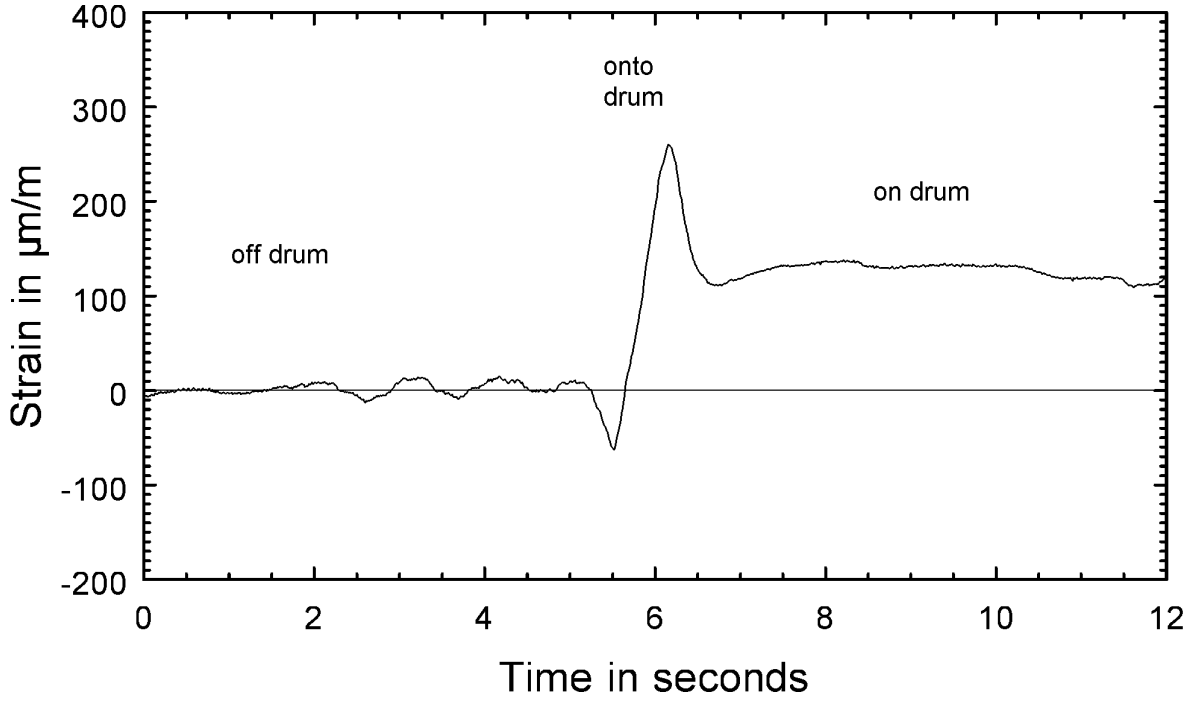

Figure 3.1: ***Strain measured on the middle crown wire of another strand when wound onto the drum.***

Nevertheless, the strains measured on the individual wires during bending of the rope were

substantially less than the wire strains measured during winder deceleration and braking. Although the actual behaviour of individual wires in a rope remain unresolved, the wire stresses generated during bending will be relatively small. Even if unequal wire lengths produced slightly proud wires during rope bending, the situation on any future winder could not be any worse than at current drum winder installations.

It was further possible to carry out measurements for the rope running off the drum at speeds of up to 10 m/s. No evidence was found that winding speed increased the stresses generated by rope bending.

Although bending stresses cannot yet be quantified exactly, all indications are that bending stresses will be significantly smaller than the tensile stresses generated by normal winding operations. Because stress variations due to rope bending will be present for drum winder operations, they will have some influence on the fatigue performance of the rope. However, the bending stresses are relatively small, and the influence on fatigue performance of the rope should not be very significant.

It is noteworthy that bending of the rope will cause relative movement between the rope strands and the wires in the strands. This relative movement could lead to fretting, which in turn could lead to accelerated fatigue crack initiation.

4 Contact stresses

The contact between the rope and a headsheave, between the rope and the winder drum surface, and between rope and rope for multi-layer drum coiling were analysed to establish how the contact stresses generated on the surface of the rope could lead to adverse or accelerated rope deterioration.

Although the section on the fatigue performance of triangular strand ropes showed that the surface degradation of the ropes removed from service did not enhance the susceptibility of the strand crown wires to the initiation of fatigue cracks, it does not mean that contact stresses by themselves could not be detrimental to rope performance. Unchecked contact stresses are the most probable cause of rapid rope surface degradation and the generation of split wires in ropes.

The details of an analysis of the contact stresses that could be generated on the surface wires of triangular strand ropes are given in Appendix D. The more significant findings are given in this section.

The rope-on-rope contact stresses generated during multi-layer coiling on a winder drum are larger than the elastic limit of the rope wire material. Flat sections are therefore created at the crowns of the rope strands. The flat sections formed are a result of plastic deformation of the outer strand wires of a rope. As the flats on the rope grow larger with usage of the rope, the contact stresses are reduced because the same contact loads are spread over larger areas.

Rope-on-rope contact is far more severe than the contact between the rope and the drum surface or the contact between the rope and the headsheave. The most severe contact is between the bottom rope layer on the drum and the second rope layer. The severity of the contact is determined by the total radial load on the second rope layer when the rope is fully wound onto the drum. It is further shown in Appendix D that the contact stress degradation of the second rope layer on a drum should be greater than that of any other rope layer.

Repeated generation of contact stresses beyond the elastic limit of the rope wire material will lead to fatigue and split wires. With such high contact stresses, cracks can be initiated after a relatively small number of loading cycles. Although the accumulation of winding cycles on a winder is

relatively low (150 per day for a deep shaft winder), split wire problems have been experienced in the past.

The high contact stresses that are generated during multi-layer coiling on a drum are a reality, and cannot be eliminated. However, appropriate measures can be introduced to limit the number of high contact stress load cycles on a given section of rope, especially in the beginning of the life of a rope.

The contact loads (and therefore the contact stresses) at the drum turn crossover points for drum coiling sleeves with a drum turn crossover every 180° will be about 65% greater than for the rest of the rope turn. Smooth drums and coiling sleeves with a turn crossover only every 360° require the rope to pass over two underlying turns at every crossover. For this case, a section of rope will be unsupported and will lead to larger contact loads and contact stresses for the same rope loads compared to coiling sleeves with a drum turn crossover every 180°. The contact stresses generated by multi-layer coiling on the drums of winders of 3 000 m will be greater than those of comparable set-ups 2 000 m deep, but will in all probability not be greater than the contact stresses experienced by ropes of 2 000 m deep winders that operate without coiling sleeves. Drum coiling sleeves, with a drum turn crossover every 180°, are therefore required to reduce contact stresses at the drum turn crossover points.

Although the torque-tension characteristics of a triangular strand rope will ensure that a rope is wound onto the drum at different rotational orientations with every winding cycle, the high loads will remain on the surface of the same section of rope. This situation if is further intensified by the modern trend to use loadcells to determine the load discharged into skips. Drum turn crossover points will be at the same location on the drum if the same load is added to the skip for every winding cycle. This is even more the case for the bottom rope layer and the first part of the second layer for which small differences in load will have little effect.

There is merit in systems that load skips by volume instead of exact loads. Loading by volume will at least ensure that actual loads will be varied, and that drum turn crossover points will be shifted around on the winder drum. The same can of course be achieved with a loadcell system that varies the load deliberately form one winding cycle to the next.

The primary method of shifting the location of drum turn crossover points and drum layer crossover points, is by pulling in the back end of a rope at the winder drum. However, to date this has been done without giving much thought to the effect of pulling in back ends. Generally back ends are pulled in at intervals of three months or six months. Taking everything mentioned in Appendix D into account, there is merit in adopting a new approach towards when back ends should be done. A procedure along the following lines is proposed, especially for future deep winders:

> For the first month after installation, do back ends every week. For the next two months do back ends every fortnight. For the next four months, do back ends monthly. For the next year do back ends every three months. After this time in service, a rope will have evenly distributed surface deformation mostly produced at lower contact stresses. The frequency of doing back ends can then be increased to every six months.

Other finding of Appendix D were:

> The radial rope loads generated will be greater for smaller winder drums. The contact loads and contact stresses between ropes and headsheaves are not even remotely comparable to that of the rope on the drum.

Slipback occurs when a rope is wound off the drum at a lower tension than during the winding up part. Slipback is not a necessary ingredient for the generation of plastic deformation on the outer rope wires.

Rope diameter never appeared directly in the estimations of contact stresses, but larger rope diameters generally carry higher loads.

Triangular strand ropes were considered in this section. The calculation of the rope contact loads will also be applicable for all other rope constructions. However, other rope constructions will behave differently when the outer surface wires are deformed plastically.

5 Field observations

The origin of the field observation part of the project was detailed in the introduction of this report. Details of the six winders that were visited are given in SIMRAC reports GAP324 and GAP439. These two reports also give details of the information collected at the winders for each visit to a winder. Each winder was visited twice a year on average.

The information collected included the measurement of rope diameter, rope ovality, and rope laylength at at least three points on each rope of a winder. Moulds of a rope were also made at each of the points at which the measurements were carried out. The moulds were then used to make replicas of the rope section, which in turn were used to determine the length of the flat sections on the outer rope wires around the circumference of a rope. The original thinking was that the rate at which flats developed around a rope section may be an indication of rope surface degradation.

At the start of the field observations in 1996, it was also reasoned that by closely observing a winder, making sure that rope maintenance procedures were acceptable, and that no other factors that could be detrimental to the rope were present (like poorly maintained headsheave grooves), authentic rope service lives would be obtained for a winder. It was further reasoned that with accurate service lives obtained, it may be possible to determine the winder parameters and operating conditions that actually influence rope life.

At the onset of the field observations it was known that, because winder rope life could be several years, accumulation of data would be slow. No conclusions were reached after the first two years of field observations (reports GAP432 and GAP439) other than that it seemed to the researchers that as soon as "outsiders" observe a winder, the mine personnel will do their utmost to ensure a good rope life.

When the field observations of GAP501 commenced at the beginning of 1998, SIMRAC made it known that winder ropes research would not be supported after 1998, and it was recognised that definitive conclusions may not be reached.

In 1998 the six winders under observations were visited eleven times, and data were collected and measurements were made as during the two previous investigations. Between the last observations of GAP439 and the first observations of GAP501, ropes were changed on three of the six observed winders. Very little new information was therefore obtained from these winders. On the other three winders the ropes were well settled, and the measurements that were obtained were not much different to that of previous visits. This was also the situation comparing the measurements of GAP324 with that of GAP439. As was the case for GAP324 and GAP439, no conclusions could be reached from the measurements obtained during the field observations of GAP501.

However, the replicas made from rope moulds taken during the field studies gave some

indications of the surface degradation at points along the lengths of the ropes of the winders observed. Unfortunately the selection of the points along the rope lengths were not directly aimed at achieving such results. Apart from points selected near the front and back ends of ropes, only one other point was selected for most of the ropes, and then it was either at a layer crossover on the drum or at a point were broken wires have occurred. Front end sections usually provided little or no information because such sections vary rarely saw operation on the drum of the winder. It was nevertheless possible to "manufacture" some results of the degree of surface degradation along the rope lengths of three of the observed winders. Appendix E gives details of the process that was followed.

One of the results obtained in Appendix E is shown in Fig. 5. It was for a BMR winder that operated in a 2 050 m shaft. The graph is of interest because it shows that the back end of the rope does not have the greatest degree of surface degradation (which is the degree of plastic deformation of the outer wires of the rope).

The section on contact stresses on the rope on a winder drum (section 4) postulated that the rope section that should experience the greatest outer wire plastic deformation should be the second rope layer on the drum and not the bottom layer (or for that matter the back end of a rope). Although more measurements along the length of a rope would be required to confirm the mentioned postulation, the results in Fig. 5 do show that the back end section of the rope was not the point with the greatest amount of plastic deformation. Unfortunately, the exact location of the measured points with regard to position on the winder drum were not recorded.

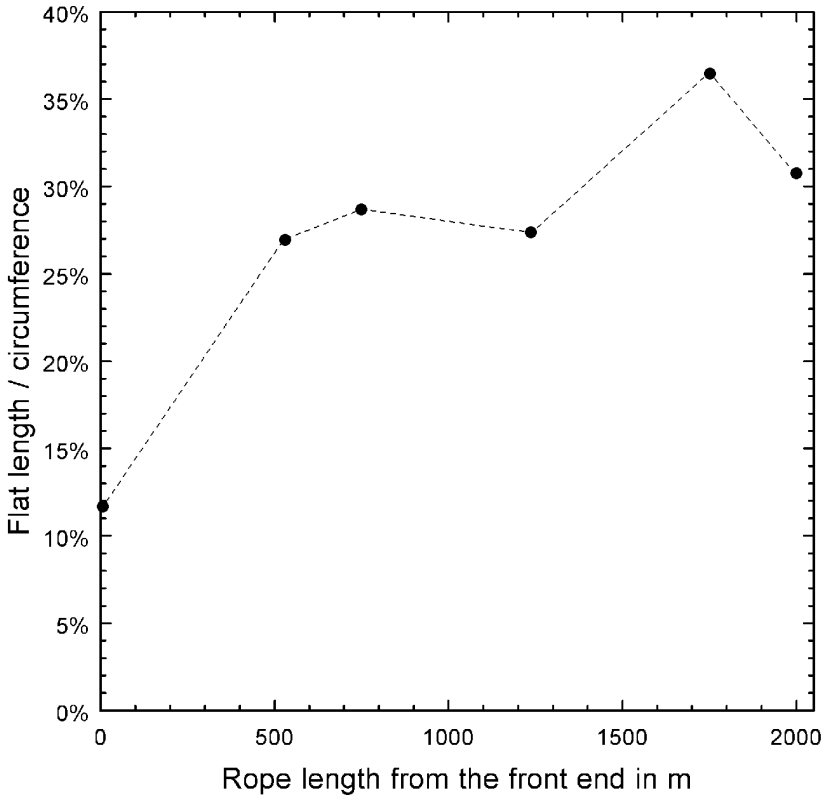

Figure 5: Rope surface degradation measured along the length of drum winder ropes that operated in a 2 050 m shaft.

If field studies of drum winder ropes are undertaken again, the measurement of the surface degradation could be aimed at locating the rope section with the greatest amount of surface plastic deformation.

6 Conclusions

Sections 2 to 5 of this report are summaries of detailed analyses shown in the appendices of this report, and each contain a number of conclusions. Only the most significant of these conclusions are repeated in this section.

Future deep shaft drum winders (especially rock winders) will operate at (dynamic) rope load ranges of close to 15% of the breaking strengths of the ropes. Under such circumstances broken wires will be generated by the tension-tension fatigue loading of the ropes. However, rope service lives of 100 000 winding cycles will be achievable for triangular strand ropes if the lubrication of a rope is maintained to minimise the effects of fretting fatigue.

The most surprising result of this report is that surface degradation (or the plastic deformation) of the crown wires of the strands of triangular strand ropes do not increase the susceptibility of wires to fatigue crack initiation.

Contact stresses experienced during multi-layer coiling on a winder drum is the primary cause for the plastic deformation or degradation of the crown wires of the rope strands. Although it was found that this surface degradation will not increase the susceptibility of wires to fatigue crack initiation, it is postulated that high contact stresses will generate their own problems (like split wires) if left unchecked. An alternative approach to the pulling in of back ends is proposed in the section on contact stresses to minimise the adverse effects of contact stresses, i.e. much more frequent in the beginning of the service life of a rope.

At dynamic rope load ranges of around 10%, triangular strand ropes should not develop broken wires from the tension-tension fatigue loading. The fact that broken wires do occur is most probably due to contact stresses experienced by the ropes on the drums.

The analysis and measurement of bending stresses in triangular strand ropes showed that the bending of ropes is still not entirely comprehended, but that the bending stresses for drum to rope diameter ratios currently employed will be considerably lower than the stresses generated by the tensile loading of a rope.

Although the findings of this report were different from what was expected or believed earlier, they were not alarming to any extent to warrant immediate changes to the regulations or specifications of SABS0294.

7 Relevance of the research to SABS0294

The current specifications in SABS0294[1] were arrived at after working group discussions over quite a lengthy period, and by giving due consideration to operational and manufacturing constraints and possible impacts on the economics of winding. The larger part of SABS0294 is a collection of best practices on current drum winders, e.g. fleet angles of the rope catenary, the specifications for flange height of the winder drum, and how the winder brakes should be tested. Only a very limited number of specifications in SABS0294 are actually of a nature that they can be supported by scientific analyses.

The investigation described in this report (GAP501) is relevant to the following aspects of SABS0294:

- Allowable rope loads: A load range of 15% of the new rope breaking strength during normal

winding, and a maximum allowable rope loads of 40% of the new rope breaking strength (envisaged to be experienced during emergency braking).
- Minimum *D/d* ratios (drum diameter and sheave diameter to rope diameter ratios): See Appendix C for details of the specification. SABS0294 allows a single deflection sheave with the specified *D/d* ratio, but only at winding speeds of less than 10 m/s.
- Recommended upper limit for winder drum and headsheave tread pressures (SABS0294 recommends values, but does not prescribe).
- Rope coiling on the winder drum: A maximum of five rope layers are allowed on the drum. Multi-layer coiling requires drum coiling sleeves with two cross overs per drum turn.
- Rope maintenance: Re-tensioning of the dead turns and pulling in of the back ends are required at intervals not exceeding 10 000 winding cycles.

In the sections that follow, a number of items are listed that should be considered for possible modifications to the regulations and the specifications of SABS0294. It is recommended that a working group should consider these recommendations before any actions are taken.

7.1 Allowable rope loads

The 15% (dynamic) load range formed and integral part of the derivation[12] of the formula for the static rope load factor of 25 000/(4 000 + *L*) included in the new drum winder regulations. Changing the rope load range limit will require a change to the "formula" in the regulations.

It was concluded that at a 15% load range broken wires will be generated by tension-tension fatigue loading of the ropes, but that rope service lives of 100 000 winding cycles will be achievable for triangular strand ropes if the lubrication of a rope is maintained to minimise the effects of fretting fatigue.

SABS0294 requires a winder to be fitted with a rope load monitoring system to ensure that required rope load range is maintained. The investigations of this report showed that it is important to maintain the rope load range to get reasonable rope service lives.

The "formula" by itself does not guarantee that a 15% (dynamic) load range will be maintained. The value of the winder accelerations/decelerations and the way in which they are introduced (ramping) will determine the load range that will be generated for a given winder installation. The 15% (dynamic) load range is of greater importance than the static "formula" of the regulations. It is very possible to maintain a 15% load range with modern winder control systems at static rope loads lower than that allowed by the "formula". The same can also be achieved by proper selection of the actual winder acceleration.

For winders operating with triangular strand ropes, consideration could be given to a regulation that will favour the 15% (dynamic) load range to the static factor of the "formula", or at least to allow winders to operate at any static factor as long as the load range limit and the maximum rope load limits are adhered to.

In the section on the fatigue performance of triangular strand ropes it was shown that such ropes will not accumulate additional damage by infrequent loading to 40% of the rope strength. If corrosion and abnormal damage of the ropes are well controlled, consideration could be given to increasing the maximum allowable rope load from 40% of the rope strength to 45% (for triangular strand ropes at least). The reason being that the 40% rope load limit may be somewhat onerous for shafts 3 500 m and deeper.

7.2 *D/d* ratios, tread pressure and contact stresses

Appendix C gives a detailed account of the reasons for the *D/d* specification included in SABS0294. The specification was included to limit possible influences of rope bending stresses on rope life. The tread pressure recommendation was included for traditional reasons (best practice). The number of rope layers allowed on the drum was limited to five to prevent possible damage from contact stresses, although the extent of radial rope loads on a winder drum was not analysed. The specification on the frequency of pulling in back ends was reached through consensus (trying to limit possible damage without making the specification too onerous).

Very few of the parameters of a winder installation can be changed in isolation. Most of the winder parameters are interrelated. Consider:

> For a given shaft depth, the static rope load factor will be determined by the formula in the regulations. For a selected maximum attached load at the front end of the rope, the rope size will be determined by the selected rope tensile grade (a limited selection). Selecting a winder speed will give a minimum drum diameter and headsheave diameter (*D/d* ratio). To be able to wind the rope of a deep shaft onto the drum without exceeding the five-rope layer limit, a certain drum width will be required. The maximum fleet angles allowed will then require a minimum catenary length to be able to accommodate the required drum width. Or the other way round: if the catenary length is set, then the drum width will be given by the maximum fleet angle required. If the length of rope cannot be accommodated in five rope layers, the drum diameter will have to be increased. For a given winding speed, an increased drum diameter will give, and require, a larger drum shaft torque, will require slower running electrical motors and more brake capacity, which in turn will increase the cost.

It is shown in this report that winding speed does not influence the magnitude of the bending stresses significantly, and that the bending stresses for *D/d* ratios of around 100 are significantly lower than the (tensile) stresses generated by normal winding operations. Although the reasons for allowing smaller *D/d* ratios for slow speed winders remain valid, consideration should be given to reducing the upper *D/d* ratio limit from 140 to 100.

The part on contact stresses in this report shows that these stresses are probably more significant than previously anticipated. Rope-on-rope contact loads will be reduced by fitting of coiling sleeves with two crossovers per turn, by employing large drum diameters, and by having fever rope layers on the drum. Larger drum diameters will, of course, lead to fever rope layers being required for a given shaft depth. SABS0294 specifies the required rope coiling sleeves, but winder drums cannot be required to be unduly large. However, the adverse effects of contact stresses generated by large contact loads can be reduced by pulling in the back end of a rope more frequently in the beginning of the life of a rope. Consideration should therefore be given to include appropriate specifications in the code of practice that will require more frequent pulling in of back ends in the beginning of the service lives of ropes, especially if drums are relatively small, and carry four or five rope layers.

Tread pressure, as specified in the code of practice, is essentially proportional to the inverse of the *D/d* ratio. Therefore, for given shaft depths and allowable rope loads and drum sizes, tread pressure is merely a consequential value rather than a selected parameter. In deep shafts the recommended tread pressure cannot be achieved. Tread pressure has no physical meaning and the tread pressure recommendation in SABS0294 should be scrapped.

7.3 Rope maintenance

The frequency at which rope back ends should be pulled in has been addressed above.

It was originally proposed that a rope should be adequately protected against corrosion, but this requirement was not included in SABS0294. It has been established that poor lubrication of the ropes will lead to increased fretting, and therefore to the accelerated generation of broken wires. SABS0294 should at least make the user aware of this fact.

7.4 General

SABS0294 allow triangular strand, round strand, non-spin and full locked coil ropes to be used. No distinction is made between the use of any of these types of rope in SABS0294. Although the investigation of the behaviour of different rope constructions was not part of the scope of GAP501, experiences of the past year indicated that non-spin ropes may be more prone to internal corrosion, and kibble winding at shaft sinking installations showed that certain types of non-spin ropes may not be properly suited for drum winding with five rope layers.

Consideration should be given to an investigation that will at least highlight possible differences in the behaviour between different rope constructions when used on drum winders and in deep shafts. Appropriate requirements can then be included in SABS0294.

8 References

1. SABS0294 *Code of Practice for the Performance, Operation, Testing and Maintenance of Drum Winders relating to Rope Safety*

2. Van Zyl, Mike: *Information on 99 drum winders and 711 discarded winder ropes.* CSIR Contract Report MST(90)MHT3, May 1990.

3. Van Zyl, Mike: *Relationship and trends of drum winder parameters.* CSIR Contract Report MST(90) MHT 10, November 1990.

4. Van Zyl, Mike: *A life prediction model for drum winder ropes.* CSIR Contract Report MST(91)MC662 February 1991.

5. Chaplin, C R: *Drum winding rope deterioration study; Summary report.* Reading University, August 1989.

6. Chaplin, C R: *Drum winding rope deterioration study; Simulation & Backslip.* Reading University, March 1990.

7. Chaplin, C R: *Drum winding rope deterioration study; Backslip - A re-evaluation.* Reading University, July 1990.

8. Hunziker, R A; Pretorius, J J; and Van Zyl, Mike: *Wear mechanisms of drum winder ropes.* CSIR Contract Report MST(92)MC1109, June 1992.

9. Hecker, G F K and Van Zyl, Mike: *Drum winder rope test facility: A feasibility study.* CSIR Contract Report MST(93)MC1233, January 1993.

10. Hecker, G F K; Wainwright, E J: *GAP324 Volume 1: Deterioration and discard of mine winder ropes.* SIMRAC report, September 1997

11. Hecker, G F K: *GAP439: Deterioration of drum winder ropes.* SIMRAC report, July 1998.

12. Hecker, G F K: *Motivation for proposed changes to Chapter 16 of the minerals Act; Rope safety regulations for drum winders.* CSIR Contract Report MST(92)MC1674, June 1993.

13. Haggie Steel Wire Ropes: *Various confidential reports on fatigue tests carried out on new triangular strand ropes during the period 1957 to 1962.* The information was made available to the project by Haggie, and collated by E J Wainwright.

14. Van Zyl, Mike: *Load ranges experienced by drum winder ropes.* CSIR Contract Report MST(92)MC996, November 1992.

15. Kenyon, John N: *Fatigue properties of steel rope wire.* Materials Research and Standards, Vol 2 No 7, July 1962.

16. Hempel, M: *Fatigue tests on steel wires.* Draht (English edition) No. 22, April 1956.

17. Becker, K: *On the fatigue-resisting ability of rope wires.* Wire Industry, July 1978.

18. Van Zyl, Mike: *GAP502: Discard criteria for drum winder ropes* SIMRAC report, September 2000.

19. Chaplin, C R: *Failure mechanisms in wire ropes.* Engineering Failure Analysis, Vol 2, No. 1, pp 45-77, 1995.

20. Van Zyl, Mike: *An Investigation onto the Behaviour and Deterioration of Winding Rope Tangent Points on Conveyance Mounted Compensating Sheaves* CSIR Contract Report MST(95)MC2491, May 1995.

Appendix A: Past fatigue tests on new triangular strand ropes

As a starting point to the investigation of the fatigue performance of triangular strand ropes, information was obtained on fatigue tests carried out in the past on new (as manufactured) triangular strand ropes. Information on fatigue tests of 85 triangular strand rope samples was supplied by Haggie Rand.[13] These tests were carried out in the period from 1957 to 1962. The purpose of the tests was to determine the effect of various base steels and manufacturing methods on the fatigue resistance of the ropes and not specifically to examine the behaviour of the ropes under different cyclic loads.

A1 Rope data

The ropes on which the fatigue tests were done were all of the same construction and size. The basic rope data is given in Table A1.

Table A1: Standard production rope data

Construction	6x28(10/12/6+3T)/F
Diameter	38,1 mm (1½")
Fibre core size	16,2 mm
Wire sizes	3,20 1,50 1,32 0,97 mm
Tensile grade	1 750 MPa
Mass/metre	6,188 kg/m
Rope lay	Right hand Lang's lay (RHL)
Rope laylength	286 mm (7,5 rope diameters)
Strand laylength	126 mm (3,3 rope diameters)

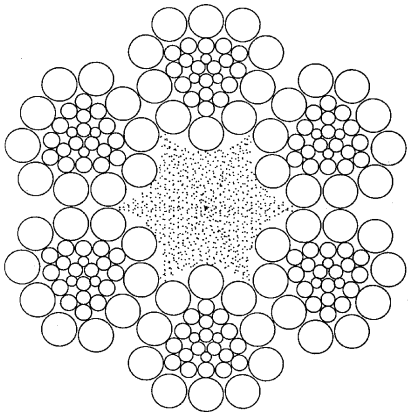

The individual ropes differed as follows:

Rope A: Standard production rope; breaking strength 1 023 kN
Rope B: Special grease used; breaking strength 1 044 kN
Rope C: Standard; breaking strength 1 063 kN
Rope D: Rope A with a 5% larger diameter fibre core.
Rope E: Swedish basic steel and special grease; breaking strength 1 023 kN
Rope F: Standard; breaking strength 1 052 kN
Rope J: Outer wires of Swedish steel, core greased; breaking strength 1 041 kN

The ropes were manufactured in the period November 1957 to July 1959. The breaking strengths of all the ropes were much the same (within ±1%), and can therefore be considered as identical.

Taking the strand laylength and the rope laylength into account, a given outer wire of a strand will re-appear on the rope surface approximately every 120 mm, and will remain visible for approximately two thirds of this distance.

The total cross-sectional steel area of all the wires in the rope was 672 mm². The cross-sectional area of one outer strand wire was 8 mm². The ten outer wires of a strand made up 72% of the cross-sectional steel area of a strand, and 12% of the total cross-sectional steel area of the rope.

A2 Fatigue of single roping wires

General information on the fatigue strength of cold drawn steel wires was obtained from various

sources.[15,16,17] A summary of the general findings is given in this section. A typical fatigue curve for a 1 800 MPa single straight steel wire is shown in Fig. A1.

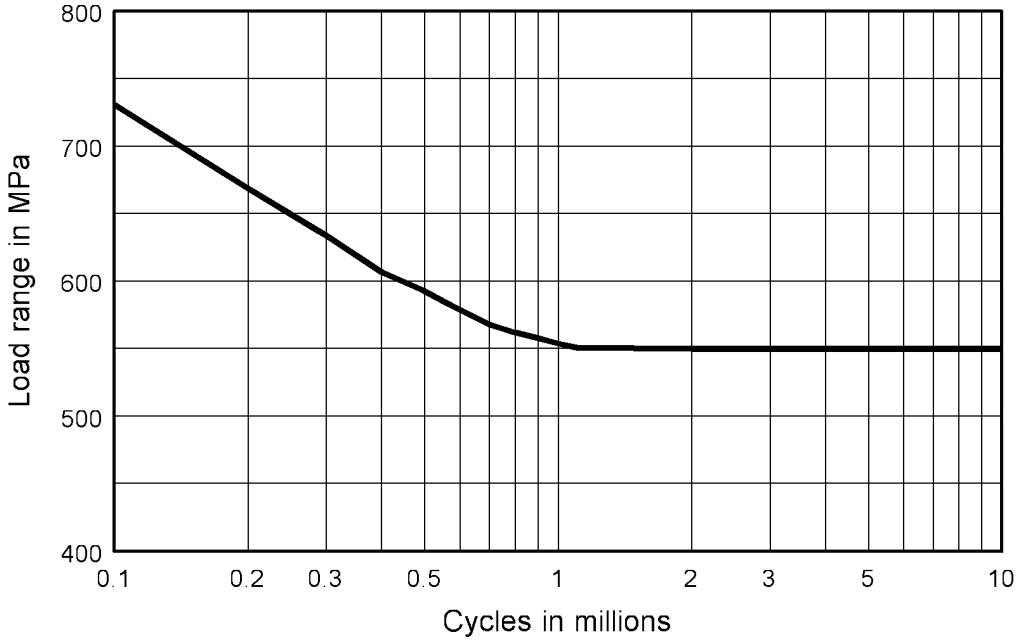

Figure A1: An example of a fatigue curve for a single roping wire

The fatigue limit of the example above is at a load range of 550 MPa, which is 30% of the breaking strength of the wire. That research has shown that the mean load during fatigue tests on single wires does not influence the shape of the curve significantly. As expected, the research also showed that the fatigue limit of a wire is influenced by its surface condition and finish. The fatigue limit of a hot dipped galvanised wire, for example, reduced to 400 MPa (22% load range). On the other hand, surface deterioration due to corrosion could reduce the fatigue limit to even lower values.

Manufacturing a rope from individual steel wires introduces residual stresses in the wires because of the wire and strand shaping processes. Residual stresses change the mean load experienced by an individual rope wire when a rope is loaded. If it is absolutely true that mean load does not have an influence on the fatigue performance of single wires, then residual stresses should not influence the fatigue performance of the wires in a rope.

When a rope is loaded in tension, the individual wires experience greater stresses than the average rope stress (based on the cross-sectional area of the wires), because the wires do not run parallel to the rope. In addition, the wires are subjected to contact stresses, which can introduce additional longitudinal and transverse stresses. The influence of these stresses is still not fully understood. A rope can also not be manufactured perfectly, therefore wires could experience stress increases due to secondary bending of wires and uneven distribution of the loads in the individual wires of the rope.

During operation of a rope on a drum winder, surface damage is introduced by contact stresses and slipping of the rope on the drum, rubbing against other rope coils during coiling, and rubbing against sheave wheel flanges. Fretting between wires and strands will also cause localised wire surface damage.
All of the mentioned additional actions could increase the susceptibility of the rope wires to crack initiation when the wires are part of a running rope, and could therefore promote the generation of broken wires.

A3 Fatigue tests and results

The rope samples were subjected to tension-tension fatigue loading. Whenever a broken wire occurred during a fatigue test, the number of completed load cycles was noted. A fatigue test was continued until a maximum of 12 broken outer wires were generated in a rope specimen. The tests usually continued for some time after the 12th broken wire was recorded due to test procedure used. Tested rope samples were then destranded and the total number of broken and cracked wires determined. There were usually several inner wires broken, but these were ignored for the purposes of this report because it was never known when an inner wire broke during a test.

A3.1 The initial tests

Initial fatigue tests were carried out on samples of Rope A to examine the effect of specimen length. The test were carried out at a mean load of 14,4% of the breaking strength of the rope, and at a load range of 20% (i.e. a minimum load of 4,4% and a maximum load of 24,4% of the breaking strength of the rope). Two specimen lengths were selected: 460 mm and 685 mm long (1,6 rope laylengths and 2,4 rope laylengths respectively).

Six specimens of the shorter length were tested and ten specimens of the longer length. The results of these fatigue tests are shown in Figs A3.1 and A3.1.1 as graphs of the number of load cycles at which broken wires occurred. Some of the tests were terminated before the maximum of 12 broken wires were registered. The records do not give reasons why these tests were terminated. No information was available on the distribution of the broken wires in a test specimen, and whether wires failed in the valleys between the strands or at other locations.

The researchers (at that time) decided that the results for the longer specimens were more consistent, and for that reason the rest of the fatigue tests were carried out on 685 mm long specimens.

A3.2 The fatigue tests

The rest of the fatigue tests were all performed at a mean load of 19,6% of the breaking strength of Rope A, and at a load range of 14,8% of the breaking strength of Rope A (i.e. a minimum load of 12,2% and a maximum load of 27% of the breaking strength of the rope). (The load range during these tests was so close to 15% that these tests will be referred to as the 15% load range tests.)

The results of the tests on 69 rope samples are given in Figs A3.2 to A3.2.6. The actual breaking strengths of the ropes were slightly different as shown in section A1. The actual load ranges (as percentages of the rope breaking strengths) are shown on the figures. All the tests were continued until each rope specimen had 12 outer broken wires. As with the initial tests, no information on the distribution and location of the broken wires in any of the specimens were available.

A4 Discussion of the results

The original reports on the fatigue tests do not give any information on the distribution of the broken wires (i.e. over how many laylengths) and whether the wires broke in the valleys between the strands or at the crowns of the strands. It is therefore not possible to determine the origins or

possible reasons for crack initiation.

If it is assumed that all the broken wires were visible, then every time an outer wire appeared on the surface of the rope, that length of visible wire could be considered as a separate test sample within the tested length of rope. From the rope and strand laylengths it was calculated that an outer wire "surfaced" every 120 mm. A rope length of 685 mm (the longer specimen length tested) would therefore have contained approximately 300 separate and identical outer strand wire samples. Each of these wire lengths could (theoretically) have developed a broken wire during a fatigue test. Each of these wire lengths also had potential fretting points at each end where the wire enters the valley between strands. The 685 mm rope length therefore, potentially, had 600 fretting points at which cracks could have initiated. The numbers per one rope laylength would be approximately 125 wire lengths and 250 fretting points.

Although the ropes that were tested only had 60 outer strand wires in total, it is known that a fractured wire could "recover" in a relatively short distance in the rope. More than one failure would therefore have been possible in the same wire of a rope during a fatigue test.

If all the fatigue tests were continued for the same number of load cycles, it might have been possible to calculate the probability of a broken wire developing after a given number of cycles. However, information on exactly where a broken wire originated would have been required, and all the samples would have had to be tested to the same number of load cycles.

A longer rope specimen has more potential crack initiation points than a shorter specimen of the same rope construction and size. Logically, more broken wires should therefore occur in longer rope specimens during fatigue tests, and broken wires should be generated more rapidly (imagine two short specimens being tested in series). Although not conclusive, this is suggested by the 20% load range tests carried out on specimens of two different lengths (Figs A3.1 and A3.1.1).

For the 15% load range tests, the different ropes (A to J) behaved in a similar fashion. Two of the tests at 15% load range on Rope A (Fig. A3.2) nearly represent the least and most number of load cycles for a given number of broken wires. Only Ropes D and E returned poorer results. Rope D (Fig. A3.2.3) was manufactured in the same way as Rope A, only with a larger fibre core. Rope E (Fig. A3.2.4) used Swedish basic steel, but so did Rope J (Fig. A3.2.6), the only difference being that Rope J had a greased core. There is no apparent reason why a larger fibre core would lead to poorer fatigue performance. (Possible explanations for the different fatigue performances are given in the main section of the report.)

The tests did show that, contrary to the general belief at the start of this project, triangular strand ropes develop fatigue cracks and broken wires at a load range of 15%. At a 15% load range, first broken wires occurred at as low as 90 000 load cycles, while another specimen required 226 000 cycles before the first wire failure occurred.

For the 15% load range case, the maximum load was 27% of the breaking strength of the rope and the minimum load 12%, with a mean load of 19,5%. For the 20% load range case, the maximum load was 24% and the minimum load 4%, with a mean load of 14%. Although the maximum load and the mean load for the 15% load range tests was higher than that of the 20% load range tests, broken wires were generated more rapidly at the higher load range.

During the fatigue tests, broken wires were generated at relatively low loads compared with the fatigue resistance of a single roping wire. The manufacturing process of a wire rope, which induces residual stress and possibly surface damage in the wires, and the additional stresses that the wires experience when part of a rope (bending, torsion) could have increased the susceptibility of the wires to fatigue.

A summary of the results of this appendix are shown as scatter plots in Fig. A4. For the 20% load

range tests, only the results of the longer specimen lengths were included.

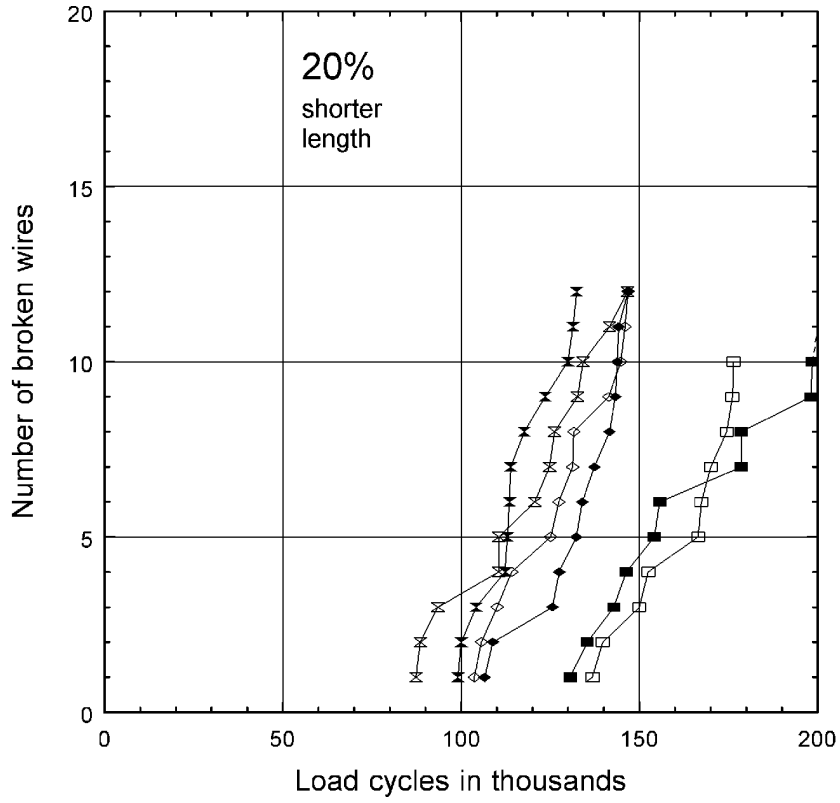

Figure A3.1: ***Rope A, shorter specimen (460 mm long): 20% load range, load cycles at which broken wires occurred, 6 tests.***

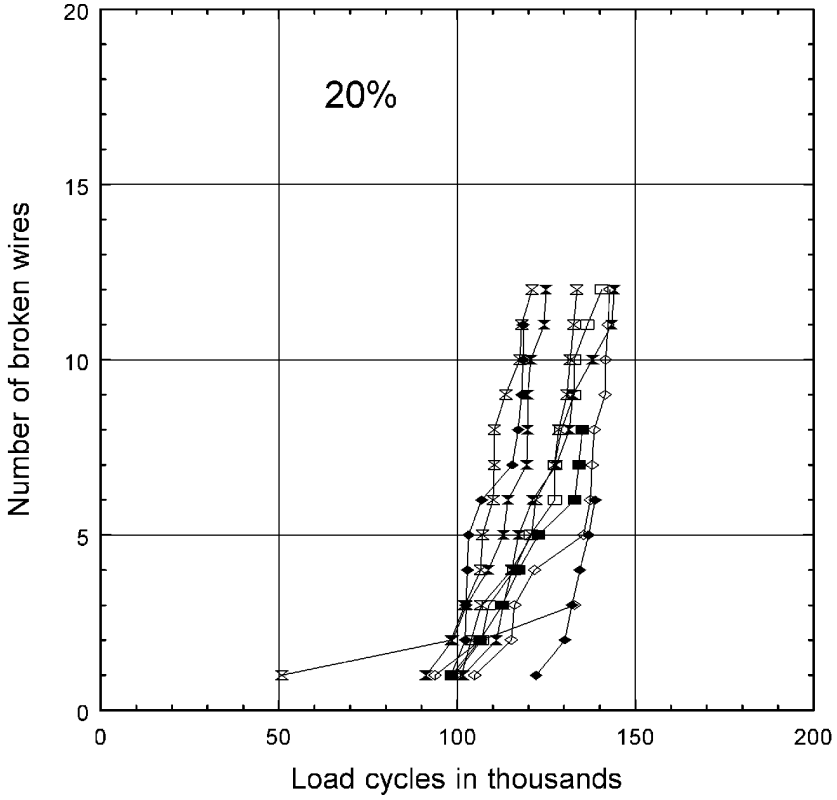

Figure A3.1.1: ***Rope A, longer specimen (685 mm long): 20% load range, load cycles at which broken wires occurred, 10 tests.***

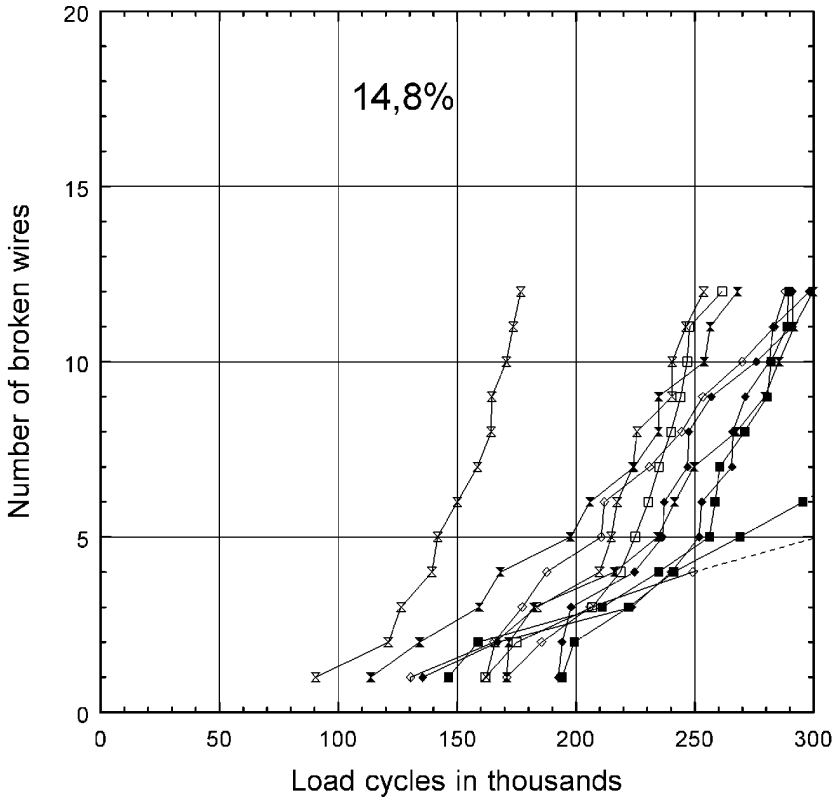

Figure A3.2: ***Rope A: 15% load range, load cycles at which broken wires occurred, 11 tests.***

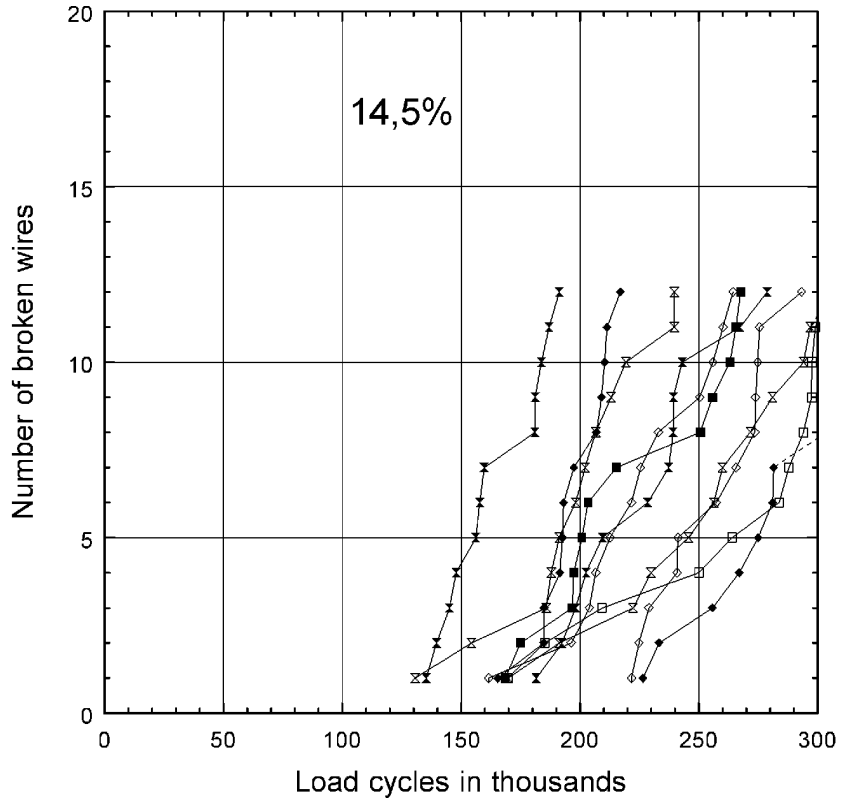

Figure A3.2.1: Rope B: 15% load range, load cycles at which broken wires occurred, 10 tests.

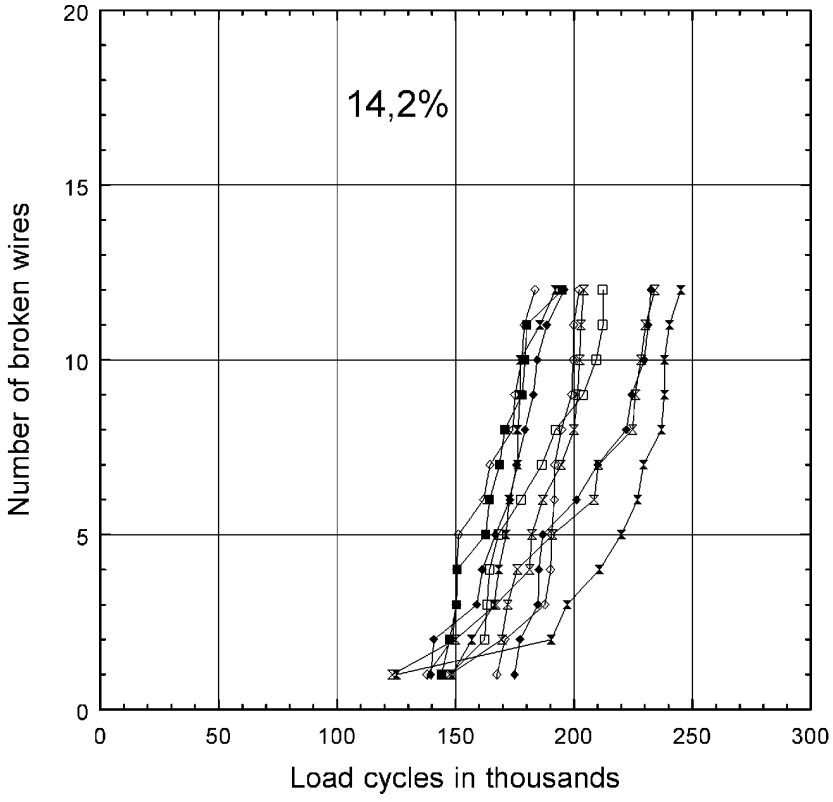

Figure A3.2.2: Rope C: 15% load range, load cycles at which broken wires occurred, 10 tests.

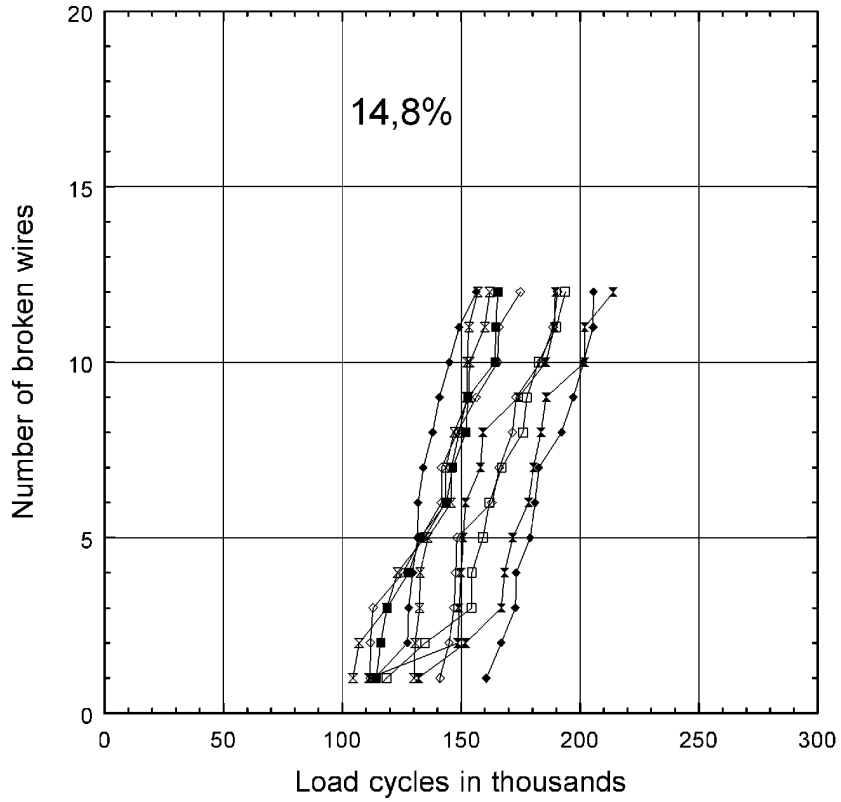

Figure A3.2.3: Rope D: 15% load range, load cycles at which broken wires occurred, 10 tests.

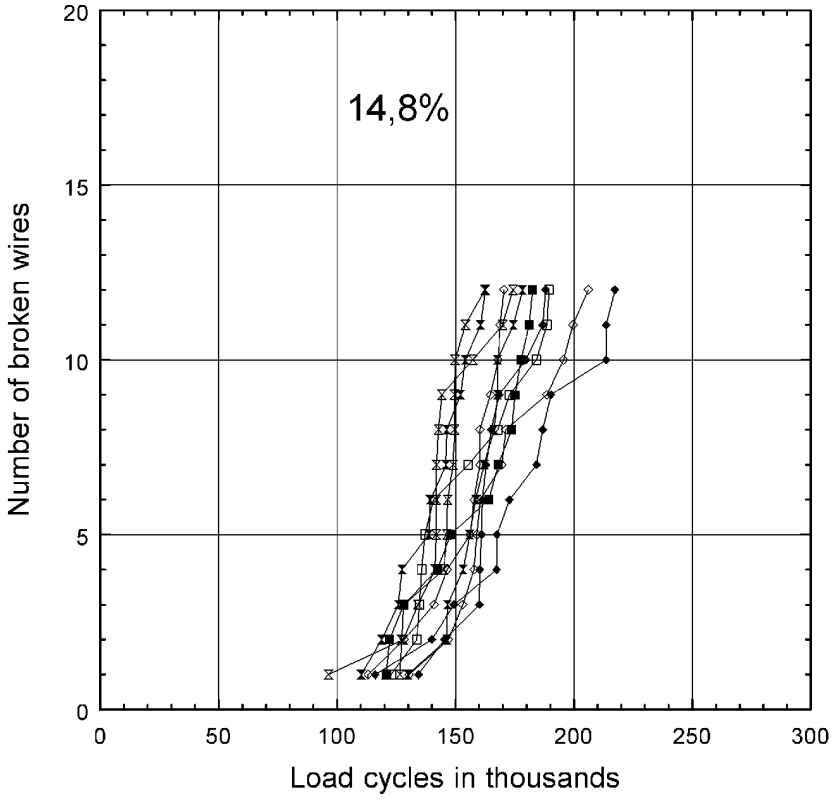

Figure A3.2.4: Rope E: 15% load range, load cycles at which broken wires occurred, 10 tests.

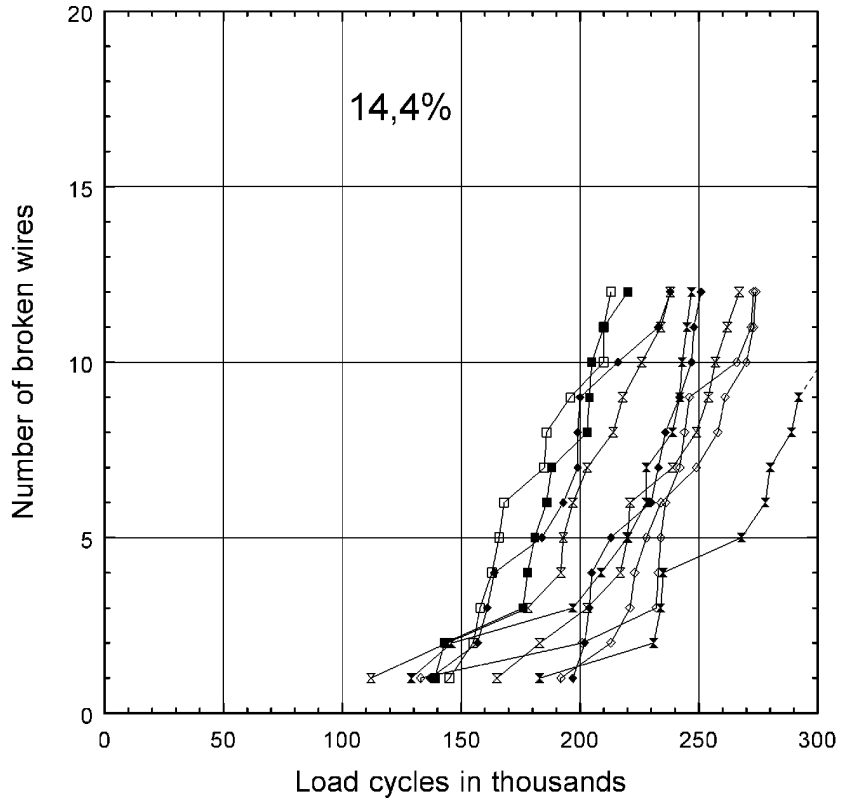

Figure A3.2.5: Rope F: 15% load range, load cycles at which broken wires occurred, 10 tests.

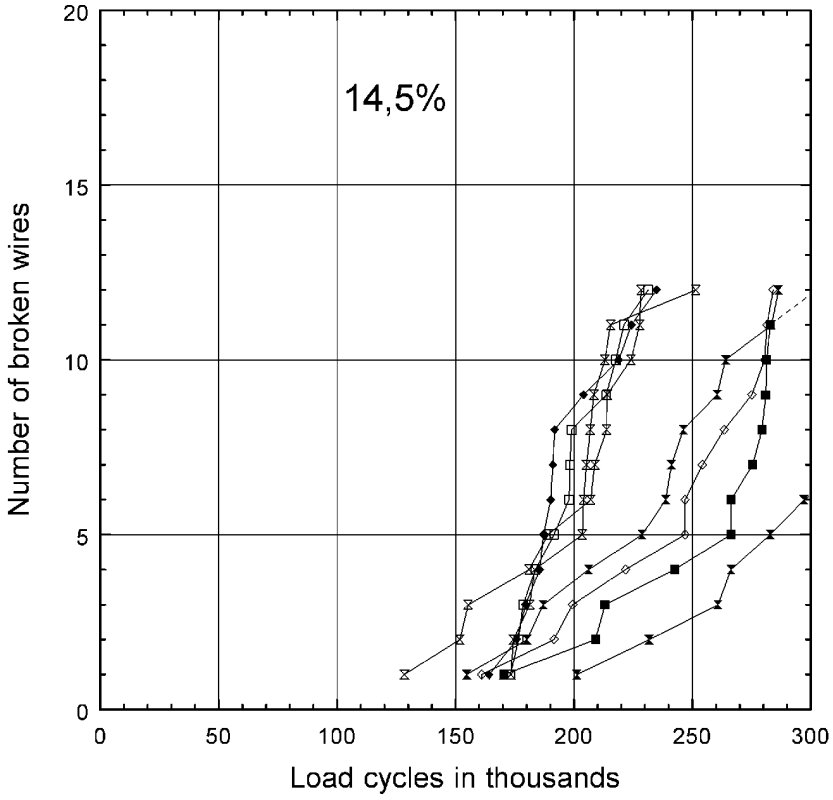

Figure A3.2.6: Rope J: 15% load range, load cycles at which broken wires occurred, 8 tests.

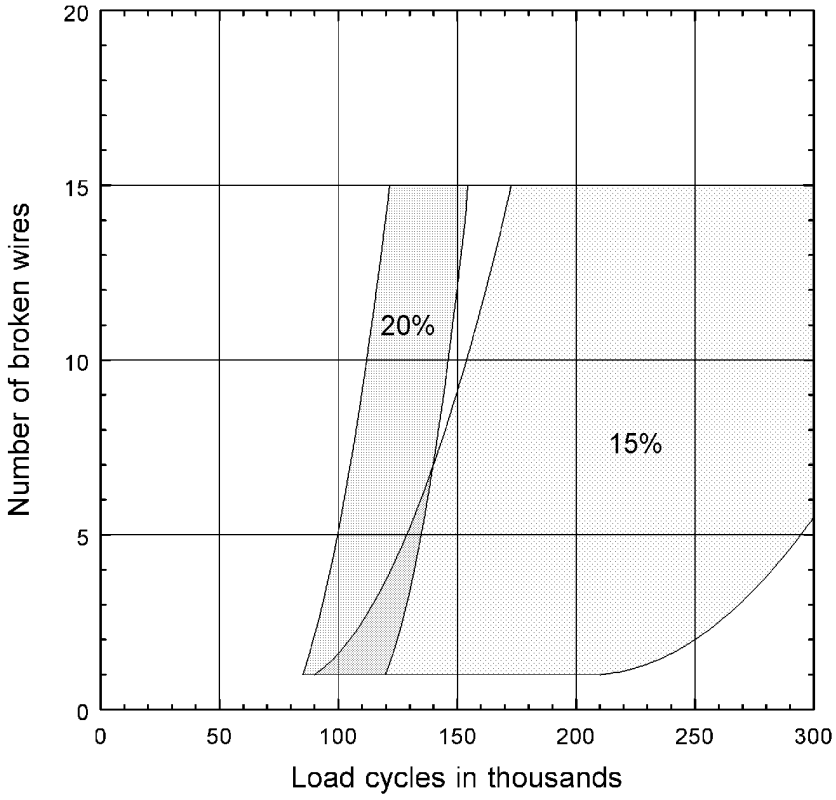

Figure A4: Scatter plots of the new-rope tests at 15% and 20% load ranges.

Appendix B: Fatigue tests on used triangular strand ropes

The primary objectives of the fatigue tests on used drum winder ropes were to determine to what extent surface damage experienced in service would accelerate the initiation of fatigue cracks in the wires of the ropes, and to determine the effect of load range on the initiation of cracks and generation of broken wires.

B1 Selected rope sections and rope data

Sections of the two underlay ropes of the West BMR at Western Deep Levels South were obtained for fatigue testing after the ropes were discarded. The four ropes on the BMR were discarded after one of the overlay ropes reached the discard criteria according to SABS0293. The two underlay ropes had relatively few broken wires (as determined by non-destructive magnetic testing of the ropes). The rope service life achieved was normal. The winder on which the rope operated was exclusively used for hoisting rock.

The two ropes had opposite lay directions. The lengths of rope obtained were from the front ends of the ropes (conveyance end), from around midshaft, and from near the back ends (drum ends). The winder and rope details are given in Table B1. A schematic of a cross-section through the rope is shown in Fig. B1.

Table B1: Winder and rope details

Winder type	BMR drum
Ropes per skip	2
Susp. length of rope	2 360 m
Length of wind	2 350 m
Winding speed	15 m/s
Skip mass	10 300 kg
Payload	20 000 kg
Rope diameter	48 mm
Rope construction	6x33(15/12/6+3T)/F
Wire diameters (mm)	2,95 2,32 2,00 1,48
Tensile grade	1 900 MPa
Mass per metre	9,95 kg/m
Breaking strengths	1 805 kN (LHL) 1 780 kN (RHL)

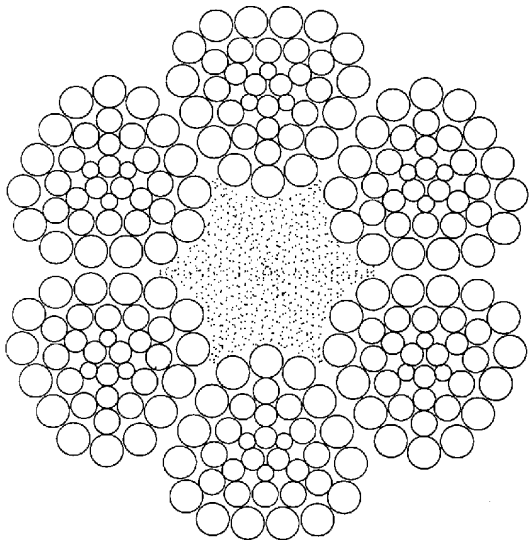

Figure B1: Cross section of a 6x33 triangular strand rope.

Stock samples of the rope set (sections cut from the ropes after manufacture) were obtained from Haggie (the rope manufacturer). The stock samples were also subjected to fatigue tests to obtain a measure of the fatigue performance of the new (unused) ropes.

After some time in service, rock winder ropes exhibit significant degrees of plastic deformation and wear of surface wires. The combination of plastic deformation and wear is sometimes referred to as plastic wear. The plastic wear was, of course, more significant towards the back ends of the ropes. The crown wires of a strand exhibit the most noticeable plastic wear.

Due to the torque-tension characteristics of a triangular strand rope, the back end laylength of the

rope in service will be longer than the as-manufactured (or zero-tension) laylength, the front end laylength will be shorter than the as-manufactured laylength, while at midshaft the rope will have approximately the same laylength as manufactured. During service, the laylengths increase every time spin is let out of the rope when the front end of the rope is released from the conveyance (for front end cutting).

Because of the plastic wear on the ropes, there will be a degree of permanent laylength change after a rope has been in service for some time. After removal from service, the (zero-tension) laylengths of the selected lengths of rope were approximately 400 mm for the front end samples, 420 mm for the midshaft samples, and 440 mm for the back end samples. The midshaft laylength was 8,75 rope diameters (after being removed from service). The stock samples had laylengths of approximately 430 mm.

The length of the fatigue specimens of 990 mm between the end fittings was determined by the maximum length of rope that could be fitted into the fatigue testing machine. This specimen length constituted around 2,3 rope laylengths and just more than 20 rope diameters.

For the rope and strand laylengths of the rope specimens tested, a strand outer wire at the crown of the strand would be at the crown of the strand again approximately every 250 mm. Therefore, all 15 outer strand wires would have passed through the crown of the strand in a rope length of 250 mm. The 990 mm long fatigue specimens therefore had approximately 60 crown wires per strand, and approximately 360 crown wires in total.

A strand outer wire would "appear" out of the ropes and "disappear" into the ropes approximately 70 mm on either side of the crown position. At each of these points, an outer wire makes contact, or could make contact, with the wires of an adjacent strand. Each of these inter strand contact points could be the origin a "fretting fatigue" crack. Taking into account the number of fretting fatigue points "lost" at the end fittings, each strand would have approximately 110 fretting points, giving a total of approximately 660 fretting points for the 990 mm long specimens.

B2 Preparation of fatigue test specimens

Before a rope specimen was cut to length, the testing length of 990 mm was firmly secured by attaching purpose-machined split flanged collars/clamps to each end of the specimen length. These collars were approximately two rope diameters long, and gripped the crown wires of the specimen firmly without causing damage to the wire surfaces and prevented relative movement between the strands during cutting. These collars further served as attachments for the split end-fittings/grips.

The cylindrical end fittings were 145 mm long with 8° cones on the inside. When the ends of a specimen were "brushed", utmost care was taken to prevent excessive strain on the rope wires at the point of transition into the termination. After brushing, the split end fittings were placed over the brushed wires and aligned by fastening the end fittings to the flanged collars. Resin mixed with silica was poured into the cones of the end fittings. When the specimens were fitted into the fatigue testing machine, care was taken to align the ends properly to minimise bending stresses at the end fittings.

To enable a tensile test after a fatigue test, an 11° resin cone was cast over the 8° termination. The standard tensile test machine end fittings could then be used.

The first set of conical end fittings were damaged during the first fatigue test (Specimen no. 1). The results of Specimen no. 1 were therefore ignored. After modifications, the end fittings performed better. The remainder of the fatigue tests (25 specimens) were completed with two

sets of end fittings.

B3 Detecting wire breaks

During the fatigue tests, the number of load cycles completed when broken wires occurred had to be recorded. The first two proper fatigue tests (specimen nos 2 and 3) were observed continuously, and the load cycles completed at each of the wire breaks were recorded manually. Because this operation was laborious, and because the occurrence of (outer) wire breaks emitted a very audible sound, it was decided to develop a wire break detector.

A microphone, sound card, and a computer were used to monitor the ambient sound during a test, and to record events that exceeded a preset level. Although other events triggered recordings, post test analysis by playing back the recorded files and simply listening to the sound was sufficient to remove events other than wires breaking.

After 98 wire breaks were recorded during 300 000 load cycles for one of the tested specimens (specimen no. 25), the specimen was not tensile tested but was opened up and all the wire breaks counted. 102 wire breaks were found. The reason why four wire breaks were not detected was that maybe the trigger level was set too high, or maybe the level of sound emitted decreased as the number of broken wires present in the rope increased. Nevertheless, the ability of the wire break detector was considered to be adequate.

B4 Broken and cracked wires

After a fatigue test was completed on a specimen, the specimen was tensile tested to destruction. The one purpose of the tensile test to destruction was to "open up" the specimen to enable the inspection of the inside of the rope. The second objective of the tensile test was to determine the breaking strength and then to try to correlate the reduction in breaking strength with the number of broken and cracked wires. However, the report on GAP502[18] showed that such a correlation on the 990 mm long specimens would not be realistic. This was not known at the time that the fatigue and tensile test were carried out.

Nevertheless, the maximum loads and other interesting results from the tensile tests are given in this appendix together with the results from the fatigue tests.

Wires that fractured completely during a fatigue test are simply referred to as "broken wires". These are the wire breaks detected with the wire-break-detector and recorded during a fatigue test.

Some wires developed fatigue cracks during the fatigue tests but did not fracture. Some of these cracks were large enough to propagate into wire failures during the tensile test carried out subsequent to a fatigue test. These partially fatigued wires were counted and reported as "cracked wires". To determine the number of cracked wires accurately, the resin terminations of a specimen were cut off after the tensile test and the rope was taken apart wire by wire.

B5 Loads applied during the fatigue tests

The new rope breaking strengths of the two ropes from which samples were cut were 1 780 kN for the right hand lay rope, and 1 805 kN for the left hand lay rope.

The fatigue tests were done at three different load ranges, namely:

> **10% load range:** The tests were done at a mean load of 535 kN; a minimum of 445 kN and a maximum of 625 kN (i.e. approximately 30% ±5% of breaking strength, or from 25% to

35%)

15% load range: The tests were done at a mean load of 535 kN; a minimum of 400 kN and a maximum of 670 kN (i.e. approximately 30% ±7,5% of breaking strength, or from 22,5% to 37,5%)

20% load range: The tests were done at a mean load of 535 kN; a minimum of 357 kN and a maximum of 713 kN (i.e. approximately 30% ±10% of breaking strength, or from 20% to 40%)

With the new South African rope factor regulations for drum winders in vertical shafts, the back end of a rope in a 4 000 m deep shaft will experience a static load of approximately 32% of breaking strength and a maximum load of around 36,5% during normal winding with full loads.

To ensure that the correct loads were applied during the fatigue tests, the load calibration of the fatigue testing machine was checked before the fatigue tests commenced.

B6 The fatigue tests and results

Apart from the three load ranges that were to be investigated, samples with three different degrees of surface deterioration (front end, midshaft, back end) were available, and left hand lay and right hand lay rope samples were available.

- Two left hand lay and two right hand lay samples of each of the three degrees of surface deterioration were tested at a 15% load range, i.e 12 samples. Except for one sample, the tests were all continued until at least 300 000 load cycles were completed.

- One left hand lay and one right hand lay sample of each of the three degrees of surface deterioration were tested at a 20% load range, i.e six samples. On average the tests continued for 150 000 load cycles.

- One back end sample of the left hand lay rope and one right hand lay sample from the midshaft section were tested at a 10% load range for 300 000 load cycles. One more left had lay sample from midshaft was tested at a 10% load range for 150 000 load cycles.

- The four stock samples, two left hand lay and two right hand lay ropes, were tested at a 15% load range for 300 000 load cycles.

A summary of the fatigue tests carried out and described in this appendix is given in Table B6.

Note: During preparation of specimen no. 2, the sample was thoroughly cleaned over its complete length, i.e. all the rope "grease" was removed. This specimen had ten broken wires after 160 000 load cycles were completed. All the broken wires developed at the inter-strand contact points. Specimen no. 3 was not cleaned at all, and had only six broken wires after 300 000 load cycles.

It was then decided not to clean any of the remainder of the fatigue specimens. The specimens were therefore tested in the condition they were when the ropes were discarded from the winder.

Table B6: Summary of the fatigue tests carried out on samples from the used ropes and the stock samples

Specimen no.	Specimen description	Load range	Load cycles

2	LHL front	15%	160 000
3	LHL front	15%	300 000
4	RHL front	15%	600 000 *
5	RHL front	15%	300 000
6	LHL middle	15%	300 000
8	LHL middle	15%	300 000
7	RHL middle	15%	300 000
9	RHL middle	15%	300 000
12	LHL back	15%	300 000
13	LHL back	15%	300 000
10	RHL back	15%	300 000
11	RHL back	15%	300 000
18	LHL front	20%	180 000
17	RHL front	20%	150 000
16	LHL middle	20%	150 000
14	RHL middle	20%	150 000
19	LHL back	20%	150 000
15	RHL back	20%	135 000
21	LHL stock	15%	300 000
26	LHL stock	15%	300 000
23	RHL stock	15%	300 000
25	RHL stock	15%	300 000
20	LHL back	10%	300 000
22	RHL middle	10%	300 000
24	LHL middle	10%	150 000

* Although this sample (accidentally) ran to 600 000 load cycles, the wire break detector only recorded events up to 375 000 cycles

The results of the tests are given in the order listed in Table B2. The specimen numbers are in the order that the tests were carried out. The results of the 25 fatigue tests are given in Tables B6.1 to B6.25, and are shown in Figs B6.1 to B6.25.

The tables of the results give the relevant specimen information, the number of broken wires that developed during the test, the number of cracked wires counted after the tensile test, and any other observation made during the test or during the inspection of the specimen after the tensile test. Just for interest, the tensile test result give the percentage reduction in strength of the fatigue specimen compared to the new rope strength.

The graphs show the number of load cycles completed when the wire fractures were recorded. All the graphs show 300 000 load cycles and 60 broken wires. Where more broken wires occurred or where the load cycles were greater, an extra graph, showing the complete test, was included.

B7 Discussion of the fatigue tests

Tensile-tensile fatigue tests at a 10% load range for 300 000 load cycles did not produce any wire fractures or partially fatigued wires in the "used rope" samples tested.

A summary of the results of the 15% load range fatigue tests on the used rope samples is shown in Fig. B7. The results from specimen no. 2 (cleaned sample) was not included in that figure

(reasons will be given). No clear differences exist between the tests carried out on samples from the front ends, midshaft and back ends. The graph shows no evidence of increasingly poorer rope fatigue performance from front to back end samples. No clear differences exist between the left hand lay rope and the right hand lay rope samples.

A summary of the results of the 20% load range fatigue tests on the used rope samples is shown in Fig. B7.1. As with the 15% load range samples there is no evidence of increasingly poorer rope fatigue performance from the front to back end samples. Comparing Figs B7 and B7.1 shows that wires fractures were generated earlier and at a significantly greater rate during the 20% load range tests than during the 15% load range tests.

Figure B7.2 shows scatter bands of the summarised results for the 15% load range and the 20% load range tests.

A summary of the results of the 15% load range fatigue tests carried out on specimen no. 2 (cleaned sample) and the stock samples is shown in Fig. B7.3. The points to note are that the best stock sample result (at 15%) was not better than the worst used rope result (at 15%), and the worst stock sample result (at 15%) was much the same as the best used rope result at 20% load range. The stock samples behaved much the same as the used rope sample that was cleaned. The results from the stock samples and the cleaned used rope sample lie perfectly between the 15% and 20% load range scatter bands shown in Fig. B7.2.

The fractured and cracked wires of (the cleaned) Specimen no. 2 (Table B6.1 and Fig. B6.1) all originated at the inter strand contact points in the valleys between the strands. Wire fractures were generated at a significantly greater rate than in any of the other 15% load range specimens. The conclusion that is drawn from this result is that a lack of lubricant increases the fretting at inter strand contact points, which lead to a greater susceptibility to crack initiation. Specimen no. 5 was partially cleaned, i.e. the valleys between the strands were not cleaned. The fatigue performance was not inferior to any of the other "un-cleaned" specimens.

The fatigue tests on the stock samples were carried out approximately eight years after the ropes were manufactured. The most probable reason for the relatively poor fatigue performance of the stock samples was poor lubrication. The rope ends from which stock samples are obtained are generally only lubricated internally, and are not lubricated externally during closing of the rope. The lubricant that was present in the rope could also have dried out during the eight years in storage. The poor lubricated state of the stock samples then led to increased fretting at the inter strand contact points during the fatigue tests. All the broken and cracked wires of the stock samples originated at the inter strand contact points.

Poorly lubricated or "dry" ropes will therefore have significantly inferior fatigue performance compared to well lubricated ropes. This fact had been mentioned by Haggie (the rope manufacturer) at a meeting of their "Rope Development Group" some years ago.

Very few crown wires fractured during the fatigue tests. Excluding the tests carried out on the stock samples, the used rope samples developed a total of 362 wire fractures during the fatigue tests. Only six were crown wires (less than 2%). All other fractures originated at the inter strand contact points. The degree of surface deterioration of the ropes (front, middle and back end samples) therefore did not have any significant influence on the generation of wire fractures. This confirms the earlier mentioned fact that no evidence could be found of increasingly poorer rope fatigue performance from front to back end samples.

Of the 344 partially fatigued (cracked) wires found upon completion of the fatigue tests on the used ropes, only 10% were crown wires. Three possible conclusions could be drawn from this:

One: While in service very few cracks were initiated in the wires at the strand crowns in a

direction crosswise to the rope wires. If such cracks were present at the start of a fatigue test, they should have been able to propagate into fractured wires.

Two: Cracks, lengthwise to the wire directions, could have been present in the wires at the strand crowns at the start of the fatigue tests. The load ranges and number of load cycles to which the rope samples were subjected during the fatigue tests were only of sufficient magnitude in a very few cases to turn such a crack through 90° and then to propagate the crack to some extent.

Three: The flattening of the crown wires could have induced compressive residual stresses in the wires, requiring larger load ranges to initiate fatigue cracks. Therefore the small percentage of crown wires that did develop cracks and fractures.

It should further be kept in mind that each fatigue test specimen had approximately 360 crown wires and 660 inter strand fretting points at which cracks could initiate. In a relatively small percentage of the available initiation points did cracks actually originate.

The used rope samples showed visible indentations at the inter strand contact points (generally referred to as nicking). Crack initiation during the fatigue tests started at the nicks in most cases.

The stock samples, which were of course never in operation on a winder, had no visible nicking at the inter strand contact points. However, the cracks in the wires of the stock samples also originated at the inter strand contact points during the fatigue tests. It therefore seems that crack initiation is a result of fretting, and not of nicking.

The one front end sample that was cleaned before the fatigue test (Specimen no. 2) was identical to the other front end samples in all other respects (laylength, inter strand nicking). Specimen no. 2, however, already had ten broken wires after 150 000 load cycles, while the other samples only started to develop broken wires after around 150 000 load cycles. It was deduced that lack of lubrication on Specimen no. 2 increased the fretting action at the inter strand contact points, and increased the susceptibility of the wires to fatigue crack initiation. This further suggests that crack initiation is more a result of fretting than merely a result of the presence of nicks on the wires.

With hindsight: It would have been of interest if fatigue tests were also carried out on "cleaned" rope samples at load ranges of 10% and 12%.

Table B6.1: Results of the fatigue test on specimen no. 2

Type: Left hand lay	Front	Load range = 15%
Load cycles completed:	157 161	Tensile test = -17%
Number of broken wires:	10	
Number of cracked wires:	25	
The specimen was **cleaned** during preparation, i.e. all visible lubrication (rope grease) removed. The broken wires were counted manually during the fatigue test. The broken wires originated from **inter strand contact** points. During the tensile test one strand failed completely at 66% of the new rope breaking strength.		

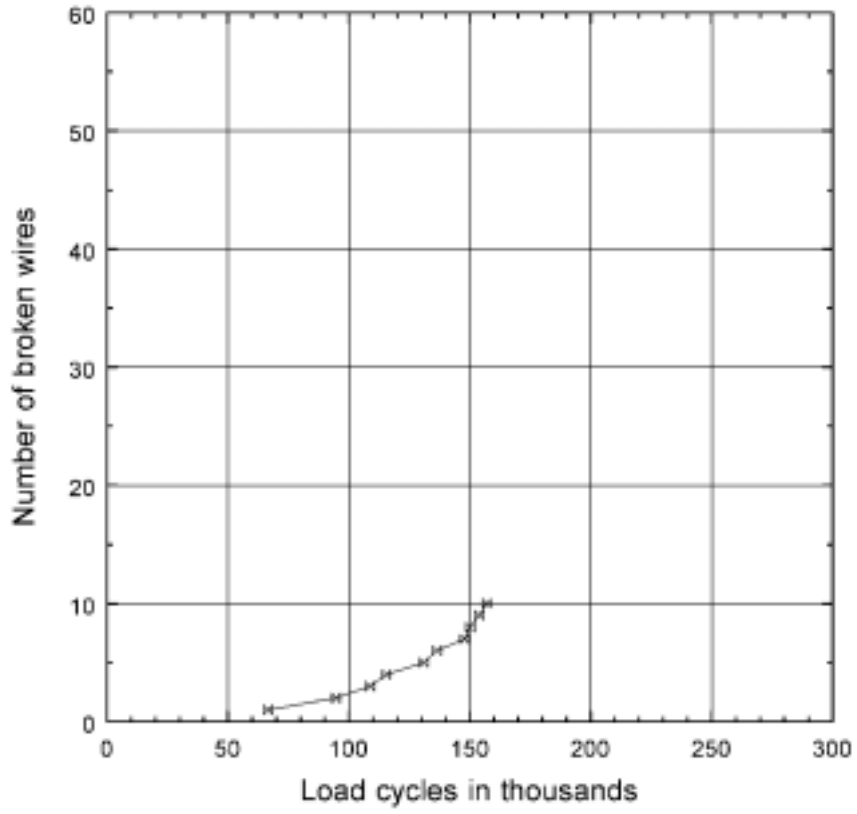

Figure B6.1: Specimen no. 2: Load cycles at which broken wires occurred.

Table B6.2: Results of the fatigue test on specimen no. 3

Type: Left hand lay	Front	Load range = 15%
Load cycles completed:	300 337	Tensile test = -9%
Number of broken wires:	6	
Number of cracked wires:	4	
The broken wires were counted manually during the fatigue test. The number of broken wires registered during the fatigue test included **one crown wire**. The cracked wires included one crown wire. The tensile test fracture occurred inside the one rope termination.		

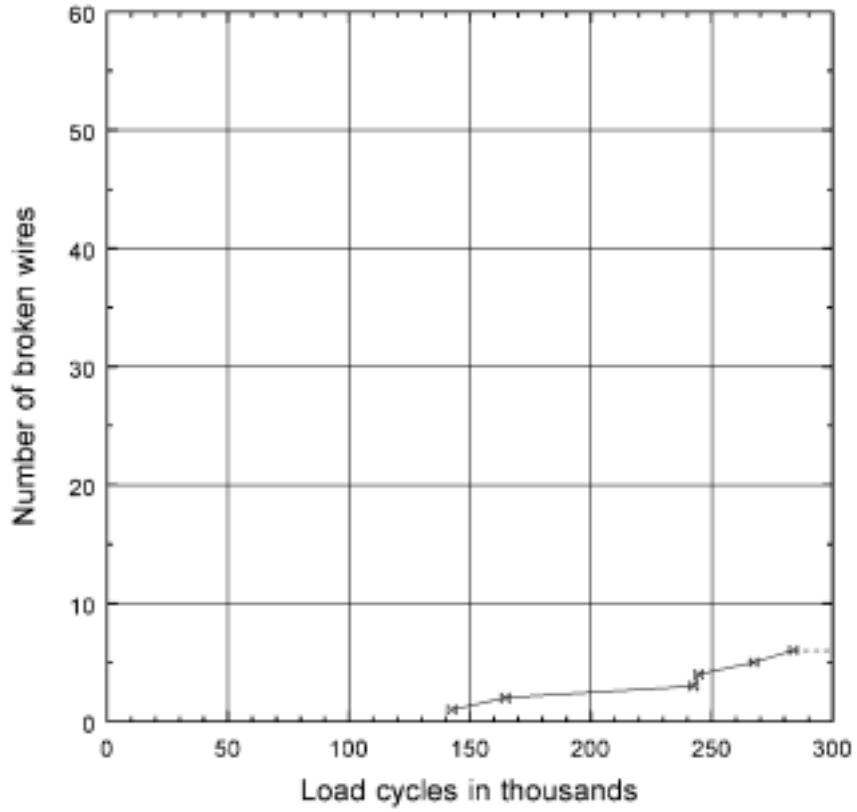

Figure B6.2: Specimen no. 3: Load cycles at which broken wires occurred.

Table B6.3: Results of the fatigue test on specimen no. 4

Type: Right hand lay	Front	Load range = 15%
Load cycles completed:	622 472	Tensile test = -24%
Number of broken wires:	11 at 375 000 cycles	
Number of cracked wires:	see notes	
The fatigue test was carried out for an **extended number of cycles**. The wire break detector stopped operating at 375 000 cycles. During the inspection after the tensile test, 25 outer fatigued wires and 11 inner fatigued wires were counted. The outer wires that were fatigued included **one crown wire**. An additional 16 outer cracked wires and 5 inner cracked wires fractured during the tensile test. Also see the additional graph on the next page. During the tensile test one strand failed completely at 40% of the new rope breaking strength.		

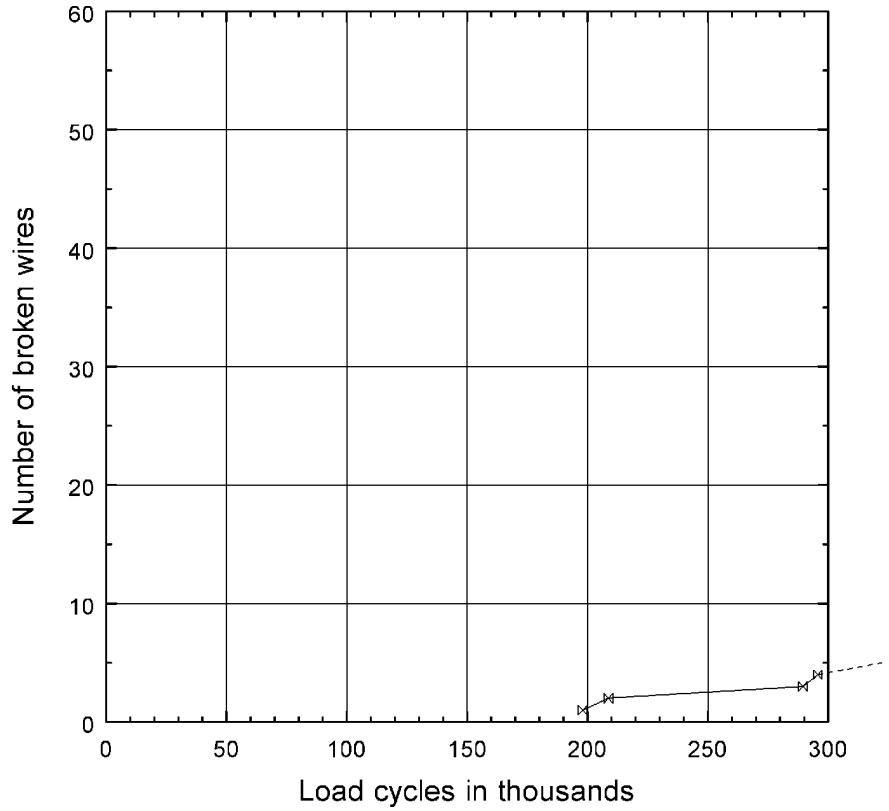

Figure B6.3: Specimen no. 4: Load cycles at which broken wires occurred.

The occurrence of broken wires in specimen no. 4 were registered until 375 000 cycles were completed. The figure below shows when they occurred.

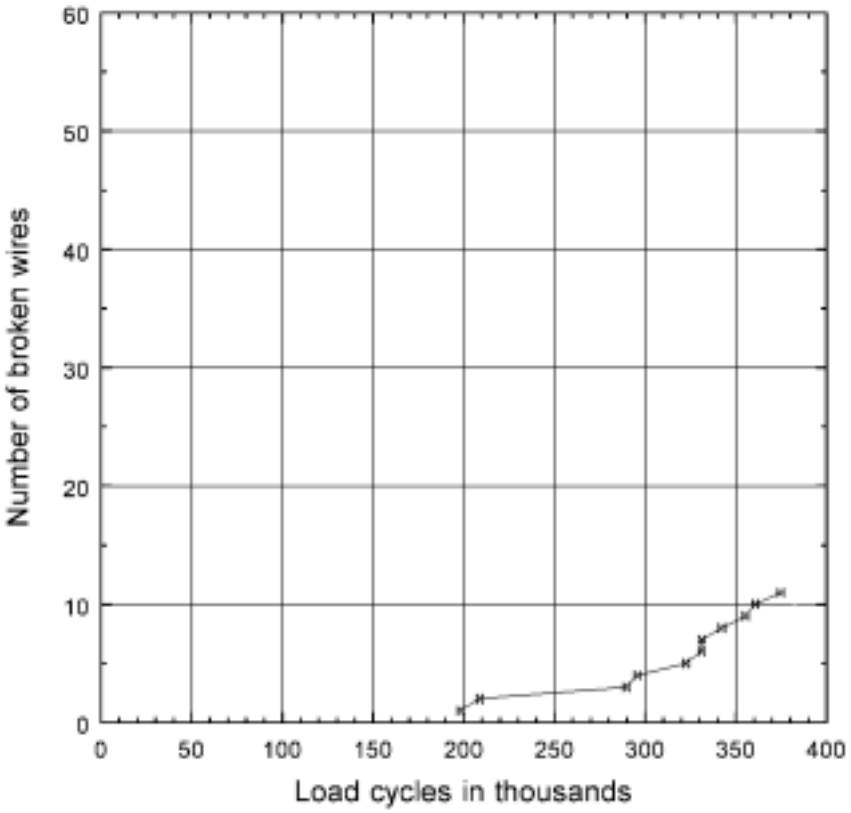

Figure B6.4: Specimen no. 4: Load cycles at which broken wires occurred.

Table B6.4: Results of the fatigue test on specimen no. 5

Type: Right hand lay	Front	Load range = 15%
Load cycles completed: Number of broken wires: Number of cracked wires:	300 315 8 4	Tensile test = -9%
The specimen was partially cleaned during preparation. The broken wires included **two crown wires**. One broken wire occurred at one of the terminations. The tensile test fracture occurred at one of the end caps.		

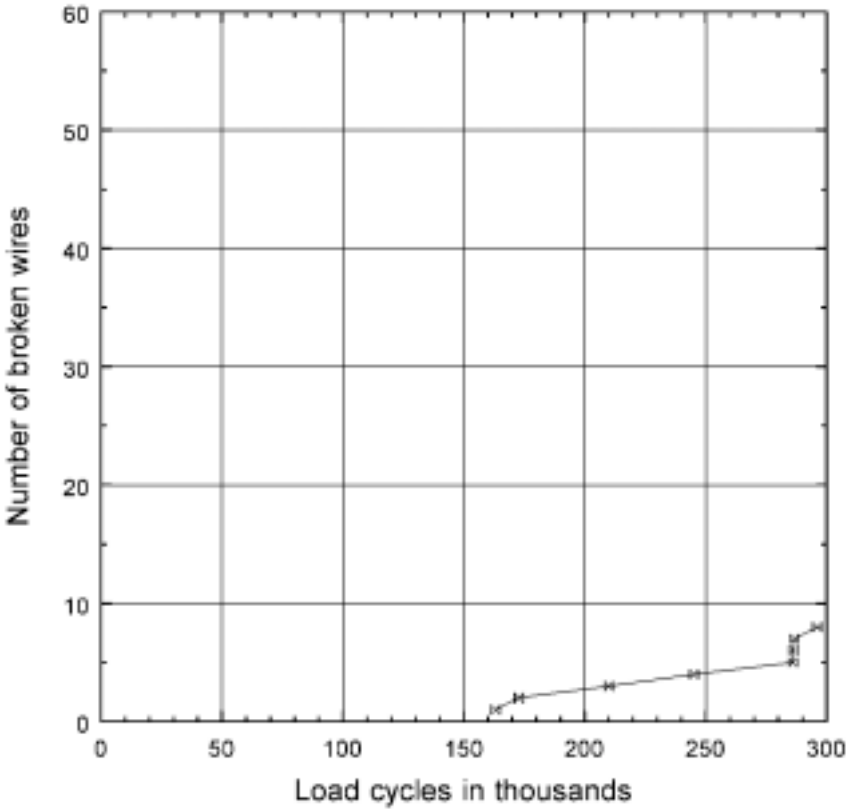

Figure B6.5: Specimen no. 5: Load cycles at which broken wires occurred.

Table B6.5: Results of the fatigue test on specimen no. 6

Type: Left hand lay	Midshaft	Load range = 15%
Load cycles completed: Number of broken wires: Number of cracked wires:	300 000 22 7	Tensile test = -17%
Three crown wires developed (partial) cracks during the fatigue test. During the tensile test, ons strand failed completely at 52% of the new rope breaking strength.		

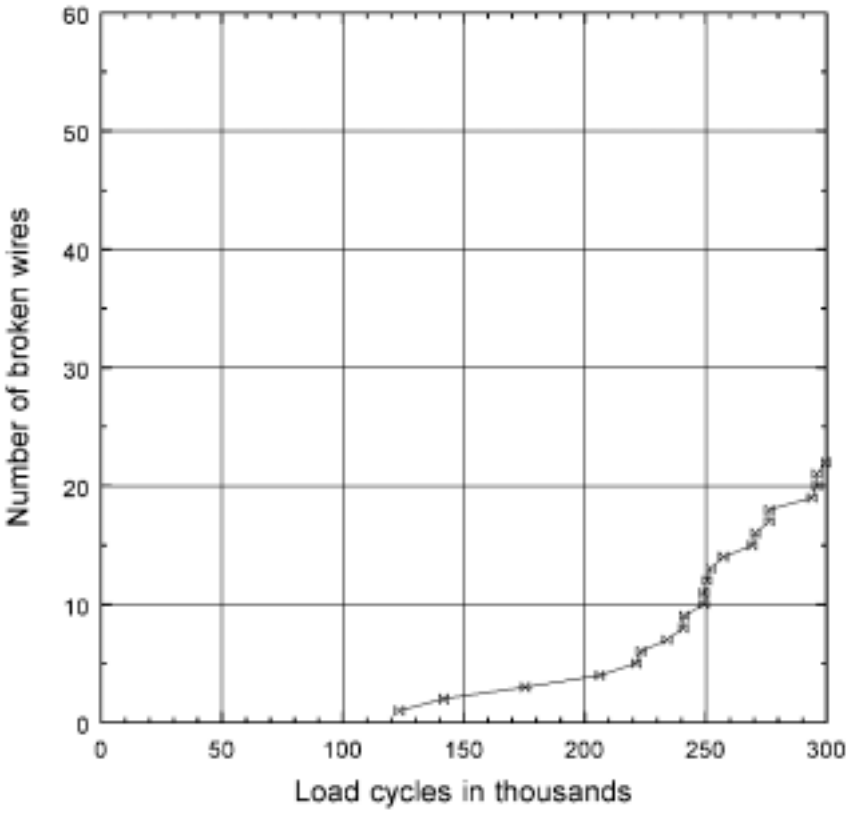

Figure B6.6: Specimen no. 6: Load cycles at which broken wires occurred.

Table B6.6: Results of the fatigue test on specimen no. 8

Type: Left hand lay	Midshaft	Load range = 15%
Load cycles completed: Number of broken wires: Number of cracked wires:	300 031 33 13	Tensile test = -25%
Two crown wires developed (partial) cracks during the fatigue test. During the tensile test, one strand failed completely at 67% of the new rope breaking strength.		

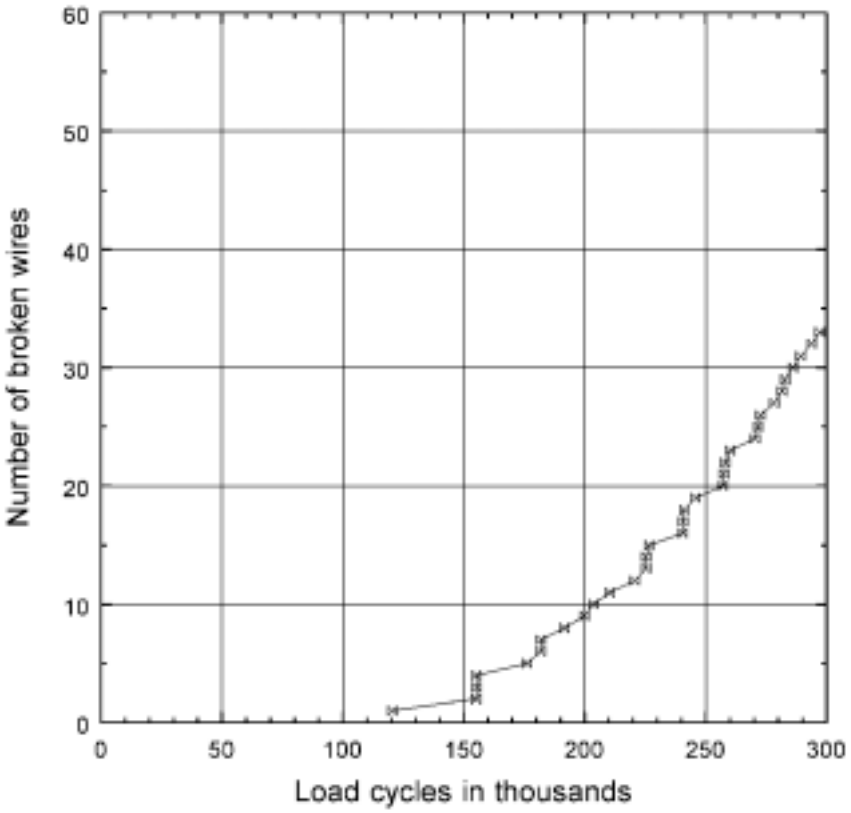

Figure B6.7: Specimen no. 8: Load cycles at which broken wires occurred.

Table B6.7: Results of the fatigue test on specimen no. 7

Type: Right hand lay	Midshaft	Load range = 15%
Load cycles completed: Number of broken wires: Number of cracked wires:	300 000 14 22	Tensile test = -17%
During the tensile test, one strand failed completely at 71% of the new rope breaking strength.		

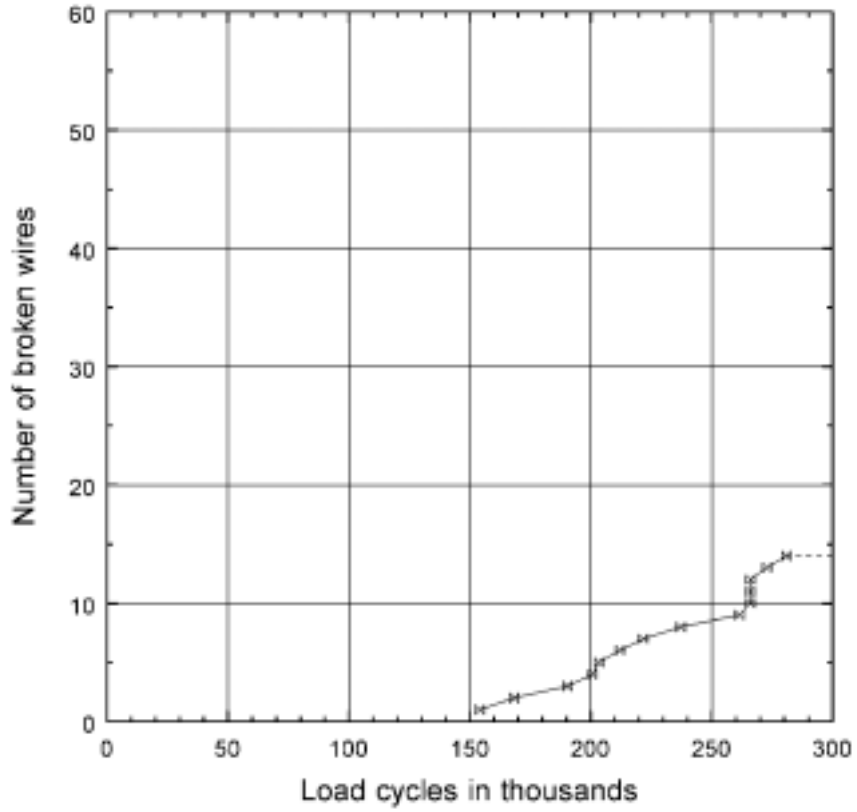

Figure B6.8: Specimen no. 7: Load cycles at which broken wires occurred.

Table B6.8: Results of the fatigue test on specimen no. 9

Type: Right hand lay	Midshaft	Load range = 15%
Load cycles completed:	290 000	Tensile test = -11%
Number of broken wires:	5	
Number of cracked wires:	14	
Testing machine problems were experienced during this fatigue test. The test was interrupted several times, at which the load on the specimen reduced to zero. Three crown wires developed (partial) cracks during the fatigue test.		

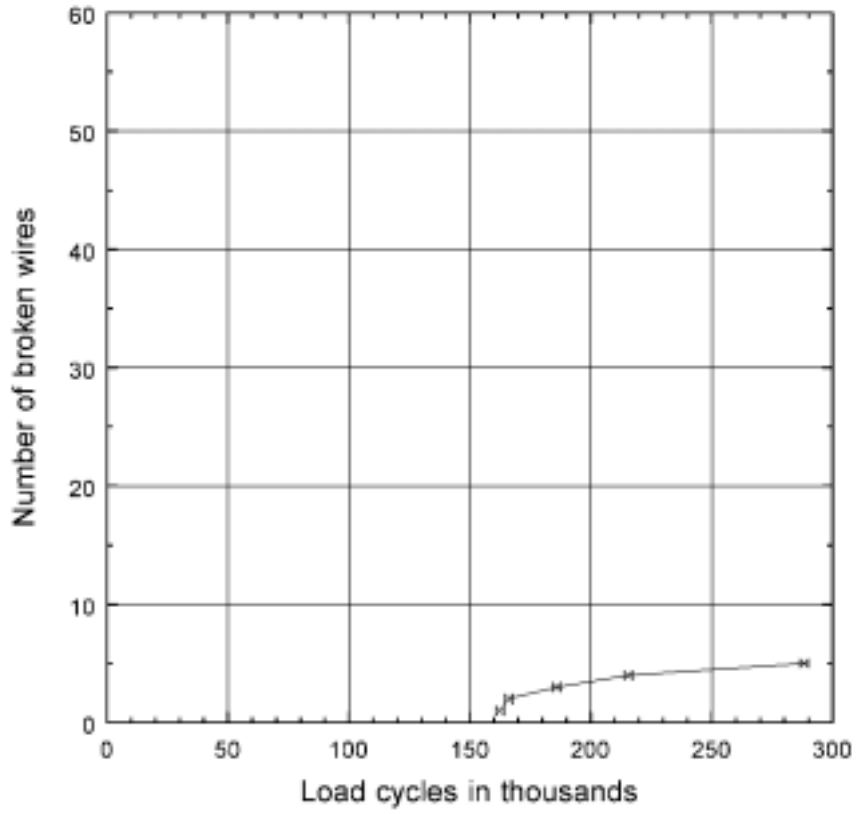

Figure B6.9: Specimen no. 9: Load cycles at which broken wires occurred.

Table B6.9: Results of the fatigue test on specimen no. 12

Type: Left hand lay	Back	Load range = 15%
Load cycles completed: Number of broken wires: Number of cracked wires:	300 000 24 30	Tensile test = -19%
Three crown wires developed (partial) cracks during the fatigue test.		

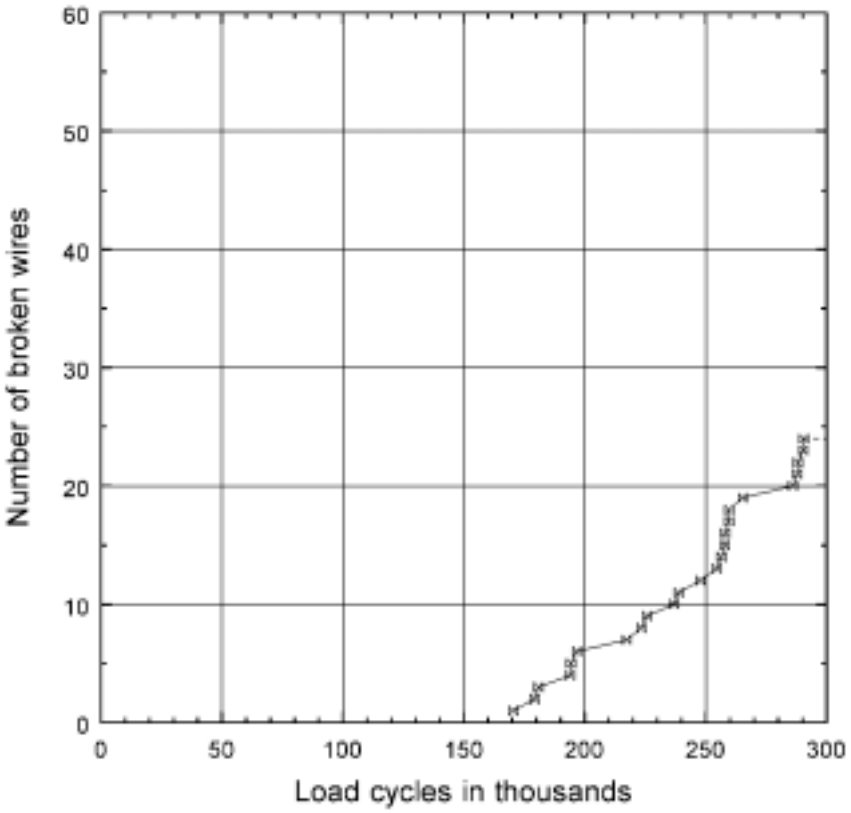

Figure B6.10: Specimen no. 12: Load cycles at which broken wires occurred.

Table B6.10: Results of the fatigue test on specimen no. 13

Type: Left hand lay	Back	Load range = 15%
Load cycles completed: Number of broken wires: Number of cracked wires:	300 000 18 25	Tensile test = -15%

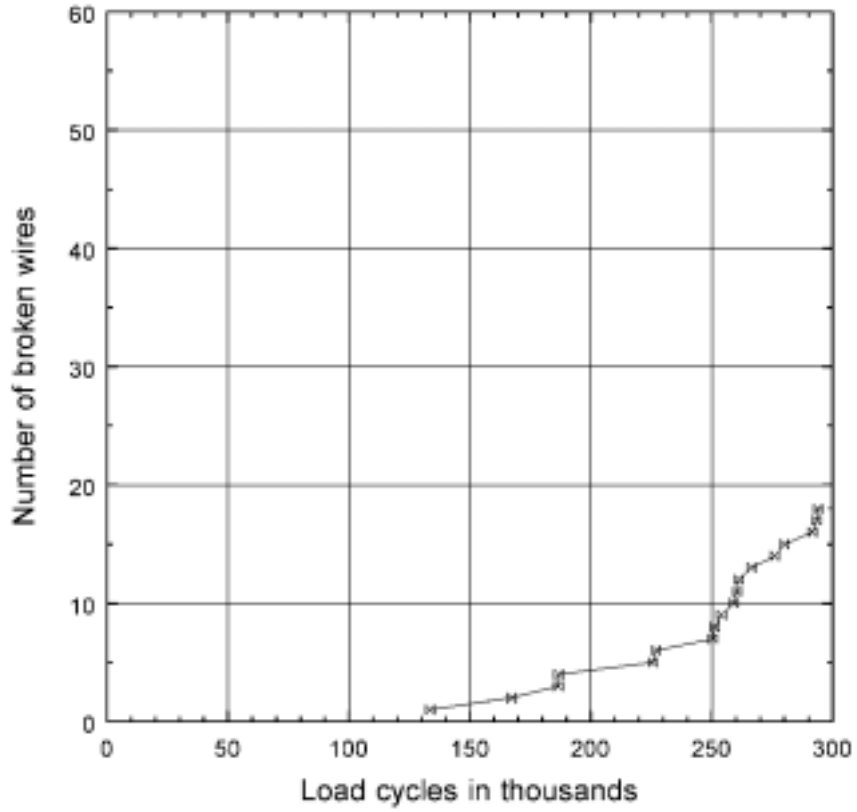

Figure B6.11: Specimen no. 13: Load cycles at which broken wires occurred.

Table B6.11: Results of the fatigue test on specimen no. 10

Type: Right hand lay	Back	Load range = 15%
Load cycles completed: Number of broken wires: Number of cracked wires:	300 000 2 14	Tensile test = -8%
The fatigue test was interrupted for a short time at 150 000 cycles. The two broken wires occurred close together at 279 228 cycles and 279 268 cycles. One crown wire developed a (partial) crack during the fatigue test.		

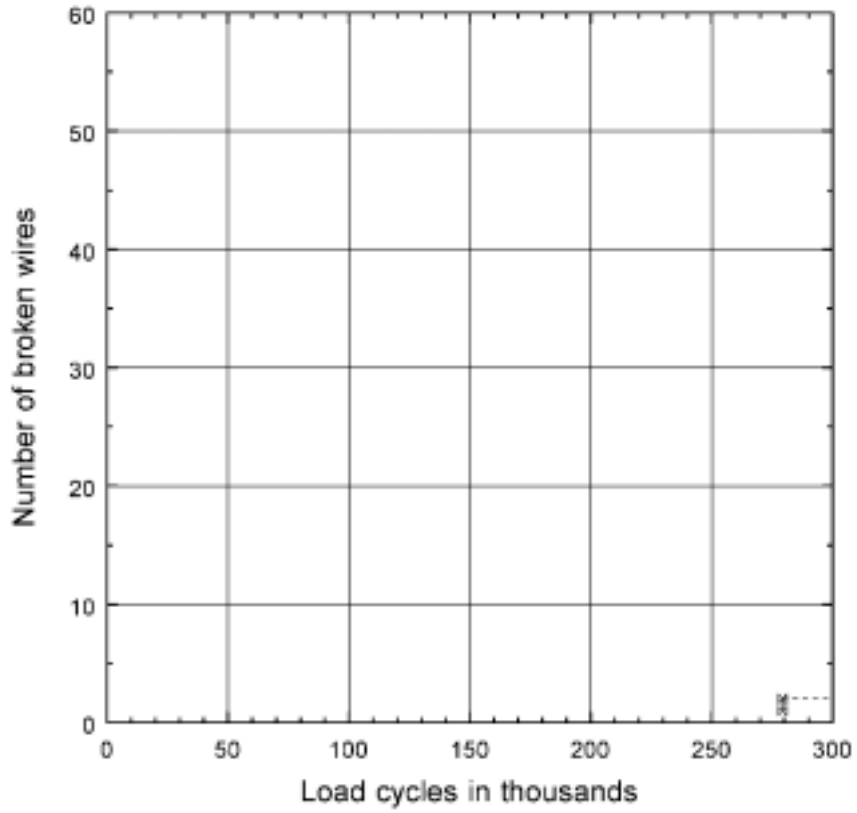

Figure B6.12: Specimen no. 10: Load cycles at which broken wires occurred.

Table B6.12: Results of the fatigue test on specimen no. 11

Type: Right hand lay	Back	Load range = 15%
Load cycles completed: Number of broken wires: Number of cracked wires:	300 000 14 13	Tensile test = -9%
Nine crown wires developed (partial) cracks during the fatigue test.		

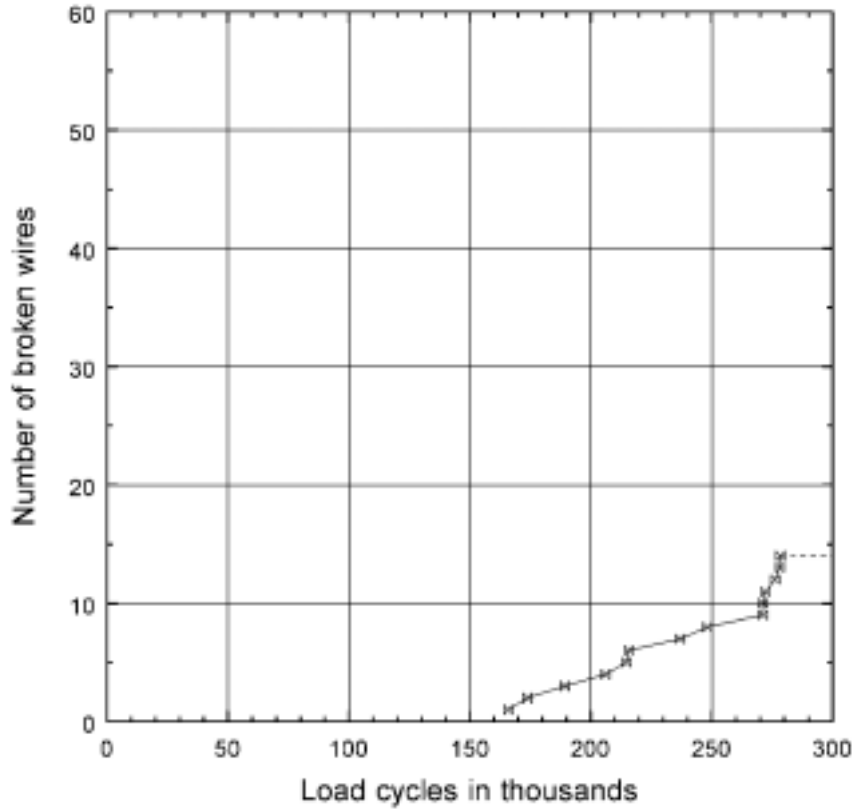

Figure B6.13: Specimen no. 11: Load cycles at which broken wires occurred.

Table B6.13: Results of the fatigue test on specimen no. 18

Type: Left hand lay	Front	Load range = 20%
Load cycles completed:	178 691	Tensile test = -46%
Number of broken wires:	94	
Number of cracked wires:	29	
A few inner strand wires developed (partial) cracks during the fatigue test. It is of interest that no crown wires broke during the fatigue test, or developed cracks large enough to fail during the tensile test. In two separate sections of wire, a second crack developed 20 mm away from the one that broke completely during the fatigue test. In both cases the second cracks had propagated more than 50% through the wire, and failed during the tensile test. Also see the additional graph on the next page.		

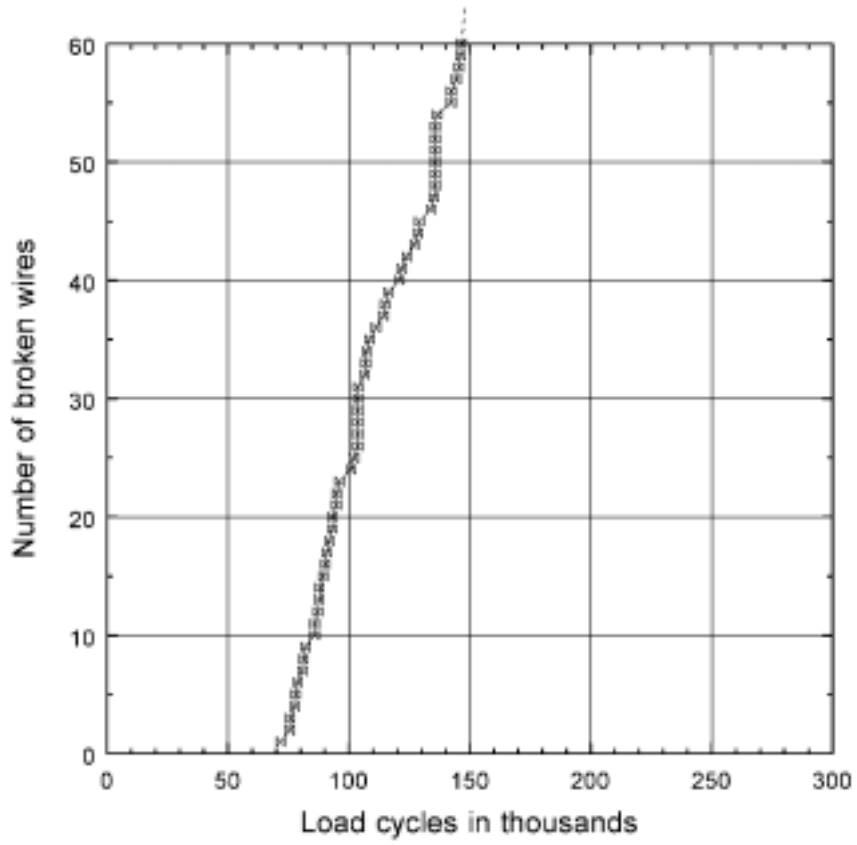

Figure B6.14: Specimen no. 18: Load cycles at which broken wires occurred.

Additional graph for specimen no. 18.

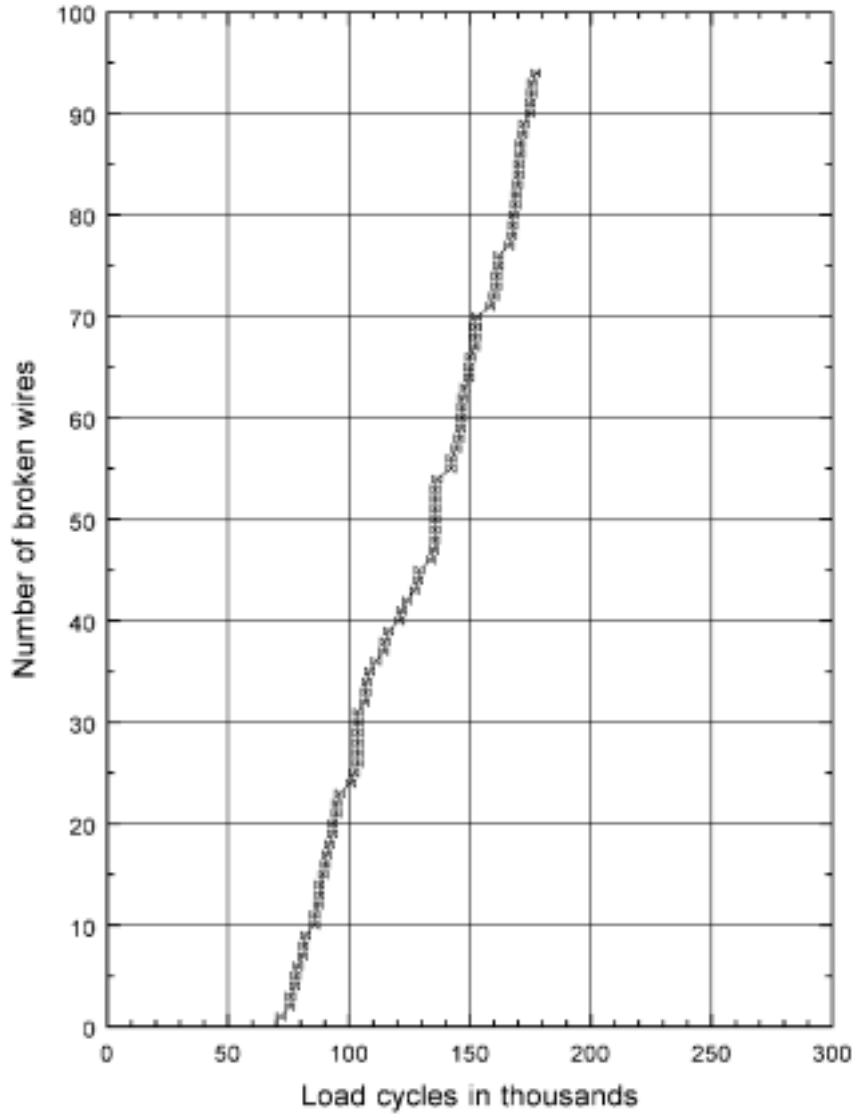

Figure B6.15: Specimen no. 18: Load cycles at which broken wires occurred.

Table B6.14: Results of the fatigue test on specimen no. 17

Type: Right hand lay	Front	Load range = 20%
Load cycles completed:	150 000	Tensile test = -13%
Number of broken wires:	14	
Number of cracked wires:	22	

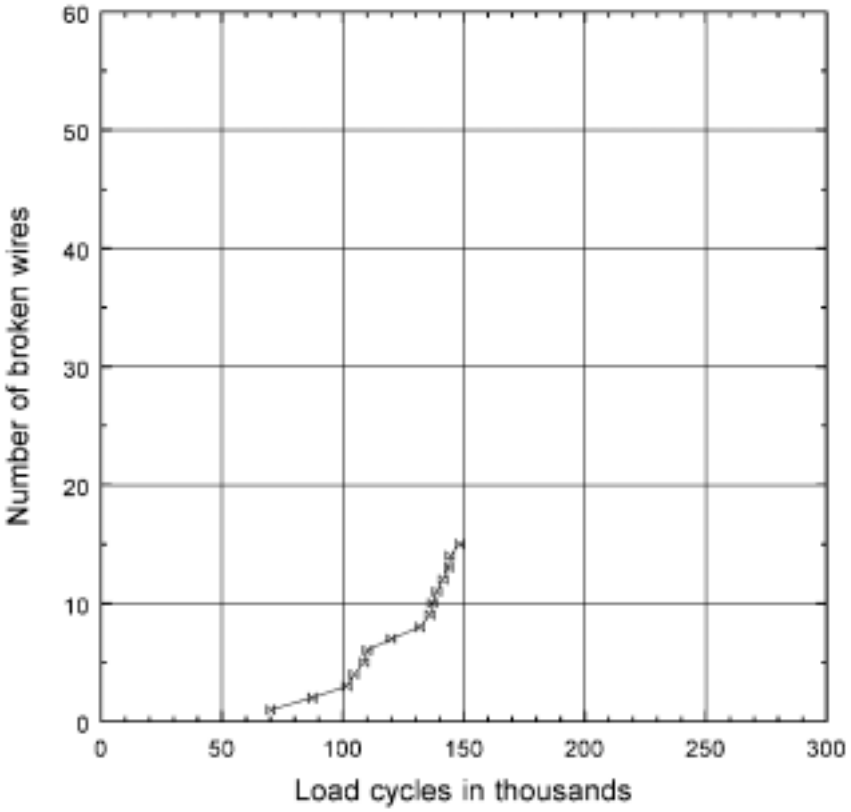

Figure B6.16: Specimen no. 17: Load cycles at which broken wires occurred.

Table B6.15: Results of the fatigue test on specimen no. 16

Type: Left hand lay	Midshaft	Load range = 20%
Load cycles completed: Number of broken wires: Number of cracked wires:	150 000 44 44	Tensile test = -27%
Two crown wires broke during the fatigue test. Ten other crown wires developed (partial) cracks during the fatigue test.		

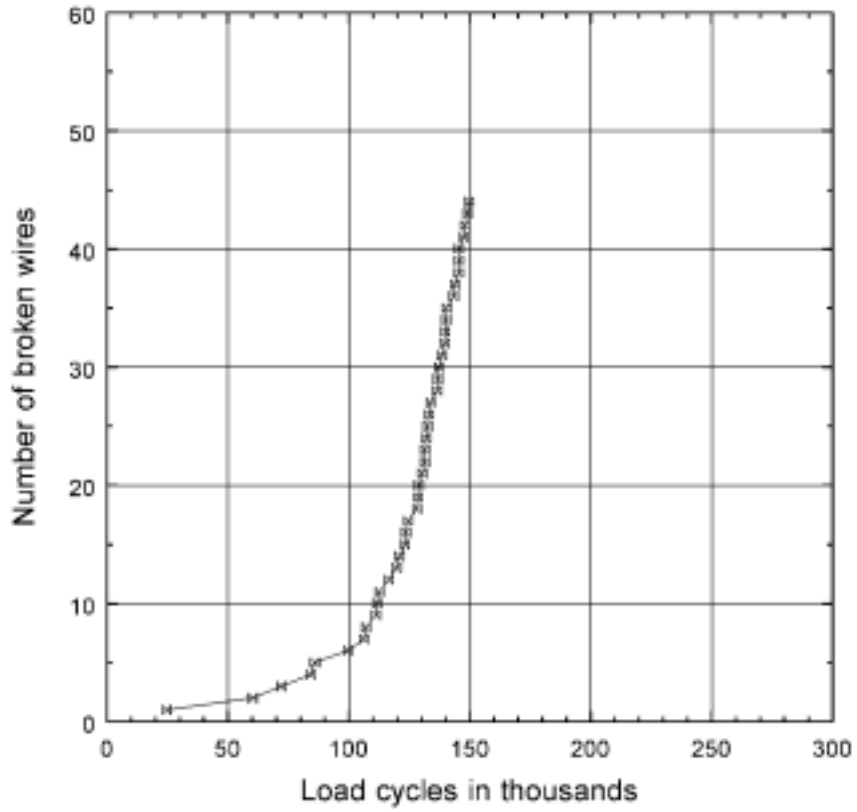

Figure B6.17: Specimen no. 16: Load cycles at which broken wires occurred.

Table B6.16: Results of the fatigue test on specimen no. 14

Type: Right hand lay	Midshaft	Load range = 20%
Load cycles completed: Number of broken wires: Number of cracked wires:	150 832 10 43	Tensile test = -13%
Seven crown wires developed (partial) cracks during the fatigue test.		

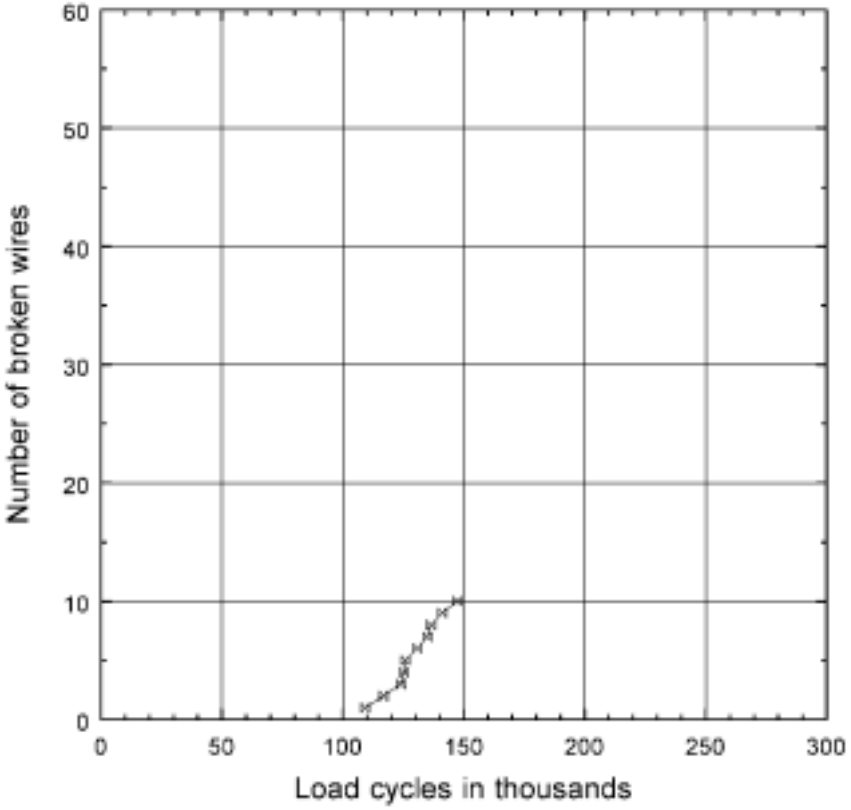

Figure B6.18: Specimen no. 14: Load cycles at which broken wires occurred.

Table B6.17: Results of the fatigue test on specimen no. 19

Type: Left hand lay	Back	Load range = 20%
Load cycles completed: Number of broken wires: Number of cracked wires:	150 000 28 25	Tensile test = -30%

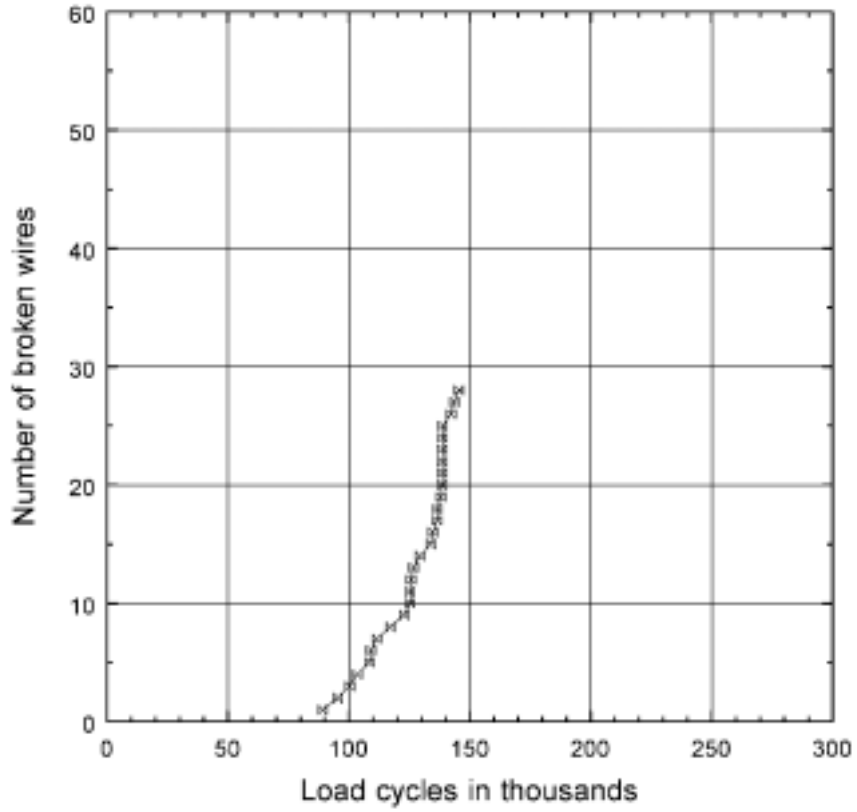

Figure B6.19: Specimen no. 19: Load cycles at which broken wires occurred.

Table B6.18: Results of the fatigue test on specimen no. 15

Type: Right hand lay	Back	Load range = 20%
Load cycles completed: Number of broken wires: Number of cracked wires:	135 234 5 10	Tensile test = -8%
Testing machine problems interrupted the fatigue test a number of times. The test was terminated just after 135 000 cycles. Seven crown wires developed (partial) cracks during the fatigue test.		

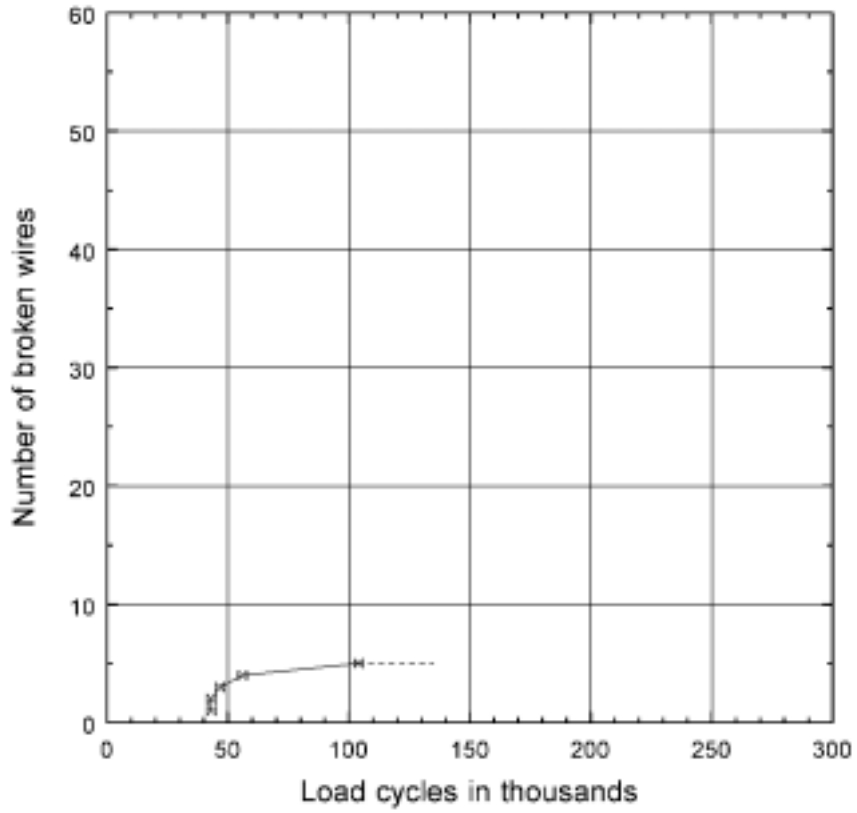

Figure B6.20: Specimen no. 15: Load cycles at which broken wires occurred.

Table B6.19: Results of the fatigue test on specimen no. 21

Type: Left hand lay	Stock sample	Load range = 15%
Load cycles completed: Number of broken wires: Number of cracked wires:	300 000 31 24	Tensile test = -18%
During the tensile test, one strand failed completely at 78% of the new rope breaking strength.		

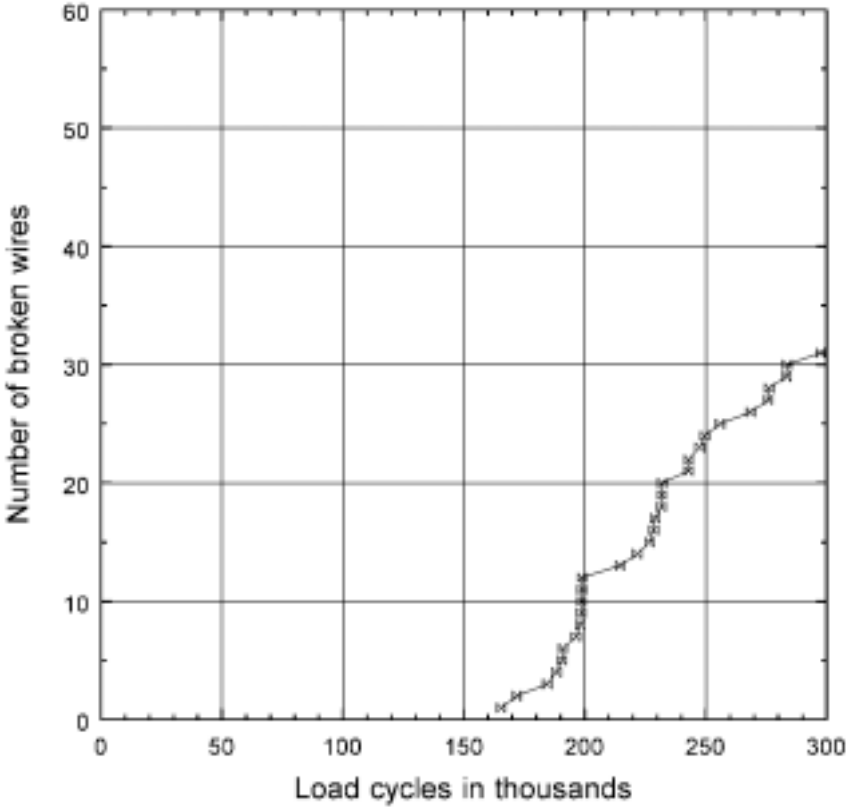

Figure B6.21: Specimen no. 21: Load cycles at which broken wires occurred.

Table B6.20: Results of the fatigue test on specimen no. 26

Type: Left hand lay	Stock sample	Load range = 15%
Load cycles completed: Number of broken wires: Number of cracked wires:	300 000 54 32	Tensile test = -34%
The load-elongation graph of the tensile test showed that one strand could have failed completely at 23% of the new rope breaking strength.		

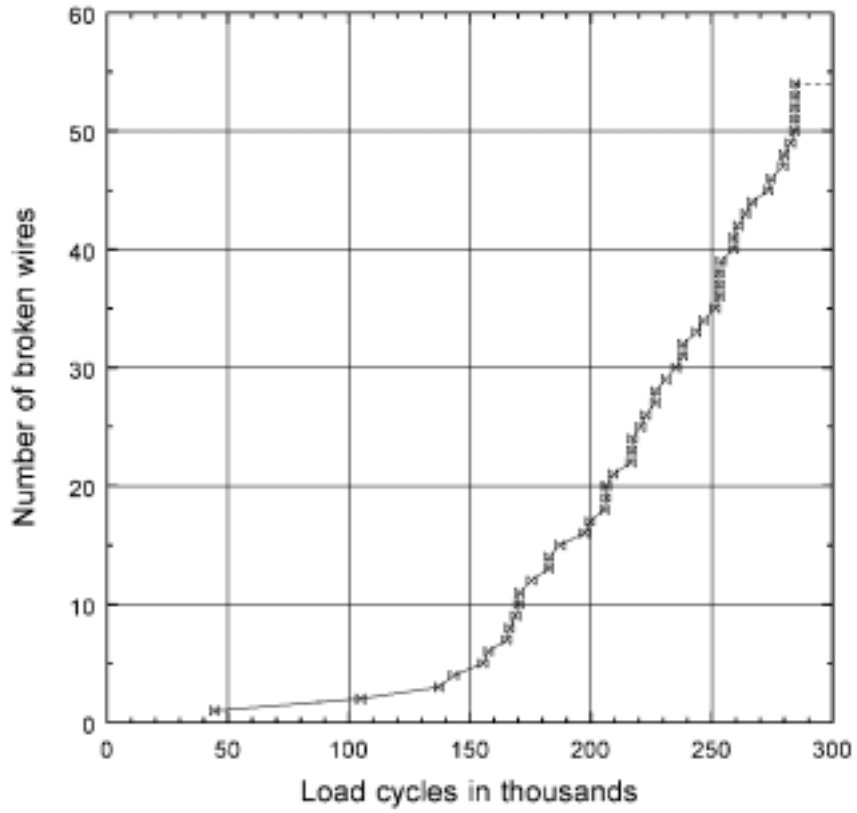

Figure B6.22: Specimen no. 26: Load cycles at which broken wires occurred.

Table B6.21: Results of the fatigue test on specimen no. 23

Type: Right hand lay	Stock sample	Load range = 15%
Load cycles completed:	300 000	Tensile test = -35%
Number of broken wires:	64	
Number of cracked wires:	33	
In one wire, a second crack developed 10 mm away from one of the fatigue fractures. The second crack had propagated 50% through the wire, and failed during the tensile test!		

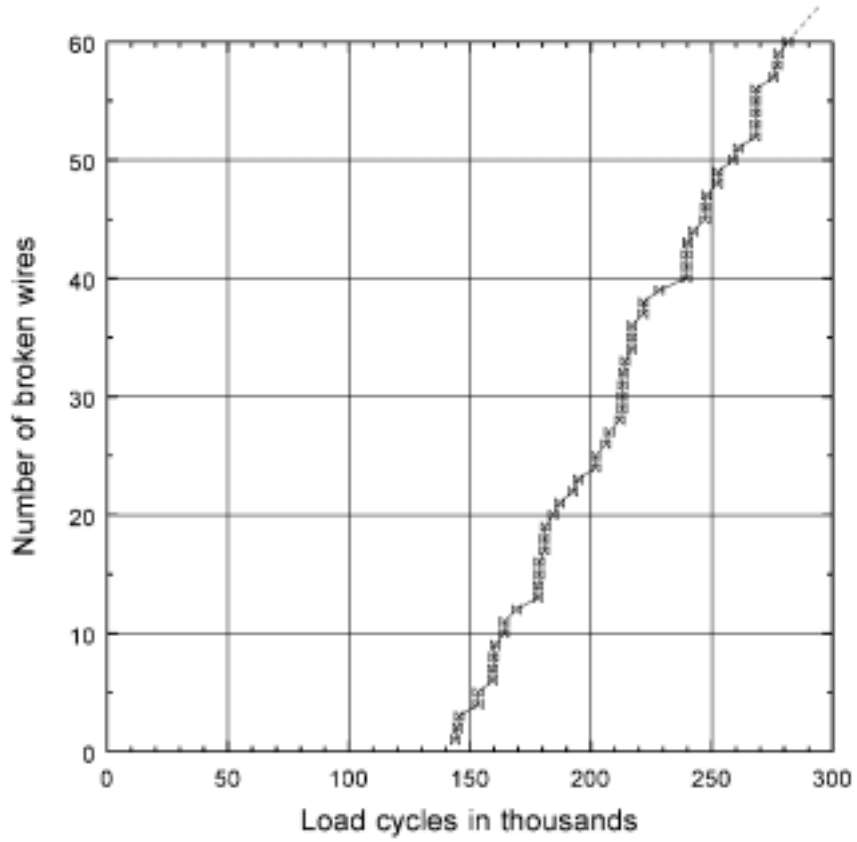

Figure B6.23: Specimen no. 23: Load cycles at which broken wires occurred.

Table B6.22: Results of the fatigue test on specimen no. 25

Type: Right hand lay	Stock sample	Load range = 15%
Load cycles completed: Number of broken wires: Number of cracked wires:	300 000 98 not counted	Tensile test not carried out
A tensile test was not carried out after the fatigue test because this specimen was used to determine the effectiveness of the broken wire detector. The number of cracked wires could therefore also not be determined. Also see the additional graph on the next page.		

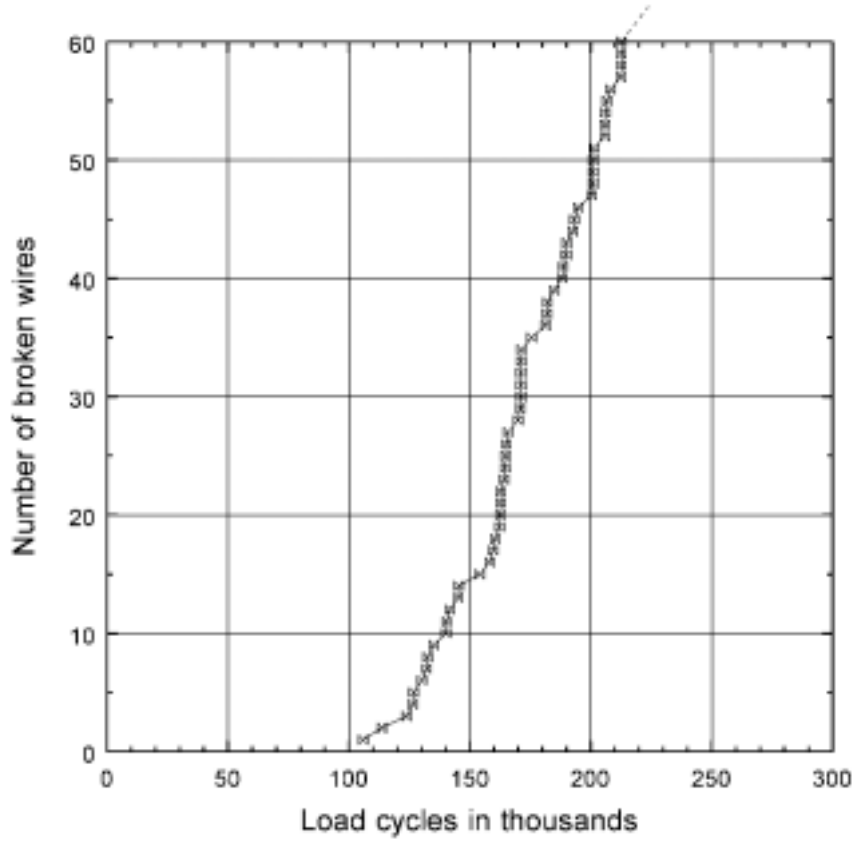

Figure B1.24: Specimen no. 25: Load cycles at which broken wires occurred.

Additional graph for specimen no. 25 to show the total number of broken wires.

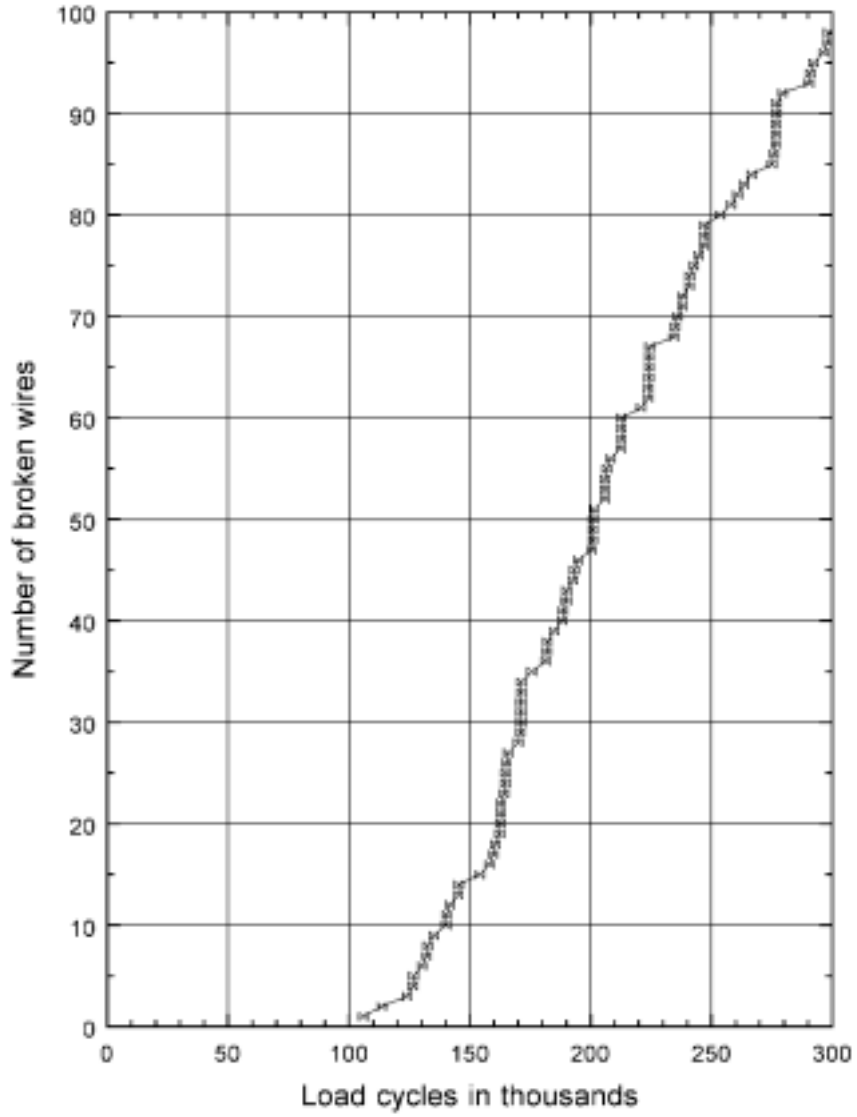

Figure B1.25: Specimen no. 25: Load cycles at which broken wires occurred.

Table B6.23: Results of the fatigue test on specimen no. 20

Type: Left hand lay	Back	Load range = 10%
Load cycles completed:	300 000	Tensile test = -5%
Number of broken wires:	0	
Number of cracked wires:	0	

Table B6.24: Results of the fatigue test on specimen no. 22

Type: Right hand lay	Midshaft	Load range = 10%
Load cycles completed:	300 000	Tensile test = -7%
Number of broken wires:	0	
Number of cracked wires:	0	
The tensile test failure occurred at the one rope termination.		

Table B6.25: Results of the fatigue test on specimen no. 24

Type: Left hand lay	Midshaft	Load range = 10%
Load cycles completed:	150 000	Tensile test = -11%
Number of broken wires:	1	
Number of cracked wires:	0	
Only one wire broke during the fatigue test, and it occurred as soon as 1 492 load cycles after the start of the test. This wire most probably already had a large crack at the start of the test. There were also two other broken wires in the specimen at the start of the test. During the tensile test, the one termination pulled out halfway, and subsequent failure occurred inside this termination, which is the cause of the 11% reduction in breaking strength.		

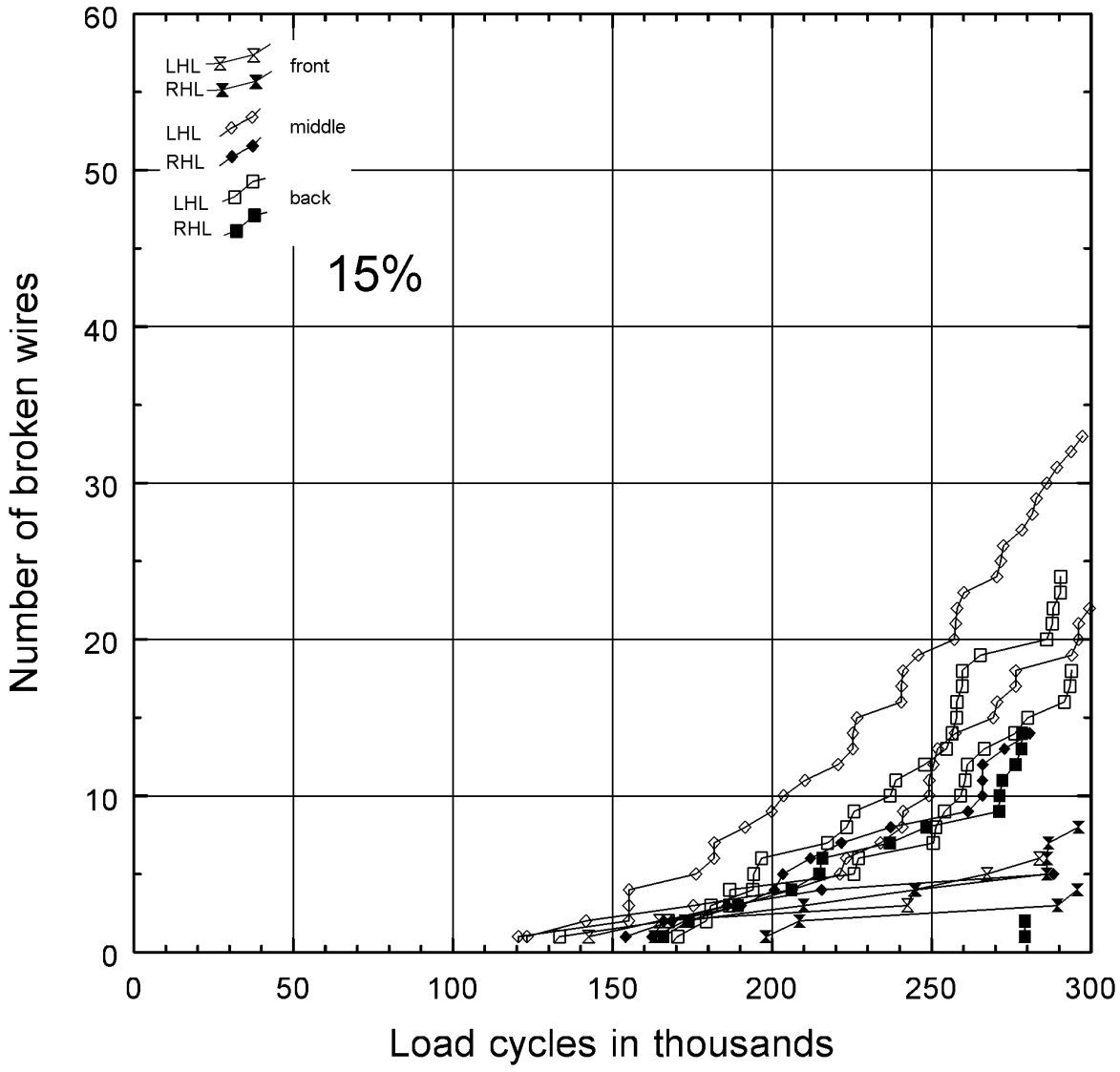

Figure B7: ***Summary of the results of the 15% load range fatigue tests.***

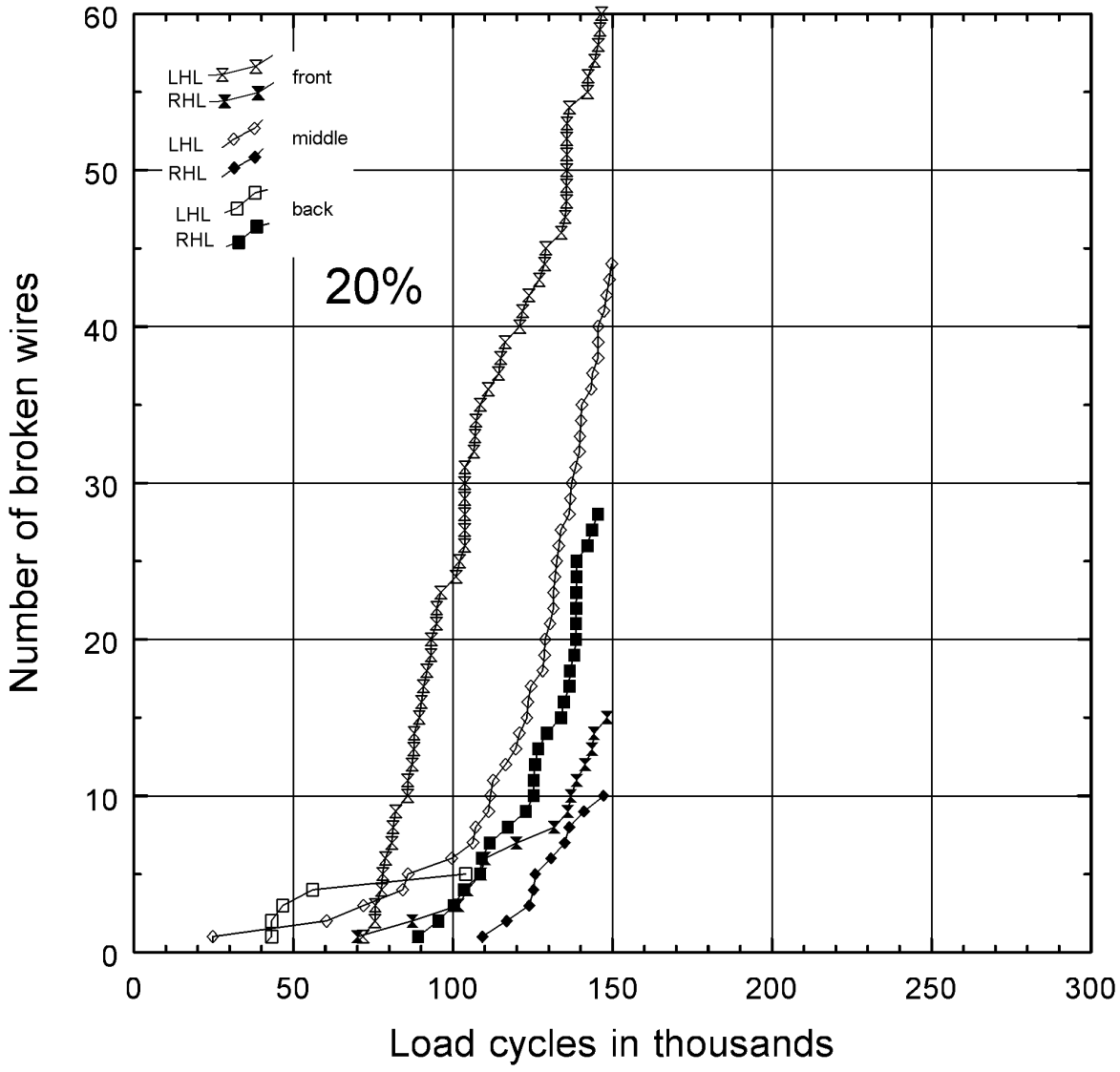

Figure B7.1: Summary of the results of the 20% load range fatigue tests.

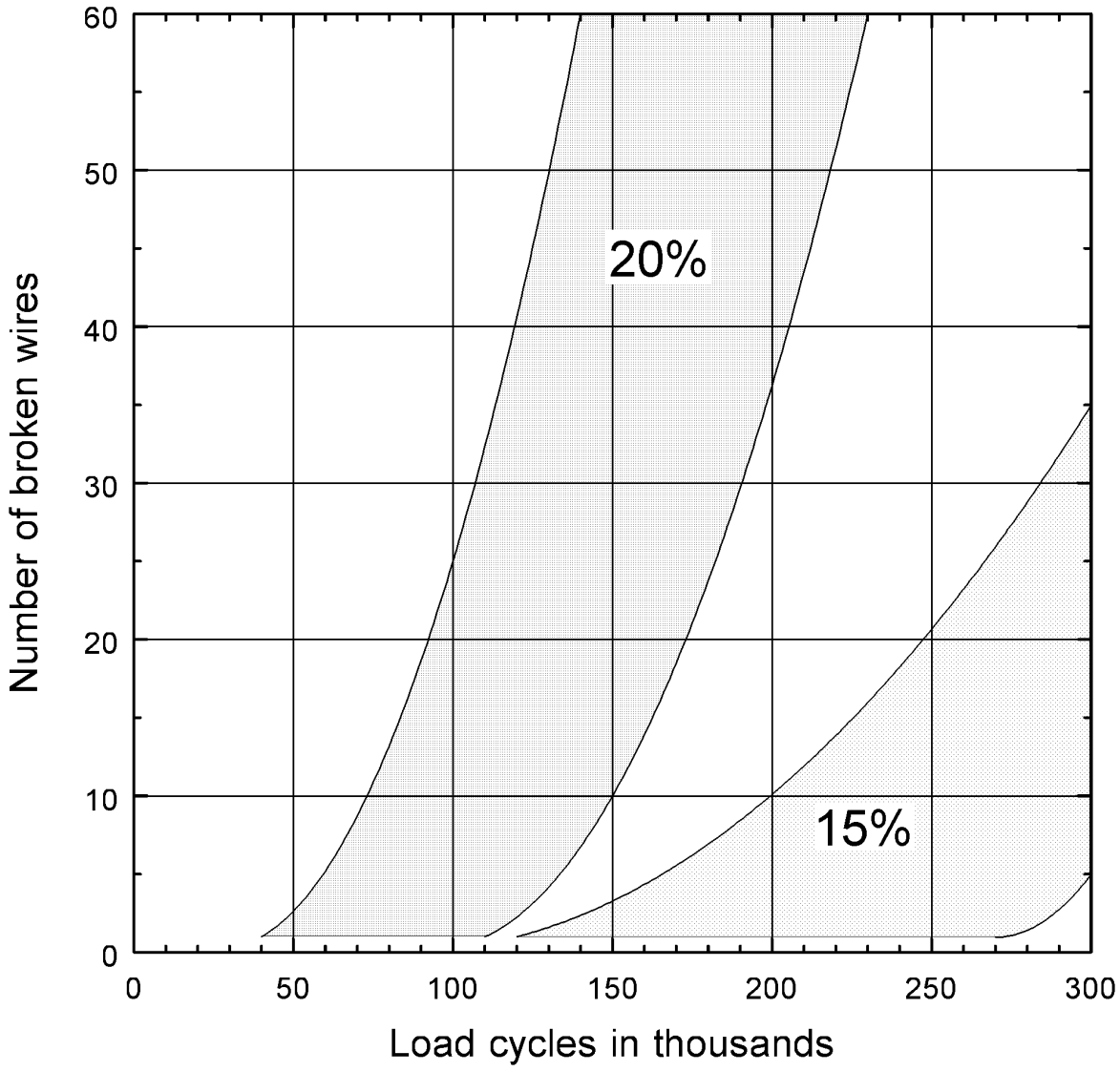

Figure B7.2: Scatter bands of the fatigue test results.

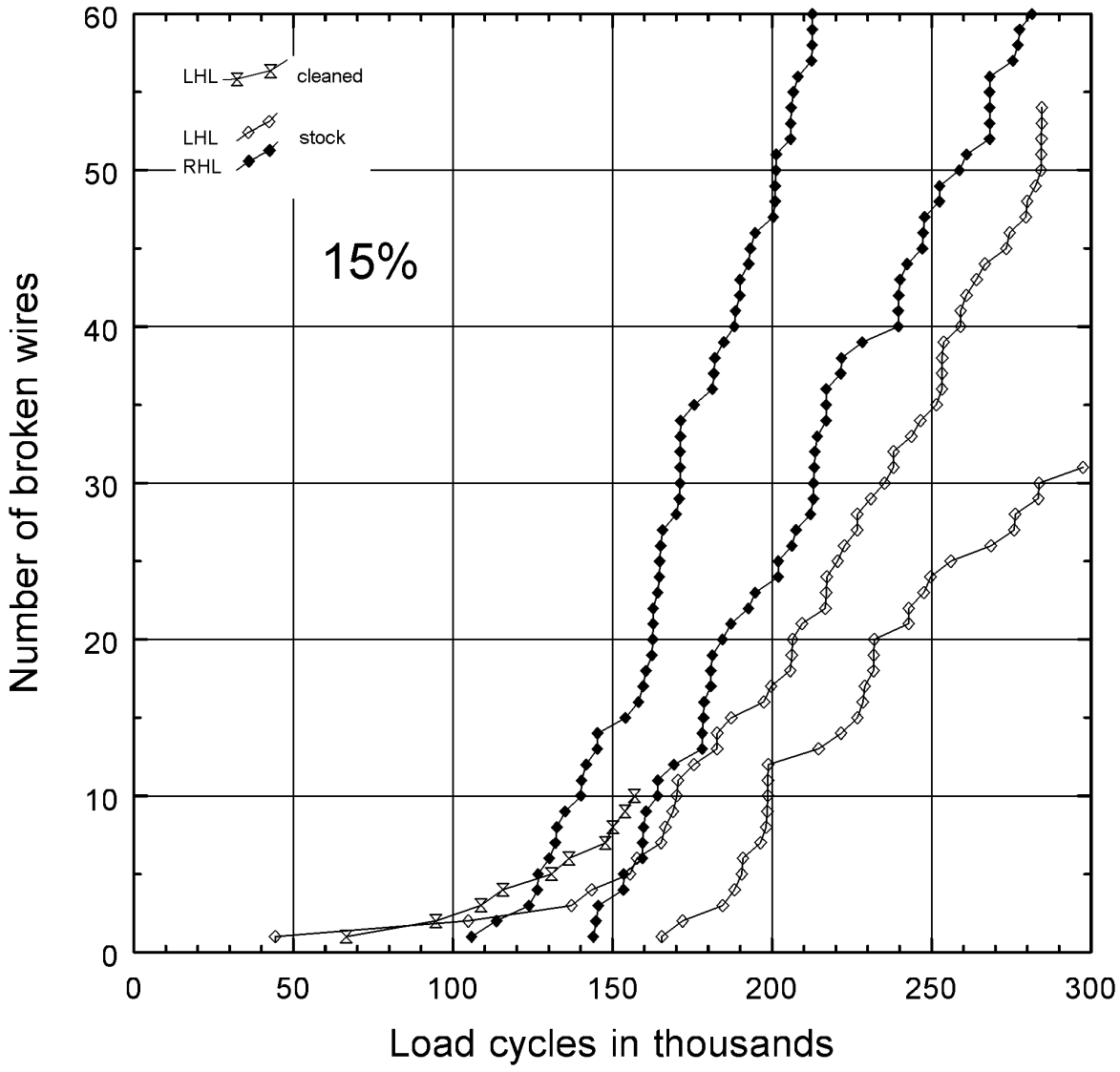

Figure B7.3: ***Summary of the results of the 15% load range fatigue tests carried out on the stock samples and one cleaned used rope sample.***

Appendix C: Bending stresses in triangular strand ropes

In this appendix, the order of magnitude of the bending stresses in the wires of a winding rope, when bent over a sheave or onto a drum, are estimated. Stresses measured with strain gauges on the wires of a rope, when the rope was wound onto and off a winder drum, are also discussed. Only triangular strand ropes are considered.

C1 *D/d* ratios

On a drum winder, *D/d* refers to the ratio between the drum diameter and the rope diameter, and the ratio between the headsheave diameter and the rope diameter. The winder code of practice[1] requires *D/d* ratios for drums and sheaves of not less than:

$$D/d = 40 + 4V \qquad \text{with } V \text{ the maximum rope speed in m/s}$$

Therefore, a winding speed of 15 m/s requires a *D/d* of 100. The code of practice further stipulates that a *D/d* of greater than 140 is not required.

The *D/d* specification of the winder code of practice is for all practical purposes the same as the recommendation in the Haggie rope catalogues (since 1976). Although the specification as shown is winding speed related, the following was noted during the drawing up of the winder code of practice:

> "The *D/d* ratio has an influence on the rope stresses and therefore also on rope life. Operating a busy winder at a small *D/d* ratio may result in such a high rate of deterioration that it could result in an unsafe situation before the next rope inspection is due.
>
> If a service winder, running at 5 m/s, is allowed to operate at a small *D/d* ratio, it will experience more damage per winding cycle than a rock winder with a larger *D/d* ratio running at 20 m/s. The service winder would, however, take much longer to accumulate as many winding cycles as the rock winder if they operate at the same depth. Slow winders will therefore be allowed to operate at smaller *D/d* values.
>
> Although specifying a *D/d* ratio which is coupled to the rope speed makes good sense, it could create the impression that the rope speed influences safety or rope life. The bending stresses in the rope could, however, be influenced by the speed at which the rope moves over sheaves and onto the drum.
>
> The lower limit of the *D/d* ratio for drums and sheaves is based on values specified in the Haggie catalogue and should conform to the smallest bend radius allowed. It was decided that the minimum *D/d* ratio should be 40 for ropes of all tensile grades. The minimum required *D/d* ratio will increase linearly with winder speed to a value of 140 at 25 m/s, after that it will remain constant, otherwise it would be restrictive to future super fast winders ($\geq$ 25 m/s). The specified values were based on experience because scientific backed values do not exist yet."

The *D/d* ratios of 99 drum winders are given in an information report[2] and analysed in another report.[3] From the information in the these reports it can be said that generally the *D/d* ratio of a drum winder is 100 or greater. The trend is now to have *D/d* ratios of not less than 100.

It is further of interest to note that the Haggie rope catalogues stated that "the additional load imposed upon a rope by bending is dependent upon rope construction, internal lubrication, speed of rope travel and shape of sheave groove, and is therefore difficult to calculate with accuracy."

The above quotes show that great uncertainty existed regarding the actual effect of bending winding ropes around sheaves and onto drums. With regard to the *D/d* ratios generally selected for drum winders, the following quote from a paper by Chaplin:[19]

> "Bending fatigue: the bending ratios (sheave diameter to rope diameter) are so high that the endurance for 'bending over sheaves' fatigue is orders of magnitude greater than actual service life. However, though small, the superimposition of these bending stresses on the stresses associated with tensile load will cause some increase in the tensile fatigue stress range."

Nevertheless, the objectives of the bending stress investigation of this project were to compare the stresses caused by bending with the stresses from tensile loading, and to try to establish whether speed has any influence on bending stresses generated when a rope is bent over a sheave or onto a winder drum.

C2 Geometrical considerations

Although most researchers tend to express their calculations and findings in terms of dimensionless parameters, it is the opinion of the author of this report that it is generally more interpretable and easier to understand if practical values of winder parameters are used. Variations in parameters (of other installations) will then merely require another calculation.

To obtain some values of the stresses in the wires of a winding rope caused by tensile loading and bending of the rope, the following parameters were selected:

Rope diameter: 48 mm, outer wire diameter 3,2 mm, 175 mm² steel area per strand
Outer rope wire tensile grade: 1 800 MPa
Maximum static rope load: 25% of breaking strength (static safety factor of 4,0)
Drum and sheave diameter: 4,8 m giving a *D/d* ratio = 100

C2.1 Tensile loading of the rope

A replica of a triangular strand rope section (taken in service) is shown in Fig. C2.1.

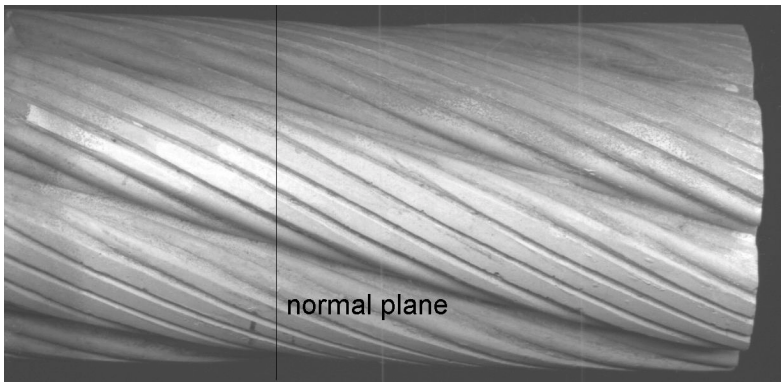

Figure C2.1: Replica of a triangular strand rope

In the as manufactured condition a strand in a rope lies at an angle of approximately 14° to the rope, and a outer strand wire lies at an angle of approximately 25° to the rope. With the increased laylengths at the back end of triangular strand ropes in service, this wire angle would then be more of the order of 20°.

If it is assumed that the stress in the outer strand wires reach 1 800 MPa at failure during a tensile test, the tensile stress in an outer wire for loading the rope to 25% of breaking strength would be 450 MPa. In steel every 1 MPa of tensile load will give a tensile strain of close to 5 μm/m. The tensile strain in a wire of an 1 800 MPa triangular strand rope, loaded to 25% of its breaking strength, will then be = 2 250 μm/m.

C2.2 Rope as a solid bar

Now if the rope was not made out of individual wires and strands, but was a solid bar of steel, bending a rope over a sheave with a *D/d* ratio of 100 would give a radius of curvature for the solid bar of 2,4 m (radius of the drum and sheave). From geometrical considerations the strain in the solid bar from bending will then be:

Strain= rope radius / sheave radius
= 48 mm / 4 800 mm
= 10 000 μm/m

The section of the bar on the inside of the bend will be in compression, and the outside will be in tension. If a rope behaved like a solid bar, it would require zero relative movement between strands so that sections of the rope in a plane normal to the rope (see Fig. C2.1) remain in that plane. If the rope has a laylength of, say, 400 mm, a strand will be in compression on the inside of the bend and 200 mm further on it will have to be in tension.

If a rope behaved as a solid bar, friction between strands and wires would be required to keep the rope "in shape". The variation in the load in a strand is estimated as ±100 kN from being in compression to being in tension. It is common knowledge that a rope does not behave in this way, and the magnitude of the friction required between strands make it impossible for a rope to behave in this way. The flexibility of a rope in bending is provided by the particular construction of wires and strands. Therefore: Bending of a rope will cause relative movement between the strands of a rope.

C2.3 Rope strands as solid members

Figure C2.3 shows a schematic of a cross-section through a triangular strand rope. The shape of a strand is somewhere between triangular and round. A triangular or round solid member bends around an axis through its centroid, irrespective of the bending direction. If the diameter of the rope shown in Fig. C2.3 was 48 mm, the distance between the centroid of the strand and the outside of the strand would vary at most between 7 mm and 10 mm.

If the construction of the rope and the wires in the strand were such that bending of the rope allowed movement between the strands, but not between wires in a strand, the strands would have behaved as solid members.

The strain at the outside of a strand from bending the strand would then at most be:

Strain (strand) = 10 mm / 2 400 mm
= 4 170 μm/m

In the outer parts of the strands that are only 7 mm away from the centroid of the strand, the

strain would be 2 920 μm/m.

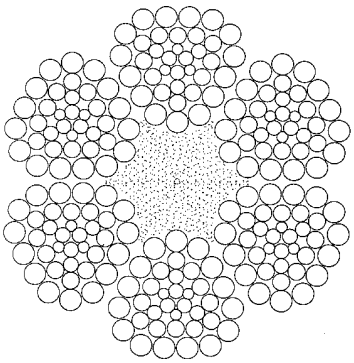

Figure C2.3: Cross-section of a rope.

These strains are greater than the strain calculated in section C2.1 for tensile loading of the rope to 25% of its breaking strength. Values for the stiffness of the strands of a triangular strand rope are not readily available, but it could be around 75% of the stiffness of steel. Maximum stress in the wires from bending strands as solid members would therefore give values of around 30% greater than the stresses generated by tensile loading.

The torsional characteristics of a triangular strand rope leads to different bending orientations during every winding cycle, which means that a section of a strand that is subjected to maximum bending stress during one cycle may be subjected to zero bending stress during the next cycle. However, it could also mean that maximum compressive bending stress may be generated in a subsequent winding cycle, which would increase the load range experienced significantly. Bending stresses larger than those generated by tensile loading of the rope will have a significant influence on the fatigue performance of the rope.

If the strands behaved like solid members, bending of a 48 mm triangular strand rope would require the same effort as bending six 12 mm diameter high tensile steel bars. The experience of handling ropes indicate that the bending stiffness of a rope should be notably less.

It is therefore improbable that the strands of a rope behave like solid members. Relative movement between the wires in a strand is required for bending of a rope, otherwise a rope would be relatively stiff in bending.

C2.4 Bending of individual rope wires

If the individual wires in the strands of a rope, as well as the strands in the rope, are all allowed to bend when the rope is bent, without any restriction or additional loads generated by friction between wires and strands, the stresses generated by bending of the rope would be the same as if each and every wire is subjected to the radius of curvature of the headsheave and winder drum.

A wire lying in a direction parallel to the length of the rope will then bend over a sheave as if only that wire alone is bent over the sheave. The D/d ratio of the wire will then be:

D/d (wire) = 4 800 mm / 3,2 mm
= 1 500

The wire strain associated with this radius of curvature is then:

Strain= 3,2 mm / 4 800 mm

= 670 μm/m

Larger outer strand wires will generate larger bending stresses.

On steel, this bending strain in the wire is equivalent to a tensile stress of 133 MPa on the outside of the bend, and a compressive stress of 133 MPa on the inside of the bend.

Where the wires run through the inside of the rope next to the fibre core (see Fig. C2.3), they lie approximately parallel to the length of the rope. On the outside of the rope and strands, a wire could lie at an angle of 20° to 30° (see Fig. C2.1). A wire at an angle at the outside of the bend (or at the inside of the bend) will not "see" the full radius of curvature of the bend, but only a fraction equal to the cosine of the angle. (The deduction of the last statement is not shown, but was done by purely considering the geometry of bending.)

For a 20° wire angle the strain and stress for the 1 500 D/d would be 94% of the parallel wire values, namely 630 μm/m and 126 MPa.

The calculated bending stress values for bending of the wires individually are only about 7% of the tensile strength of the wire material and approximately one quarter of the stress due to tensile loading.

It is of interest that a wire on the side of the rope (on the "neutral axis" of the bend) will have a radius of curvature slightly smaller than the bend radius if it lies at an angle between parallel with the rope and 50°, with the maximum decrease in curvature of about 9% at an angle of 35°. The reduced curvature will of course increase the bending stresses accordingly. The deduction of the geometries that produced this statement is also not shown. There are so many other unknowns regarding the bending of wire ropes that, for the moment, the mentioned situation should only be noted.

Most of the literature surveyed arrived at approximately the same results as shown above, except that in some cases the conversion from strain to stress is (erroneously) based on the elastic modulus of the rope instead of the elastic modulus of steel.

C2.5 Unequal wire lengths due to bending

The path that an individual wire follows through a rope and through a bend in the rope could repeat itself in a given length of curvature. For example: An outer strand wire at the crown of the strand and on the outside of the bend will appear again at the crown of the strand and on the outside of the bend a number of rope laylengths further down the bend.

A common error noticed in literature studied is that some of the authors assumed that such a situation would repeat itself every laylength of the rope. Only in very special cases where the strand laylength and the rope laylength are matched in the correct fractions would the same outer wire be at the crown after every laylength. Strand lengths, of course, repeat themselves every rope laylength.

When an outer wire appears at the crown on the outside of the bend again, all other strand outer wires would have followed a path of the same wire length. If the total bend length is a multiple of this mentioned "same" length then unequal outer strand wire lengths may not induce any extra or additional tensile or compressive stresses in the wires, provided that the rope allows relative movement between the wires in a strand. However, bending a rope over a headsheave, especially if the laylength of the rope varies along its length, will seldom lead to the ideal matching of the rope laylength and the bending length.

Furthermore, the inner strand wires and the centre part of a compound triangular strand rope

would not be matched for bending lengths with the outer wires of a strand. However, being closer to the core of the strand, the unequal lengths would be less than that of the outer strand wires, and therefore generate lower stresses. Generally, failure of outer strand wires are the more common occurrence for triangular strand ropes operating on drum winders. Inner strand wires are therefore of secondary importance.

Bending a winding rope over a headsheave has a given arc length of bend, whether ideal or not. Bending the rope onto a winder drum changes the situation continuously from the ideal to the worst (most unequal length situation). The exact behaviour of a rope bent onto a drum would therefore not be readily predictable.

The calculation of the (worst) unequal outer strand wire lengths for bending a rope around a sheave or onto a drum will require a substantial analysis of the spatial geometry of a rope and its strands and wires. Such an analysis is not part of the scope of this investigation. The magnitude of unequal wire lengths, and the accompanying stress variations, can only be established through the execution of such an analysis.

C2.6 What could be expected in reality

If unequal wire lengths in the rope due to bending are disregarded for the moment, bending of a rope can result in the following:

- The individual wires in the rope bend in an unrestricted manner and generate bending stresses as calculated in section C2.4.
- A crown wire on the outside of a strand and on the outside of the rope curvature could have additional tensile stresses if the strand and rope do not allow unrestricted relative movement between the wires and the strands during the bending action.

The basic case would then be that a wire will bend and generate bending stresses according to the radius of curvature of the bend. Friction between wires and strands of the rope could increase the stresses in crown wires on the outside of the bend. Unequal wire lengths could increase or decrease the wire stresses to an unknown degree.

C3 Bending stress measurements

Bending stress measurements on a rope in service were decided on to obtain a measure of the magnitude of bending stress when a rope is wound onto a winder drum, and to obtain more information on the behaviour of a rope in bending. The measurements were not intended for the full quantification of the behaviour of a triangular strand rope in bending.

It was also decided to attempt the measurement of the stresses when the rope was wound onto the drum and off the drum at different speeds. If the interaction between wires and strands was purely frictional, winding speed should not have an influence on the stresses generated, but if some visco-elastic interaction was present, speed would have an influence. The influence of speed on the generated bending stresses had always been a contentious issue. It was planned to carry out strain gauge measurements at slow speeds, 1 m/s and 2 m/s, and that measurements at 5 m/s and 10 m/s would be attempted.

The bending stresses were measured with the aid of strain gauges on a rock winder at Cooke no. 1 Shaft of Randfontein Estates.

C3.1 Winder and rope information

The winder and rope information of the rock winder were as given in Table C3.1.

The stress measurements on the rope wires were carried out on the underlay rope near the drum, and with an empty skip approximately at midshaft.

Table C3.1: Winder and rope information of the rock winder at Cooke no. 1 Shaft

Shaft depth	950 m
Drum diameter	4,88 m
Skip mass	7 930 kg
Rock mass	10 000 kg
Rope diameter	48 mm
Construction	6x32
Outer wire diameter	3,1 mm
Rope mass	9,81 kg/m
Tensile grade	1 800 MPa
Breaking strength	1 780 kN

The actual rope diameter was 46,3 mm at the section where the strain gauges were installed. At that section the angle between a strand and the rope was approximately 20°, and the angle between a crown wire of a strand and the rope was approximately 28°.

Following the calculations of wire stresses given earlier in this appendix, the tensile stress in the rope near the drum with an empty skip at midshaft should be around 125 MPa for this winder. The bending stress from bending the 3,1 mm wire around the 4,88 m drum would be around 112 MPa for a crown wire at a 28° angle (a bending strain of approximately 560 μm/m).

For this winder, the first natural period of longitudinal rope load oscillations for the conveyance at midshaft and an empty skip attached was calculated to be in the order of 1,2 seconds.

C3.2 Winder preparation

The winder was wound up and down a number of times with empty skips to settle the rotational orientation of the rope. This was done to limit the rope rotation during short winding trips after installation of strain gauges on the rope.

C3.3 Installation and calibration of strain gauges

One strain gauge was installed on each of two adjacent rope strands. At the time of installation, the strain gauged sections were approximately 4 m from the winder drum. The strain gauges, with 1 mm long grids, were installed on crown wires in the centre of the strands, and positioned such that they would be on the very outside of the bend when the rope was wound onto the drum.

The two strain gauges were connected to suitable strain gauge amplifiers and a computerised data acquisition system. The sampling frequency of the data acquisition system was set at 4 000 samples/second per strain gauge channel. Appropriate digital filters could then be employed to filter out "noise" recorded with the measured signals without affecting the actual signals.

The complete system (strain gauge amplifiers and data acquisition system) was calibrated by shunting each strain gauge with a 33 kΩ resistor at the strain gauge. The shunt resistor generated

compressive strains at each strain gauge of 1 812 μm/m. The calibration of the system with a shunt resistor at the strain gauges took care of the following possible measurement errors:

- Signal output direction for compression and tension;
- reduction in output from the 70 m long strain gauge leads; and
- did not require exact values of the gain settings on the strain gauge amplifiers and the analog-to-digital converter of the data acquisition system.

C3.4 Test procedure and results

C3.4.1 First site visit

Strain gauges were installed on the wires of two adjacent strands as described earlier. The strain gauged strand closer to the drum was designated "no. 1" and the adjacent one, further away from the drum, "no. 2" strand.

The rope section with the strain gauges was then wound slowly onto the winder drum and then off the drum. The winding speed was estimated at 0,3 m/s. The strain measurements (against time) are shown in Figs C3.4.1 and C3.4.1.1 respectively for winding onto and off the drum. Zero strain was taken as the situation at which the strain gauges were installed. The following was noted from the graphs:

- The behaviour of the strain gauged wires on the two adjacent strands was totally different.
- No. 2 strand behaved more like expected, but the measured strain was only 60% of the expected. When no. 2 came off the drum, the behaviour was approximately a mirror image of going onto the drum. No. 2 did not return to the set zero value after it left the drum, but showed a 50 μm/m tensile strain.
- The behaviour of no. 1 was totally unexpected: It started off going into compression, turned around and started to go into tension, after which the strain direction changed again and ended up in 100 μm/m compression on the drum! Going off the drum also showed strain direction changes but not to the same degree as going onto the drum. No. 1 returned to the same strain state after being wound off the drum than to that before it was wound onto the drum.
- Stopping the winder from creep speed will generate some (longitudinal) rope load oscillations. Figure C3.4.1.1 show such load oscillations measured by the strain gauges. The oscillation period was as expected, but no. 2 showed strain amplitudes of only a fraction of that of no. 1.

Possible explanations for the behaviour of the two strain gauged wires are:

- The fact that no. 2 did not properly "take part" in the longitudinal rope load oscillations may indicate that the strain gauged wire was slightly loose, although it did not seem that way when the strain gauge was installed. Being not "part of the rope" allowed the wire to bend individually. The fact that the full expected bending strain was not achieved could be ascribed to the fact that the wire was not completely loose; it did show some longitudinal load oscillations.
- The behaviour of the no. 1 wire could have been caused by wire length adjustments during the bending of the rope (as explained in section C2.5). Friction forces of approximately 150 N would be required to generate 100 μm/m of strain in a 3,1 mm diameter wire. Additional friction of at least four times this force would be required to nullify the outer surface strain generated by pure bending of the wire.

The frictional force on a wire of 700 N to 800 N, required to produce the observed behaviour of the no. 1 wire, seems slightly large, but only the mentioned geometrical analysis of unequal wire

lengths generated by rope bending could prove or disprove the explanation given.

After the on-and-off at creep speed, the measurements were repeated for winding speeds of 1 m/s and 2 m/s.

The measured strains for creep, 1 m/s, and 2 m/s are compared in Figs C3.4.1.2 to C3.4.1.5. In these figures the measured strains were plotted as function of distance that the rope travelled (obtained from multiplying the winding speed with time). This was done to compare the measurements more readily, because at 2 m/s the strain variations took place more rapidly than at creep speed. The graphs of the strains measured at the different speeds were displaced from one another in the figures to show the behaviour at each speed more clearly. The zeroes of the two strain gauges were not adjusted at all during the measurements. Whenever friction is involved in a system, strain gauge measurements will show some hysteresis and will not always return to the original zeroes.

Figure C3.4.1.2 shows no. 2 wire (the loose one) being wound onto the drum and the different speeds, and Fig. C3.4.1.3 shows the behaviour when wound off the drum. The graphs show a slight increase in bending strain onto the drum at the higher speeds, but the shapes of the graphs remained similar.

Figure C3.4.1.4 shows no. 1 wire being wound onto the drum at different speeds, and Fig. C3.4.1.5 shows the behaviour when wound off the drum. The graphs show different behaviours at different speeds, and also different behaviours between winding onto and off the drum. Reversals of strain directions are, however, evident at the different speeds, indicating a possibility of wire length adjustment postulated earlier.

After the 2 m/s run, the rope was wound onto the drum at 5 m/s. The strain gauged rope section had to be wound into the catenary for quite a distance to enable the winder to accelerate to 5 m/s before that section of rope reached the drum. During acceleration of the winder, the rope rotated and the strain gauges were destroyed when wound onto the drum.

It was then decided that it would not be possible to do a 5 m/s run onto the drum but that a 5 m/s run off the drum may be possible. At that stage the winder had to be put back into service, and the investigation could only be continued at a later date. Unfortunately this meant that it would not be possible to locate the same two strands and wires of the measurements described above for the continued investigation.

C3.4.2 Second site visit

Strain gauges were again installed on the wires of two adjacent strands as described earlier. The strain gauged strand closer to the drum was in this case designated "no. 4" strand and the adjacent one, further away from the drum, "no. 3" strand.

The rope section with the strain gauges was slowly wound onto the winder drum, but the recording of the strains when that section was wound off the drum was missed. The section was then wound onto the drum again, off the drum, and onto the drum again at slow speed.

The strains measured on the wire of no. 3 are shown in Fig. C3.4.2, and on no. 4 in Fig C3.4.2.1. The "off-the-drum" behaviours of the wires on the two strands were of the same shape, but the "onto-the-drum" behaviours of no. 3 and no. 4 were completely different. The "onto-the-drum" behaviour of no. 3 was more comparable to that of no. 1 of the first site visit described in the preceding section.

The strain gauged rope section was then wound off the drum and back onto the drum at 1 m/s. The behaviours of both strain gauged wires are shown in Fig. C3.4.2.2. The behaviour was for all

practical purposes the same as that at slow speed.
The strain gauged rope section was wound far enough onto the drum to provide sufficient length of rope to accelerate the winder to 5 m/s before that section came off the drum. The strain gauged section was then run off the drum at 5 m/s followed by normal deceleration and stopping of the winder. The behaviours of both strain gauged wires (no. 3 and no, 4) when wound off the drum at 5 m/s are shown in Fig. C3.4.2.3. The off-the-drum behaviours at 5 m/s were not different to that measured during slow speed winding or at 1 m/s.

To put the strains measured during this site visit into perspective with strains generated during tensile loading of the rope, the strains measured during the "off at 5 m/s" are also shown for the period of normal winder deceleration and stopping in Fig. C3.4.2.4. The strains generated during deceleration and stopping are greater than that measured due to bending of the rope. The graph also shows that both strain gauged wires "participated" during tensile loading of the rope.

Nothing additional to that mentioned before can be said about the measurements of this section, except that very little evidence of visco-elastic rope behaviour could be observed at a speed of 5 m/s.

After normal deceleration and stopping of the winder, the rope rotated and displaced the strain gauges by approximately 150° to the required positions. The strain gauges therefore had to be re-installed before the off at 10 m/s could be attempted.

C3.4.3 Third set of strain gauges

The strain gauges could be re-installed on the same strands as the no. 3 and no. 4 of the preceding section, but of course not on the same wires. To get the strain gauges on the outside of the bend, the new strain gauges were approximately 160 mm from the previous ones. The new positions were designated "no. 3a" and "no. 4a."

Unfortunately no. 4a stopped functioning every time that the strain gauged section was wound unto the drum (most probably the open leads at the strain gauge made contact with the rope when the rope was bent, causing a leakage-to-ground problem). The tests of this section therefore only describes measurements from no. 3a.

The strain gauge section was first wound slowly onto the drum, then slowly off the drum, and then back onto the drum at an even slower speed. The behaviour is shown in Figs C3.4.3, C3.4.3.1, C3.4.3.3, and C3.4.3.4. The strain gauged wire on this strand behaved differently to the other wires on which strains were measured, and it did show some tension after being wound onto the drum. When wound off the drum, the behaviour was very different to any of the other measurements: The strains went further into tension instead of returning to (approximately) the same state as before it was wound onto the drum. When the rope was wound back onto the drum, the strains returned to the values measured after the rope was wound onto the drum for the first time.

To provide enough rope to accelerate the winder to 10 m/s, the strain gauge section and the strain gauge leads had to be wound onto the drum for nearly five drum turns (70 m). During acceleration to 10 m/s, the strain gauge leads starting looping around the drum. The leads cutting through the magnetic fields in the proximity of the winder motor generated substantial noise on the signals. Fortunately the noise could be filtered out in such a way that the essence of the actual measured strains could be retained.

Figure C3.4.3.3 shows the strains measured when the strain gauged section left the winder drum at 10 m/s. The measured strains were not much different in magnitude or shape than those measured when the rope was slowly wound off the drum. No evidence of visco-elastic rope behaviour in bending could be observed for a rope speed of 10 m/s.

After the strain gauged section left the drum, the winder brakes were applied to stop the winder. The strains measured during the off at 10 m/s, the braking and after stopping the winder are shown in Fig. C3.4.3.4. As before, the strains generated during braking and stopping were significantly greater than that measured due to bending of the rope. The graph also shows that the strain gauged wire "participated" during tensile loading of the rope.

Although the measurements on the wire described in this section showed tension after bending, reversals of strain direction during bending were still present.

For the sake of interest:

> Figure C3.4.3.4 shows that from 10 m/s the winder came to a stop in approximately 4 seconds, which gives an average winder deceleration of 2,5 m/s² (which is an acceptable value for braking). The average strain increase during braking, measured with the strain gauges, was of the order of 300 μm/m.
>
> The static rope load at the time of braking was 475 m of rope plus an empty skip, which gives a total static weight of 123 kN (6,9% of rope breaking strength). The average emergency braking deceleration expressed as a fraction of static is 2,5/9,8 = 0,26.
>
> Emergency braking as shown should therefore add 0,26 x 123 kN = 31 kN to the rope load, which is 1,8% of rope breaking strength, or 32 MPa of stress. This stress gives a strain of approximately 160 μm/m.
>
> Although the calculations above were estimations, the actual tensile strains measured during braking were nearly double the estimated strains. A possible explanation could be that the outer wires of a strand carry the major part of the rope load (especially at rope loads of less than 10% of breaking strength).

C4 Summary

The strains measured during bending of the rope were never close to the tensile values calculated for bending wires as individual members.

The measurements exhibited evidence that the effect of unequal outer strand wire lengths generated by rope bending is far greater than the strains generated by the pure bending of the wires. The mechanics and geometry of rope bending is therefore far more complicated than anticipated. The same conclusion was reached after an investigation of the rope behaviour at conveyance mounted compensating sheaves of Blair multi-rope winders.[20] The analysis of the bending of a rope will require an extensive investigation of the geometry of the wires in a rope.

The stress variations measured during normal winding operations (deceleration and braking) were greater than any of the strains measured during bending of the rope. The proportion of rope load carried by outer strand wires could be significantly greater than the average wire load, especially at relatively low rope loads.

No evidence was found that winding speed increases the stresses generated by rope bending.

The strain gauge measurements were only carried out on one crown wire of each of five different rope strands. Wire behaviour in bending, other than those measured, therefore remains very possible.
Although bending stresses cannot yet be quantified exactly, the indications are that bending stresses will be significantly smaller than the tensile stresses generated by normal winding operations. Because stress variations due to rope bending will be present for drum winder

operations, they will have some influence on the fatigue performance of the rope. However, the bending stresses are relatively small, and the influence on fatigue performance of the rope should not be very significant.

The measured rope behaviour could be specific to the winder on which the measurement were carried out, the rope construction, the position along the length of the rope, and the amount that the rope laylength increased or decreased (from as-manufactured) for the shaft position and the amount of rope spin lost.

If the measurement of bending stresses in the wires of a winding rope is ever attempted again, strain gauges should be installed on as many adjacent outer wires of a single strand as possible. High speed winding on and off the drum will not be necessary, but the rope behaviour for tensile load variations should be investigated as well.

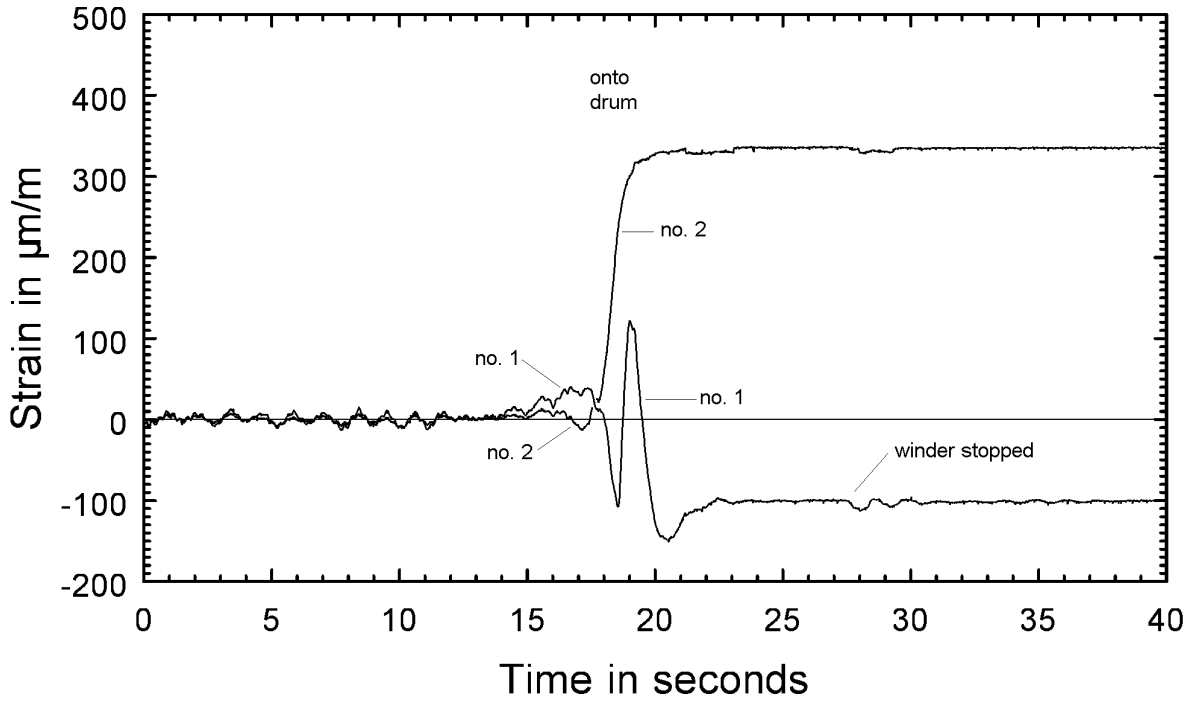

Figure C3.4.1: ***Strand nos 1 and 2: Winding slowly onto the drum.***

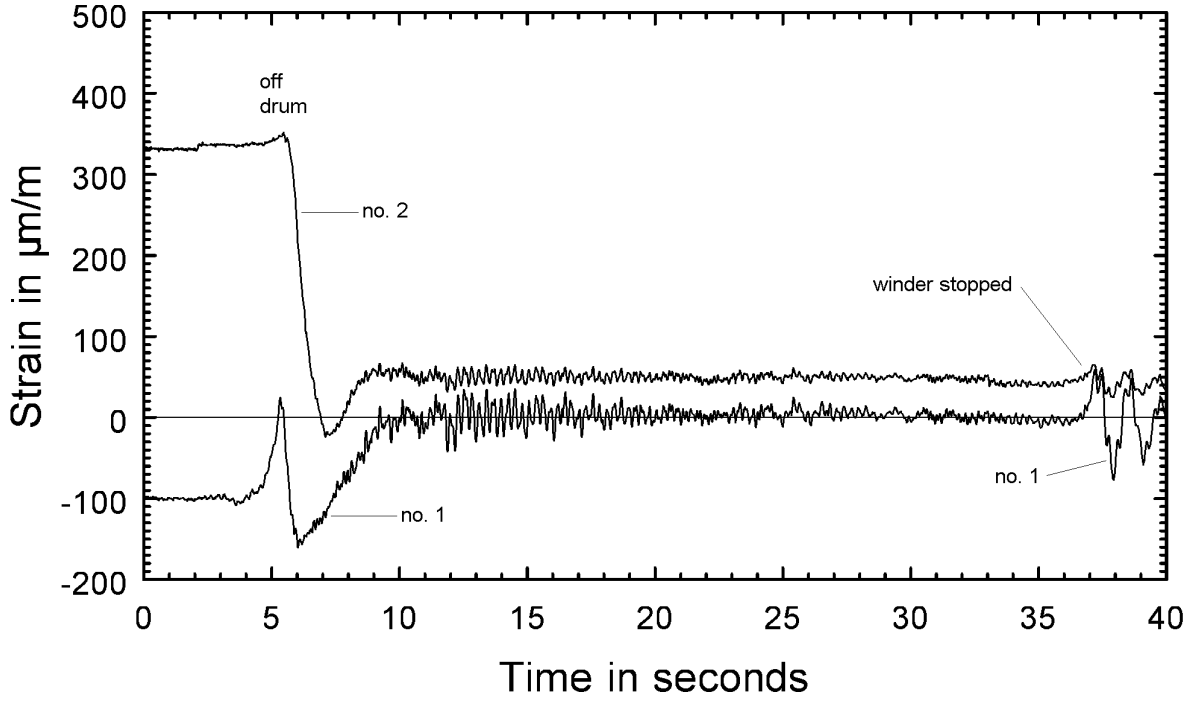

Figure C3.4.1.1: ***Strand nos 1 and 2: Winding slowly off the drum.***

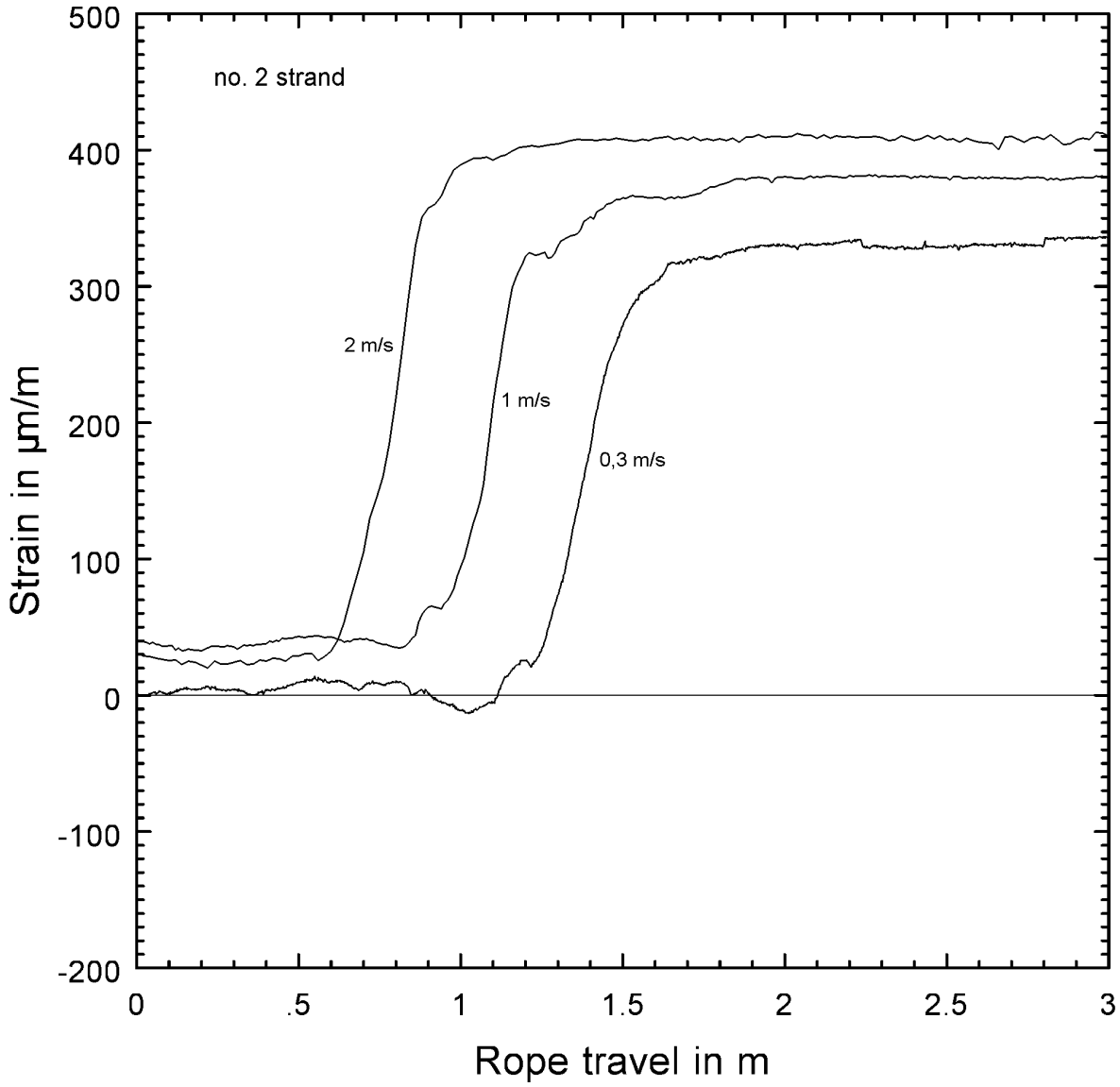

Figure C3.4.1.2: Strand no 2: Onto the drum at different speeds.

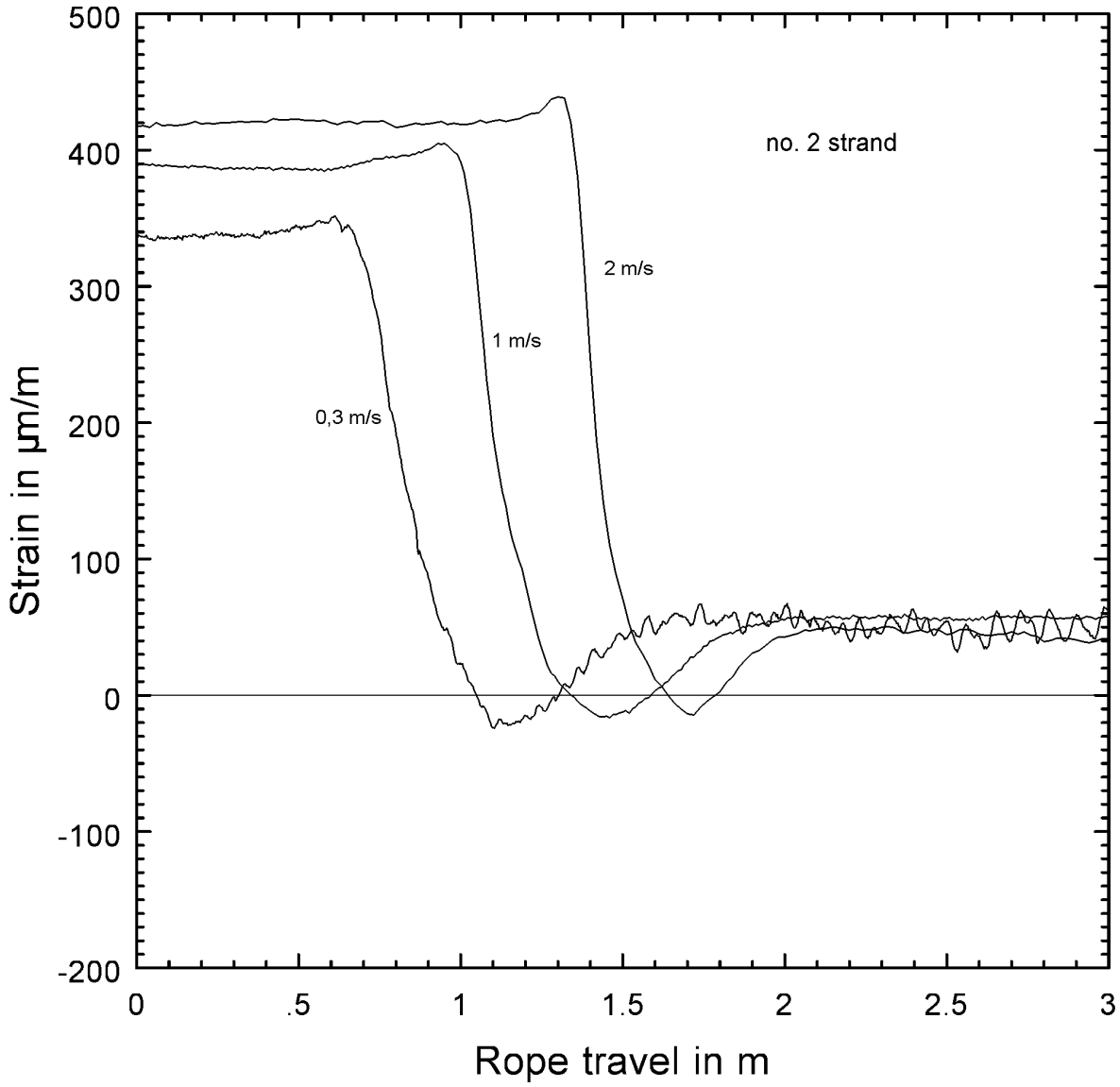

Figure C3.4.1.3: ***Strand no 2: Off the drum at different speeds.***

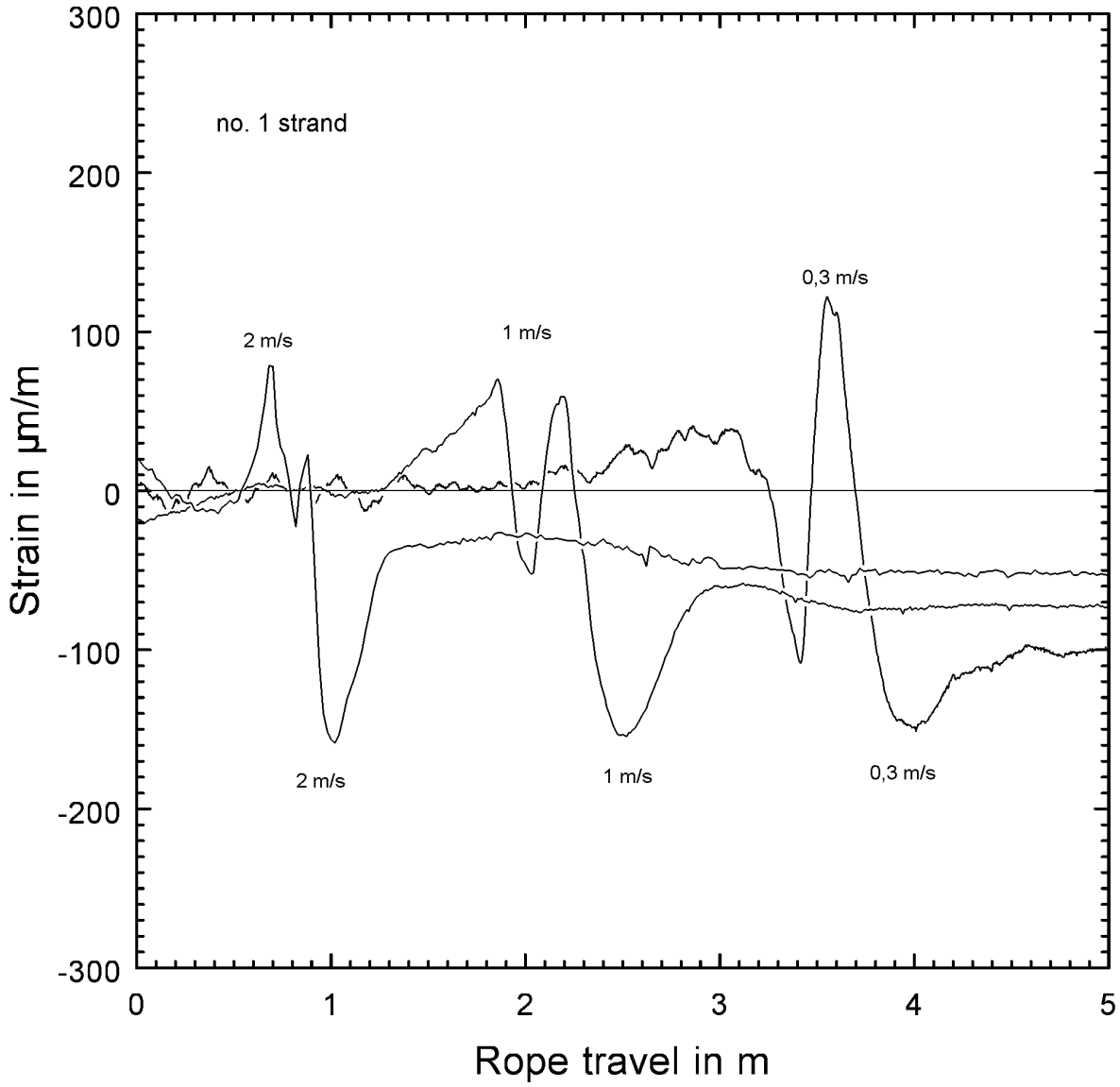

Figure C3.4.1.4: ***Strand no 1: Onto the drum at different speeds.***

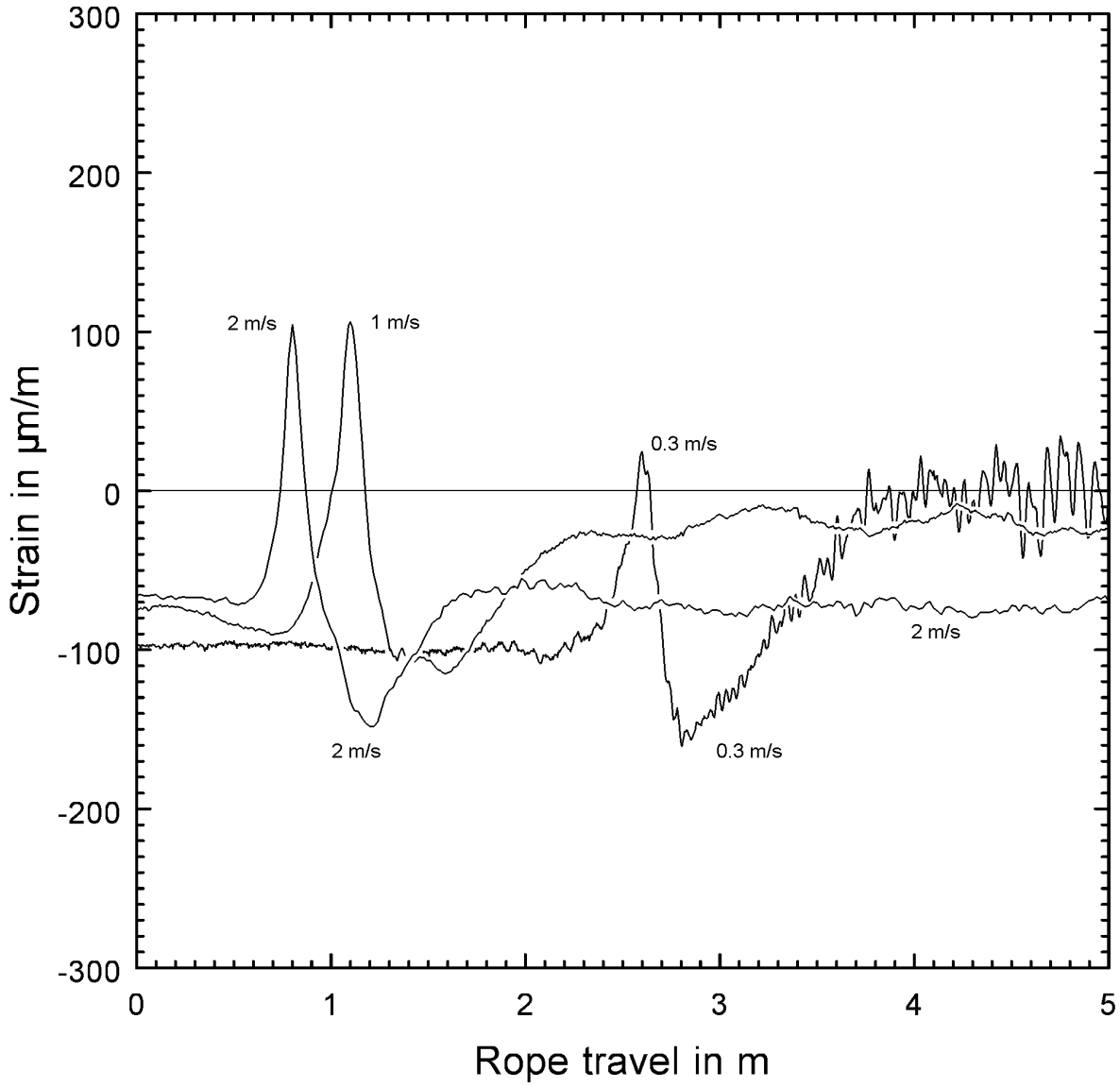

Figure C3.4.1.5: ***Strand no 1: Off the drum at different speeds.***

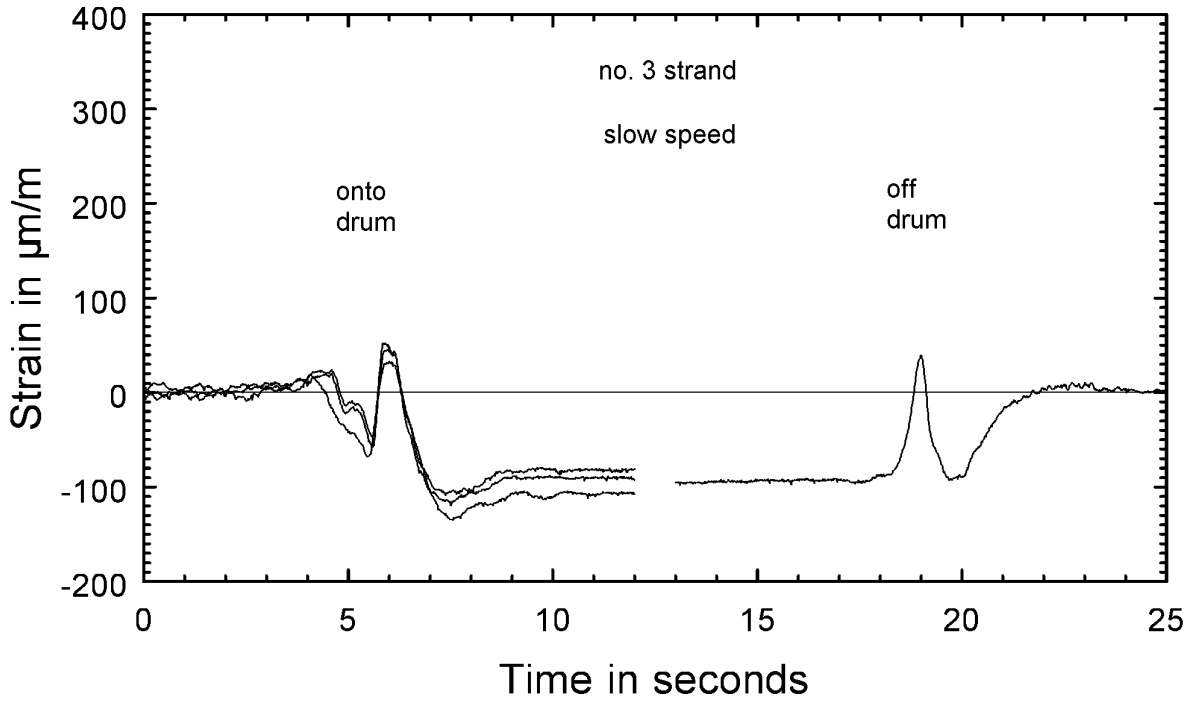

Figure C3.4.2: ***Strand no 3: Slowly onto and off the drum.***

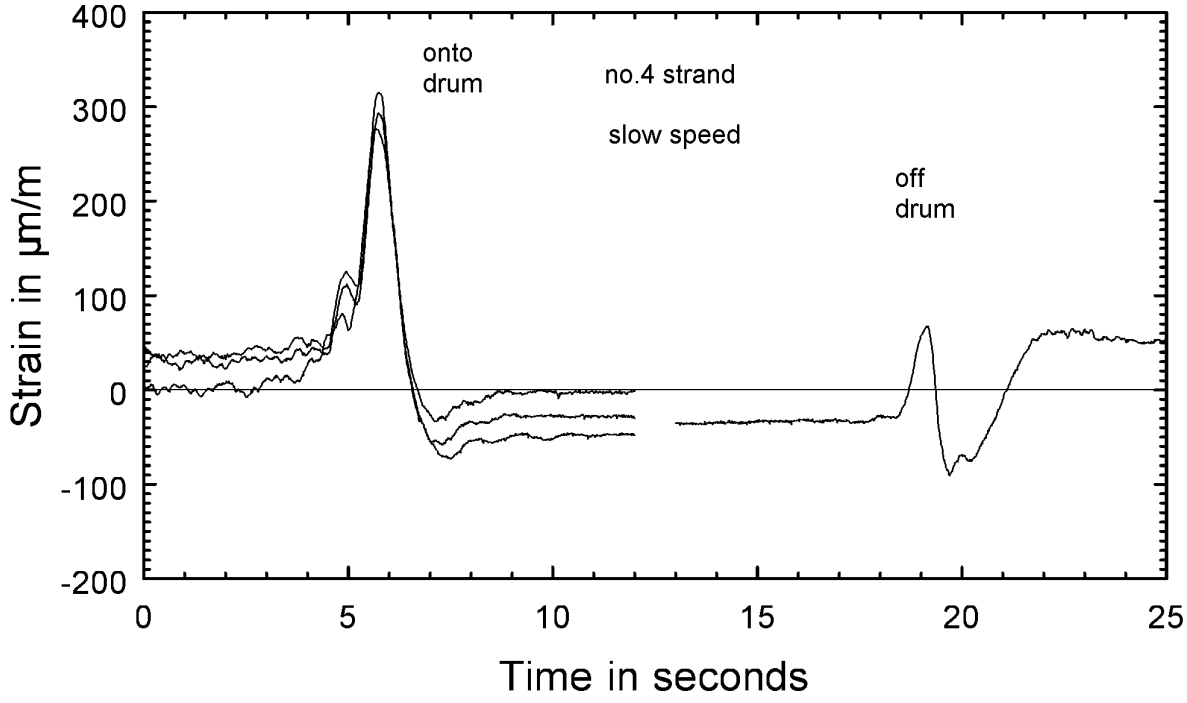

Figure C3.4.2.1: ***Strand no 4: Slowly on and off the drum.***

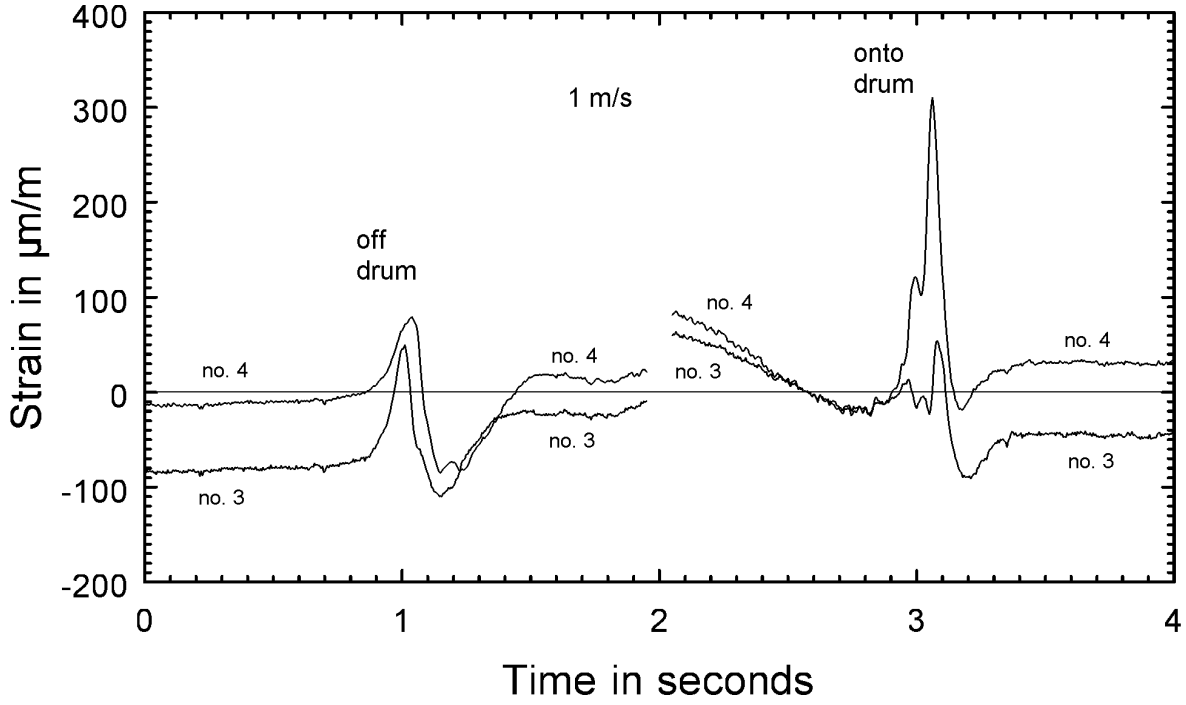

Figure C3.4.2.2: ***Strand nos 3 and 4: Off and onto the drum at 1 m/s.***

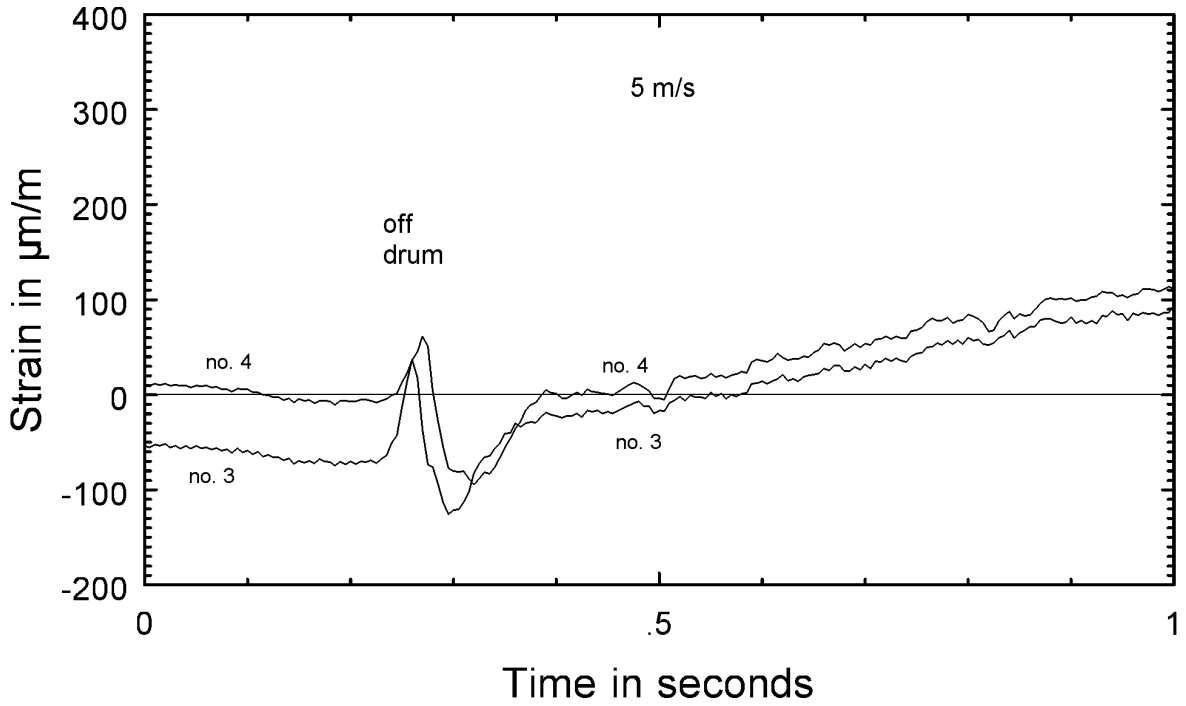

Figure C3.4.2.3: ***Strand nos 3 and 4: Off the drum at 5 m/s.***

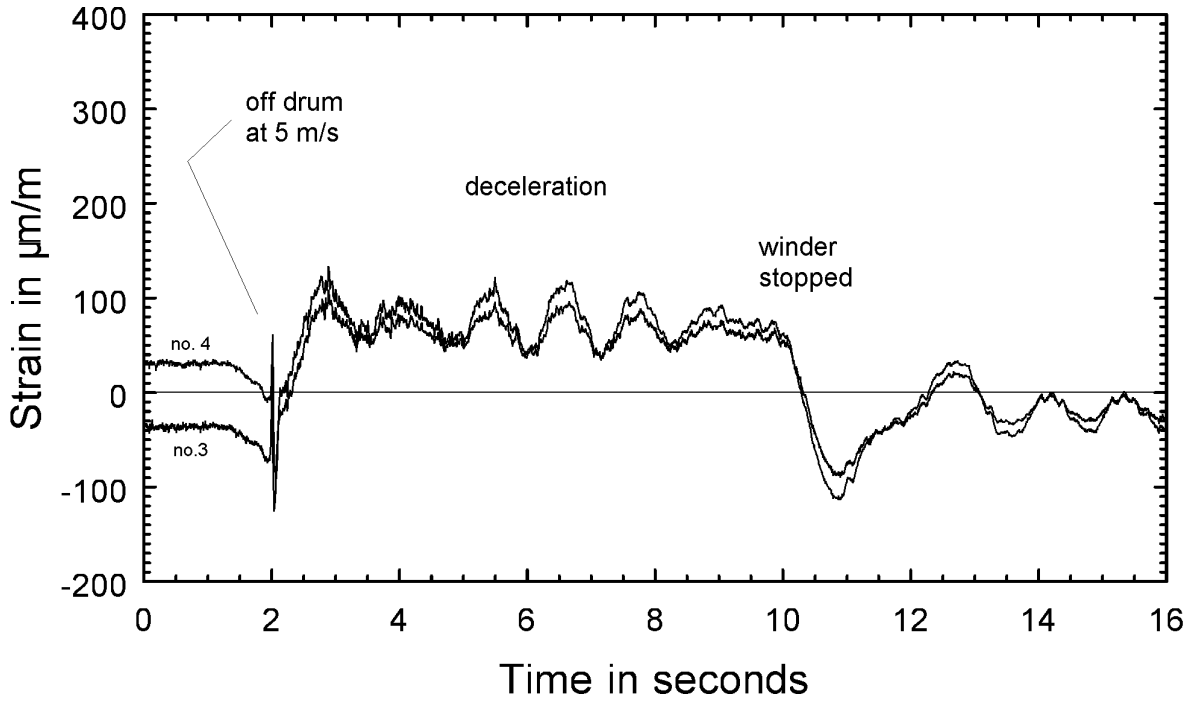

Figure C3.4.2.4: ***Strand nos 3 and 4: Off drum at 5 m/s, decelerating and stopping.***

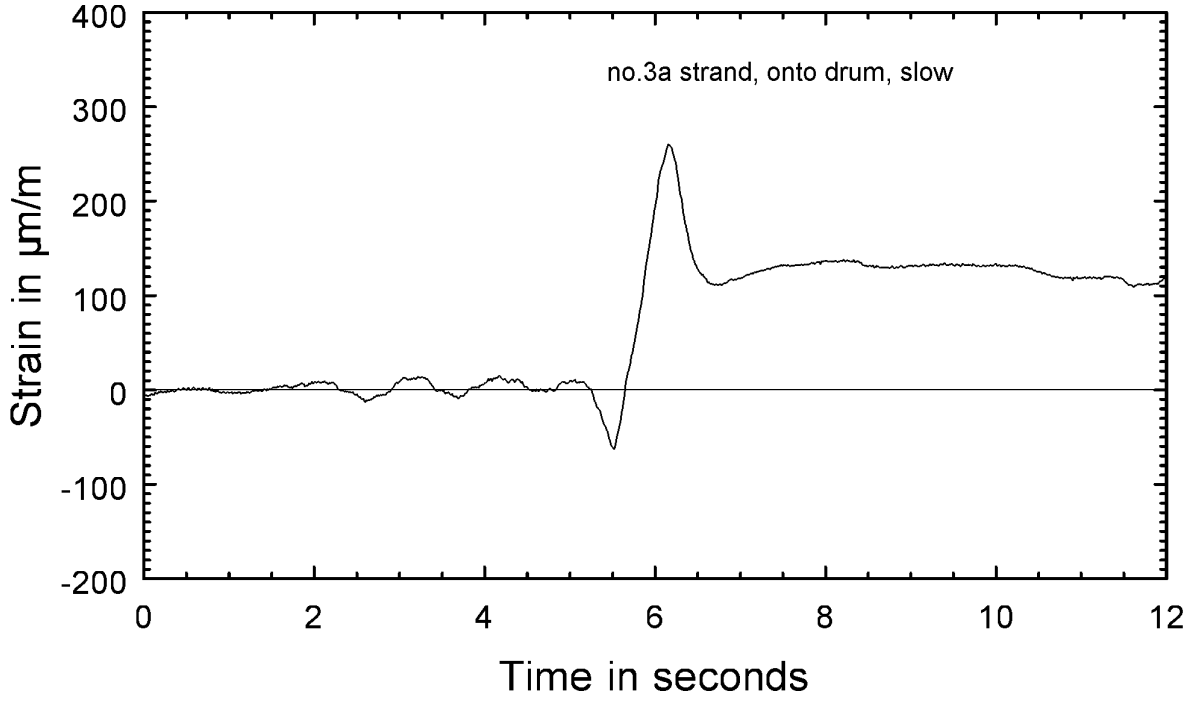

Figure C3.4.3: ***Strand no 3a: Onto the drum, slow.***

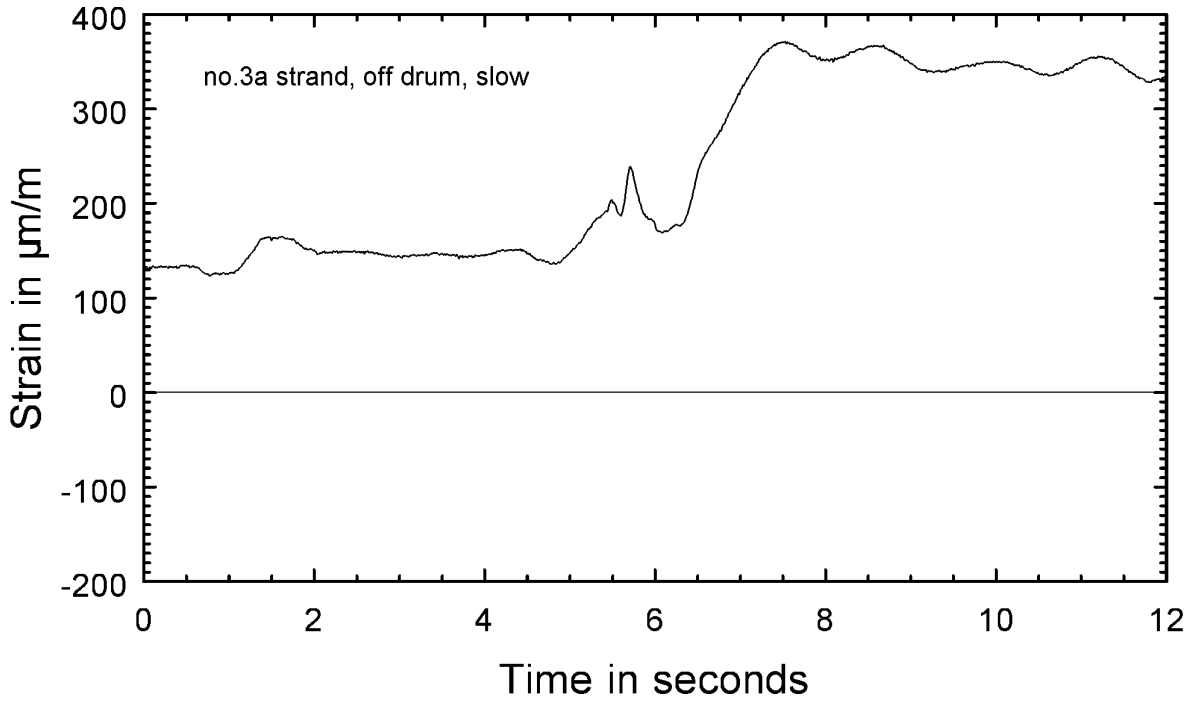

Figure C3.4.3.1: Strand no 3a: Off the drum, slow.

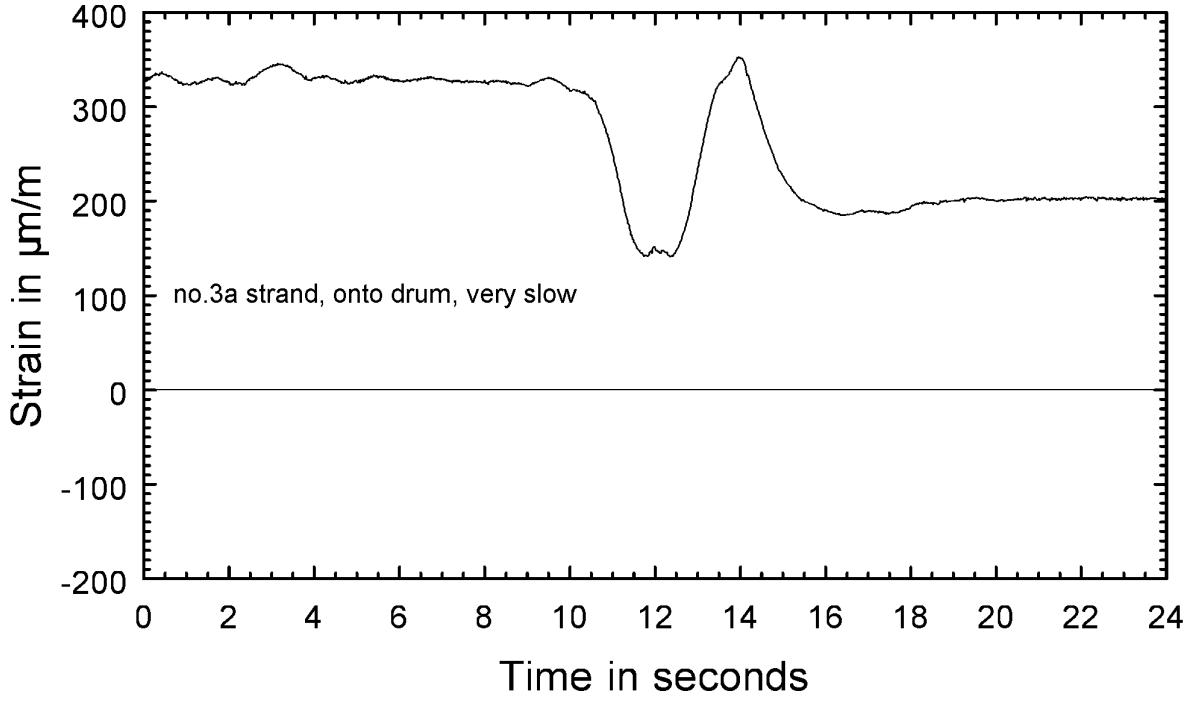

Figure C3.4.3.2: Strand no 3a: Onto the drum, very slow.

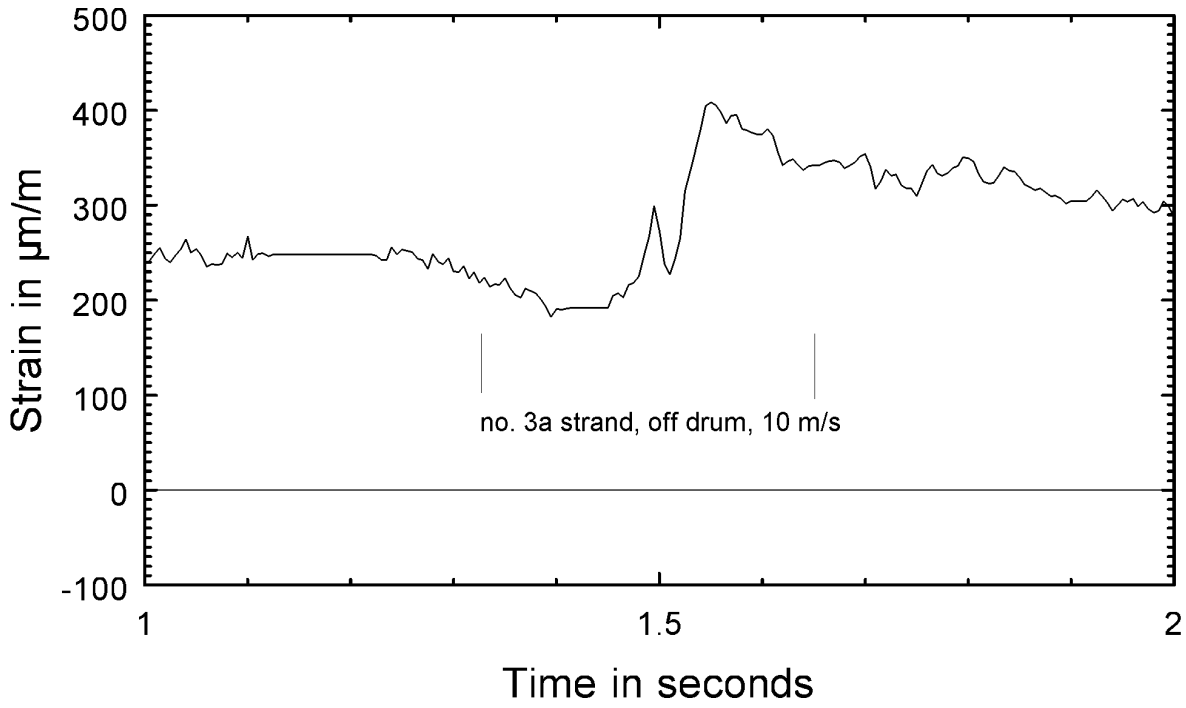

Figure C3.4.3.3: ***Strand no 3a: Off the drum at 10 m/s.***

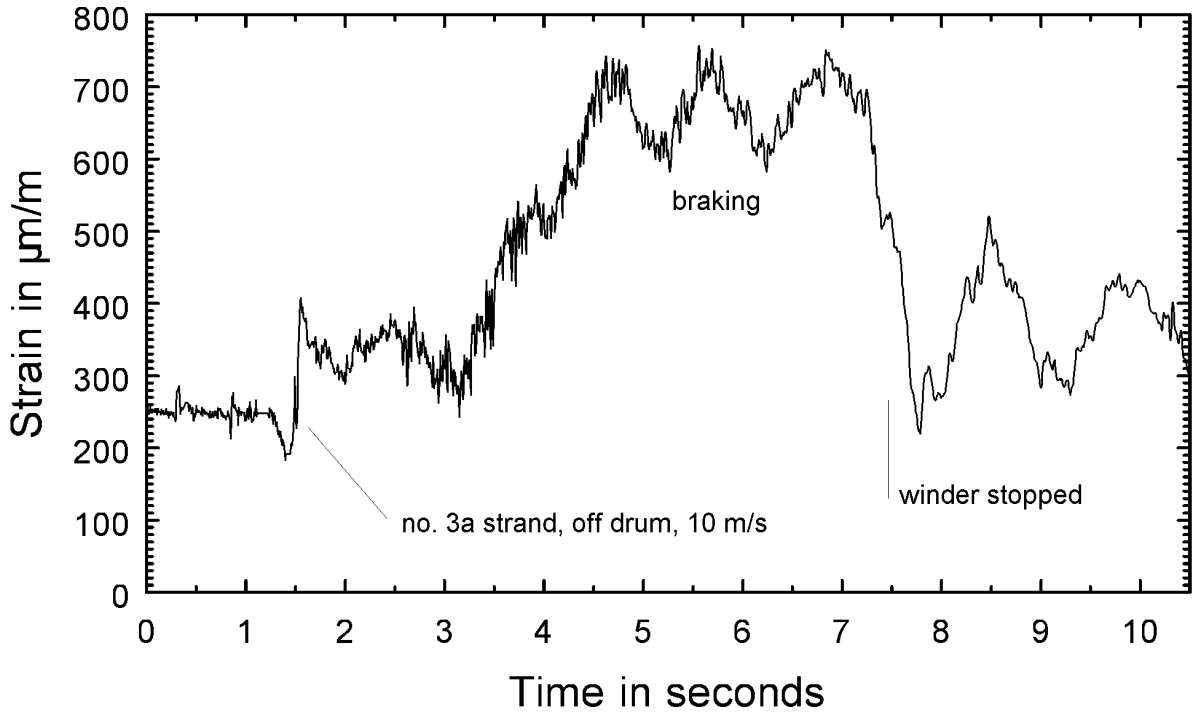

Figure C3.4.3.4: ***Strand no 3a: Off drum at 10 m/s, braking and stopping.***

Appendix D: Contact loads on drum winder ropes

The investigation described in this appendix is an initial study of the contact loads created between rope turns when the rope is wound onto a winder drum. The surface conditions of actual winder ropes were then used to calculate maximum values for the contact loads.

D1 Radial loads

When a rope under tension is wound over a sheave wheel or onto a drum, the rope exerts a radial load on the sheave or drum. Figure D1 illustrates how the radial load (F_r) is calculated from the tensile load in the rope (F_t).

Consider a cylindrical drum with diameter, D, and radius, r.

Let the length of the rope arc described by the angle of 2 α be equal to s.

The two rope tensions, shown as F_t, each has a component at right angles to F_r, and in line with F_r.

The radial force generated by the rope tensions over the arc 2 α is therefore:

$$F_r = 2 F_t \sin(\alpha)$$

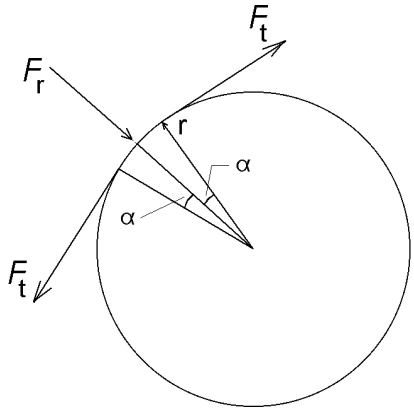

Figure D1: Calculation of radial loads generated by a rope.

For small angles (and small arc lengths):

$$\sin(\alpha) = \alpha$$

The value of the angle, 2α, is equal to the arc length, s, divided by the drum radius, r :

$$2\alpha = s/r$$

If the radial load generated by the rope is expressed as a force per unit length of rope, R, then:

$$R = F_r/s$$

Substituting from the above gives:

$$R = F_t/r \quad \text{or} \quad R = 2 F_r/D$$

Therefore, the radial rope load increases (linearly) with rope tension. For an infinitely large drum radius, the radial load will be zero. The radial load increases as the drum radius or diameter is decreased.

As an example: If the rope tension is 500 kN and the drum or sheave diameter is 5 m, the radial load generated by the rope on the drum or sheave will be 200 kN/m (i.e. 200 kN for every metre length of rope).

D2 Radial rope loads on a winder drum

When the bottom rope layer is wound onto a winder drum, there will be contact loads between the drum surface and the rope turns. Winding a second rope layer onto the drum will generate contact loads between the second rope layer and the bottom rope layer. The radial rope loads of the second layer will increase the radial loads of the bottom layer, and therefore the contact loads between the bottom rope layer and the drum. Adding more rope layers will compound the contact loads of underlying rope layers.

Rope loads, radial rope loads, and the compounding effect of adding layers of rope on the drum are illustrated in the sections that follow by means of a case study.

D2.1 Winder and rope parameters for the case study

The winder parameters for the case study given in Table D2.1 is that of a winder that would typically be designed to operate from a depth of 3 000 m.

Table D2.1: Winder and rope parameters for the case study

Shaft depth	3 000 m	Skip mass	6 200 kg
Headsheave diameter	6,10 m	Rock mass	15 500 kg
Drum diameter	6,10 m	Rope mass	10,1 kg/m
Drum width	2,00 m		
Rope diameter	49 mm	Rope turns on drum	167
Dead turns	10	Rope layers	4,4
Rope turns/layer	38		

The number of dead turns was selected as ten. The coiling diameter was assumed to be the same for all rope layers in order to simplify the calculations that follow in this appendix. The number of turns when the rope is fully wound onto the drum, given in Table D2.1, includes the dead turns. The shaft depth and length of wind was taken as the same also to simplify calculations, i.e. the skip will be wound right up to the sheave.

The rope tension in the dead turns was assumed to be the same as that of the back end of the rope. The actual dead turn tension will depend on the loads used for doubling down, and will remain static, i.e. will not vary with changes in back end rope loads.

D2.2 Rope loads at the winder drum

As the rope is wound onto the winder drum, the suspended rope length in the shaft gets shorter, and the rope load at the drum decreases. The rope loads (tension) for the case study are given in Fig. D2.2 for empty and full skips.

D2.3 Radial rope loads

When the rope is wound onto the drum at the rope tensions shown in Fig. D2.2, radial rope loads will be generated by each length of rope. The radial rope loads generated when a section of rope is wound onto the drum, calculated from the rope tensions and the drum diameter, are shown in Fig. D2.3. The radial loads of Fig. D2.3 are also the loads that will be generated when the rope is wound over a headsheave of the same diameter as the drum.

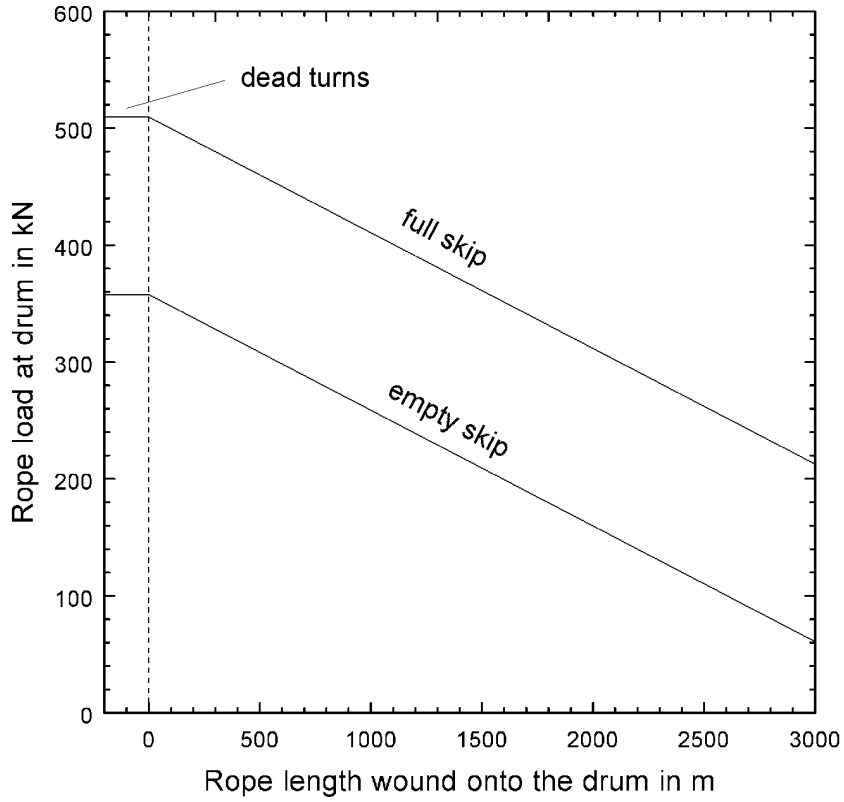

Figure D2.2: Rope loads at the winder drum.

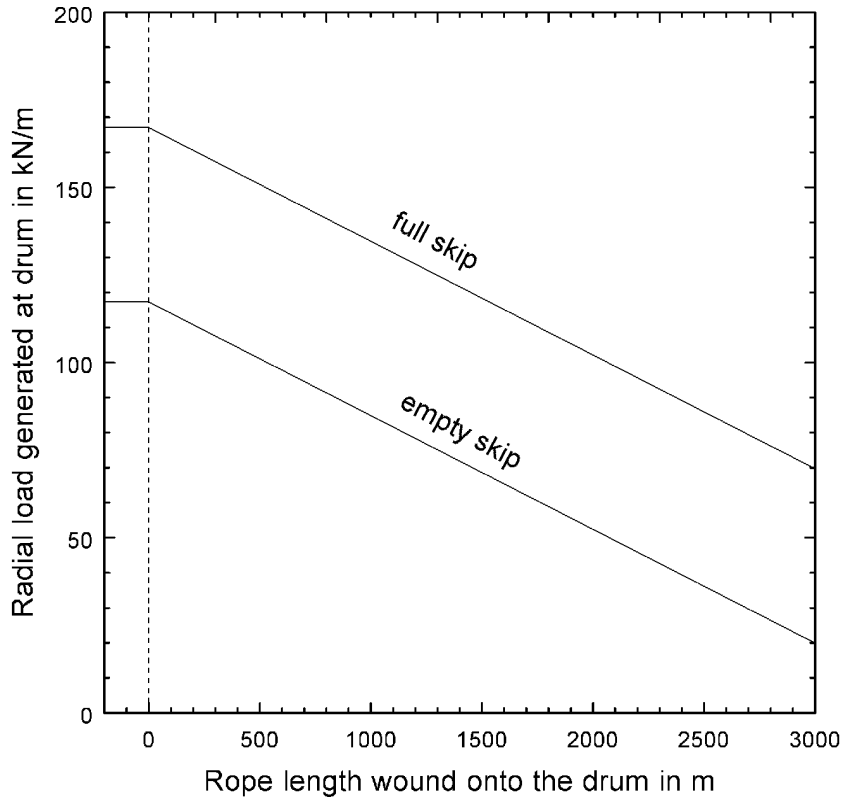

Figure D2.3: Radial rope loads when a section of rope is wound onto the drum.

When a rope with a loaded skip attached is wound onto the drum, the rope tension in the rope is "locked-in" on the drum, and will remain locked-in after the skip is off-loaded. The rope slip-back that takes place during unwinding after off-loading, resets the rope load equilibrium between the loaded skip tension and the empty skip tension. The radial load on the rope (the friction load) will change from the "full skip" line of Fig. D2.3 to the "empty skip" line during slipback.

When a load is taken down the shaft after the rope was wound onto the drum with an empty conveyance, the slip of the rope will be in a forward direction. The friction load will then change from the "empty skip" line of Fig. D2.3 to the "full skip" line during the forward-slip of the rope on the drum.

D2.4 Multi-layer coiling on a drum

The radial rope loads generated when a section of rope is wound onto the drum with a full skip (shown in Fig. D2.3) can also be plotted as a function of the position of the rope turns as wound onto the drum. Such a plot is shown in Fig. D2.4 for the full skip loads.

For actual coiling on a drum, the turns of a subsequent rope layer will lie in the valleys between the turns of the underlying rope layer. This is reflected in the rope turn positions shown in Fig. D2.4.

When a new rope layer is wound over another layer on the drum, the radial loads of the new layer will be added to the layer(s) already on the drum. Maximum radial loads will be reached when the full length of rope is wound onto the drum with the maximum suspended load (full skip or conveyance).

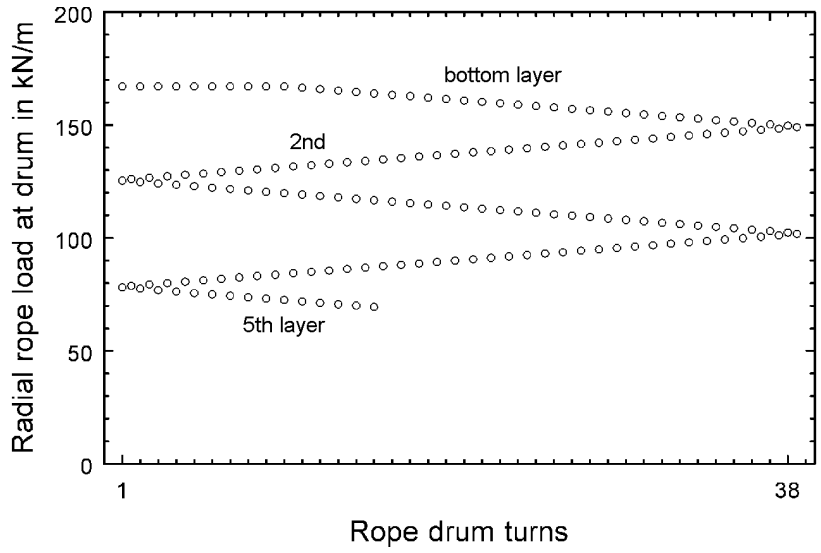

Figure D2.4: ***Radial rope loads when a section of rope is wound onto the drum shown for rope turn positions.***

D2.4.1 Addition of radial rope loads on a drum

Two methods of adding the radial loads of rope layers to underlying layers are given in this section: A simple method and a more analytical method. The basis of each of the methods is shown in Fig. D2.4.1. Coiling sleeves, used on the drums of all modern winders, leave gaps between turns of the order of 2 mm.

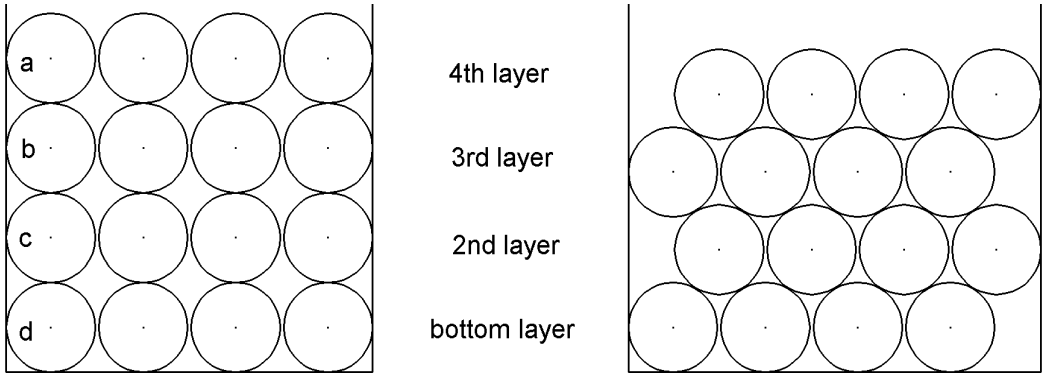

Figure D2.4.1: Two methods of adding radial rope loads together.

On the left-hand side of Fig. D2.4.1 rope turns are simply shown as lying directly on top of one another. If the rope turns are interpreted as cylinders, each of weight *W*, the load of each of the cylinders of the top (fourth) layer will be *W*. The weigh of "*a*" will be transferred to "*b*", given a total load on "*b*" as 2*W*, and so on. The load between "*d*" and the "drum surface" will therefore be 4*W*.

The addition of load for the more realistic picture shown on the right hand side of Fig. D2.4.1 works out the same as that of the left hand side for rope turns not close to the "drum cheeks". The rope turns closer to the drum cheeks (not more than one half the number of rope layers) show some variation in the total weight. The total weight on the bottom layer of the very narrow "drum" shown on the right hand side of Fig. D2.4.1 will be 2½*W*, 4*W*, 5*W*, and 4½*W* from left to right, as opposed to the average or "middle of the drum values" of 4*W*.

For the 3 000 m winder under consideration, the total radial loads of the rope layers are shown in Fig. D2.4.1.1. The total radial load includes the load generated by the turn itself, i.e. the loads shown are the radial loads required to support the rope turn in a specific layer. The small circles connected by the dashed lines in Fig. D2.4.1.1 are the loads calculated for the rope turns lying in the valleys of the underlying layer (proper analysis). The solid lines are for the simple calculation that assumed that rope turns lie directly on top of one another. As expected, the two methods of calculating the total radial load for a rope layer give the same result for the drum turns away from the drum cheeks.

Drum coiling sleeves that produce a rope turn crossover every 180° of drum rotation, require a rope to run across the underlying rope turn at a crossover point before settling in the next valley. At the crossover points, the rope turns will lie directly on top of one another, producing the same total radial loads as the rope turns in the valleys. Therefore, and at least theoretically, the turn crossover points on the drum for "crossover every 180°" coiling sleeves do not generate total radial loads greater than the rest of the drum turns. This finding came as a surprise to the author of this report. The radial load generated at a turn crossover point will in reality be slightly larger than calculated above because the radius of curvature of the rope at a crossover will be slightly smaller than the radius of curvature for normal coiling. This smaller radius of curvature (and the coupled increase in radial load) can be calculated by taking the crossover length into account.

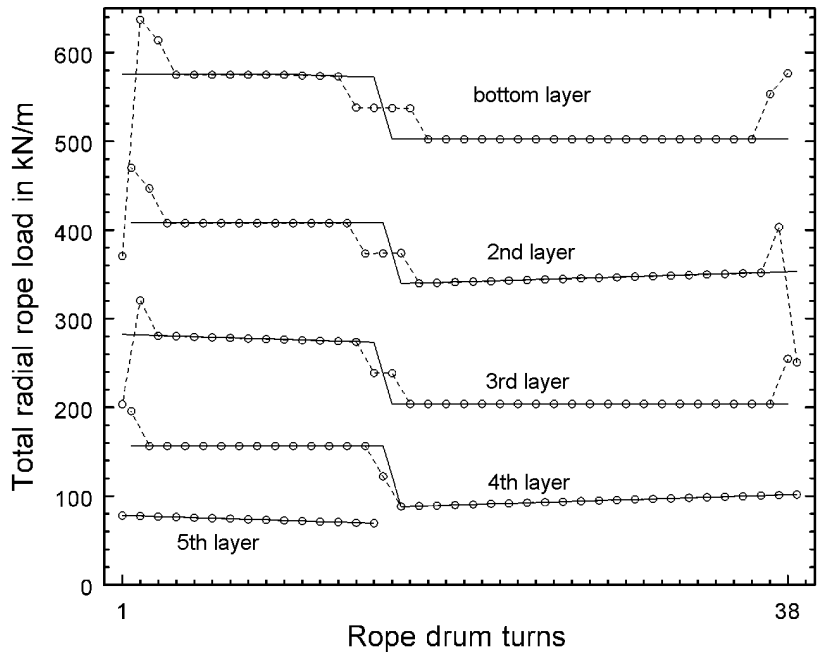

Figure D2.4.1.1: Total radial rope loads for the case winder.

Drum coiling sleeves (or smooth drums) that produce a rope turn crossover only every 360° of drum rotation, require a rope to run across two rope turns before settling in a valley. The portion of rope that runs across the valley will be unsupported, which will result in larger contact loads for the same radial rope loads. Contact loads are discussed later.

The relatively small differences shown in Fig. D2.4.1.1 between the total radial loads calculated with the two methods mentioned are not of great significance compared to other unknowns and variables that will be shown later in this appendix.

Although it was shown in this section that the total radial loads for coiling sleeves with crossovers every 180° are the same as the other total radial loads, it will be shown later in this appendix that the contact loads between rope turns will be different at the crossover points.

D2.4.2 Varying the drum coiling parameters

For the sake of interest, the winder drum parameters were varied to demonstrate how they could influence the total radial rope loads. First, the drum diameter was made 10% larger, which resulted in radial rope loads 10% smaller and fewer drum turns required for the full length of rope (four layers on the drum). The total radial loads calculated with the "simple" method are shown in Fig. D2.4.2.

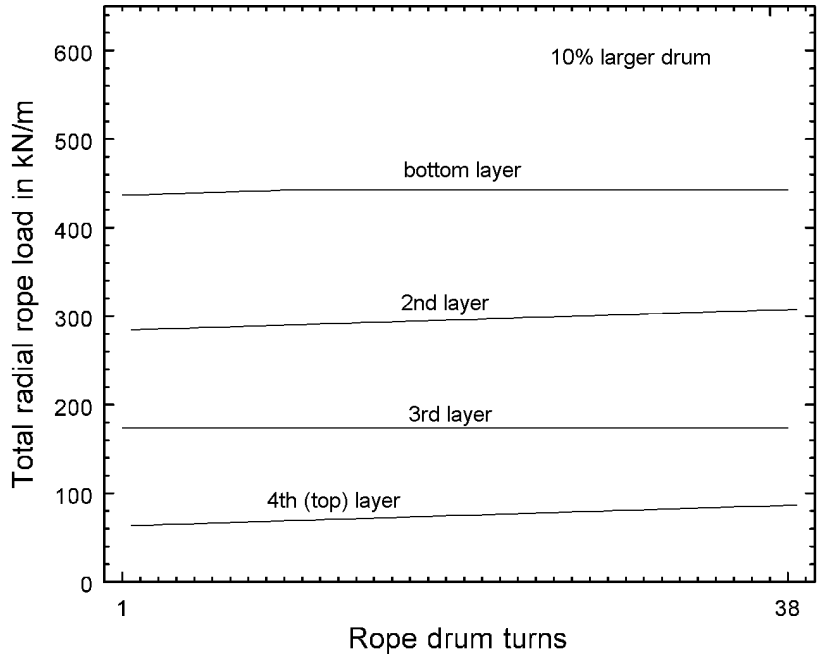

Figure D2.4.2: Total radial rope loads for the case study winder with a 10% larger drum.

Keeping the drum diameter at the original 6,1 m diameter, but increasing the width to 2,63 m will allow 50 rope turns per drum layer, and require only 3,3 layers in total. Decreasing the drum width to 1,68 m will allow only 32 rope turns per layer, and require 5,2 rope layers on the drum; i.e. part of a sixth rope layer will be required. The total radial rope loads of the rope layers are shown in Fig. D2.4.2.1 for the 50 rope turn/layer case. The total radial rope loads of the rope layers are shown in Fig. D2.4.2.2 for the 32 rope turn/layer case.

The above examples show how the total radial rope loads change with different winder drum widths and diameters. The winder code of practice[1] permits a maximum of five rope layers on the winder drum. For the case winder, five rope layers equates to a total radial rope load of approximately 600 kN/m on the bottom rope layer on the drum.

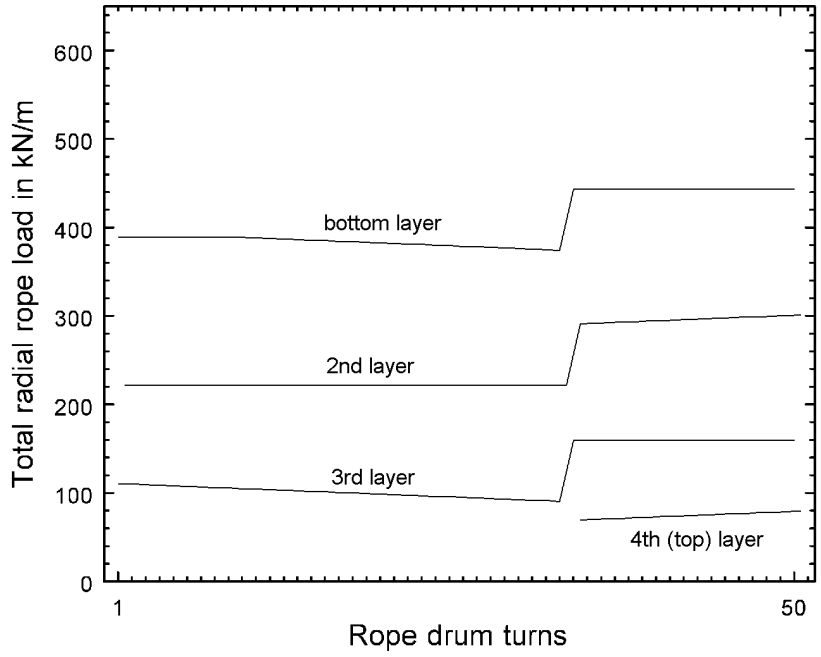

Figure D2.4.2.1: Total radial rope loads for the case study winder with 50 rope turns per drum layer.

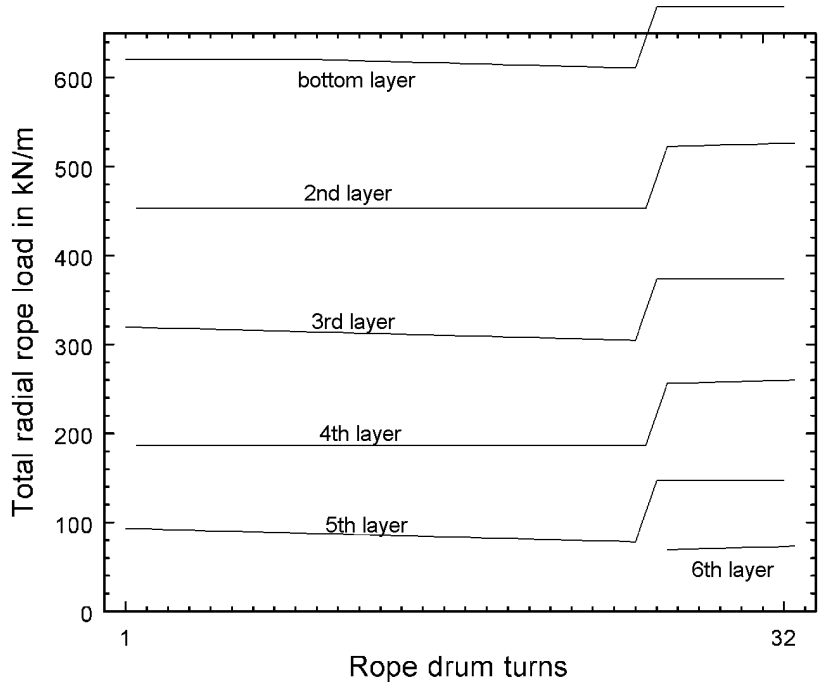

Figure D2.4.2.2: Total radial rope loads for the case study winder with 32 rope turns per drum layer.

D3 Contact loads and contact stresses

When a rope is wound over a flat sheave or onto a flat drum surface, the contact between the rope and the underlying surface will be as shown in the drawing on the left hand side of Fig. D3. The contact load, *c*, will be equal to the radial load, *r*, of the rope. For multi-layer coiling the contact load between the bottom rope layer and the drum will increase to the value equal to the "total radial rope load" of section D2.4.1.

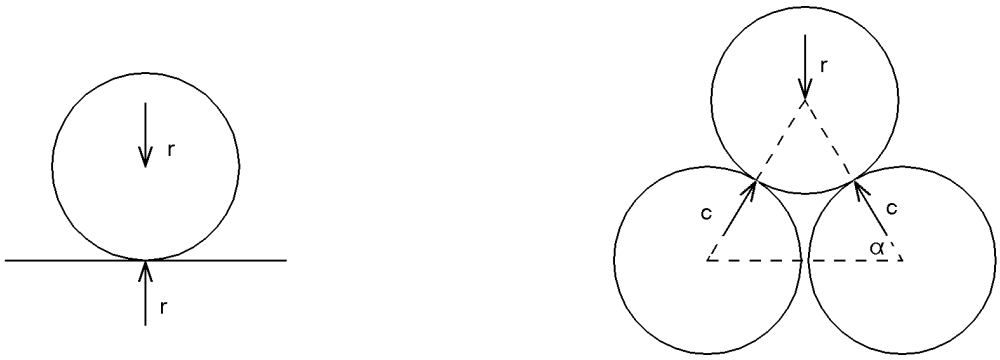

Figure D3: Radial rope loads and contact loads.

The turns of the second and subsequent rope layers on the drum will lie in the valleys between the rope turns of the previous rope layer. The contact between rope turns will be as shown in the drawing on the right hand side of Fig. D3. The angle, α, will be 60° for no gaps between rope turns, and will reduce to 58° for rope turn centres 1,06 diameters apart. For a radial or total radial load on the rope of *r*, the contact load between rope-and-rope, *c*, will be:

$$c = \frac{r}{2\sin\alpha}$$

$$= 0{,}6\,r \qquad \text{for } \alpha = 56°$$

At the rope turn crossover points on the drum, $c = r$

If the rope is considered as a smooth cylinder, the contact between the rope and rope or between rope and a flat surface will be a line contact. Deformation of the rope surface will create a contact area along the line contact. The contact area will determine the contact stress on the rope surface.

Headsheaves are grooved with a groove diameter slightly larger than the rope diameter. The rope will deform to "fill" the groove of a headsheave, and the contact between the rope and the headsheave groove could easily be 60° of the circumference of the rope. Contact stresses in the rope will therefore be substantially lower than for rope-on-rope contact, especially considering that headsheaves do not have extra radial loads added as for multi-layered coiling on winder drums.

The drums of modern drum winders all have coiling sleeves. The grooves of the coiling sleeves will have much the same effect as the groove of a headsheave. The contact between the bottom rope layer and the coiling sleeve should also be at least on 60° of the rope circumference. If the contact area for the rope in the groove of the coiling sleeve is only five times that of rope-on-rope contact between the bottom and the second layer, the contact stresses between the bottom layer

and the rope will be substantially lower than between the rope turns of the bottom and second layer.

Therefore, without any further calculations, and by simply considering the contact loads and estimated contact areas, it can be concluded that the worst contact stresses will be generated between the second and bottom rope layers. The contact stresses will be determined by the total radial load of the second rope layer on the drum.

The rope-on-rope contact loads for the case winder are shown in Fig. D3.1. At the drum turn crossovers the contact loads will be approximately 65% greater than shown.

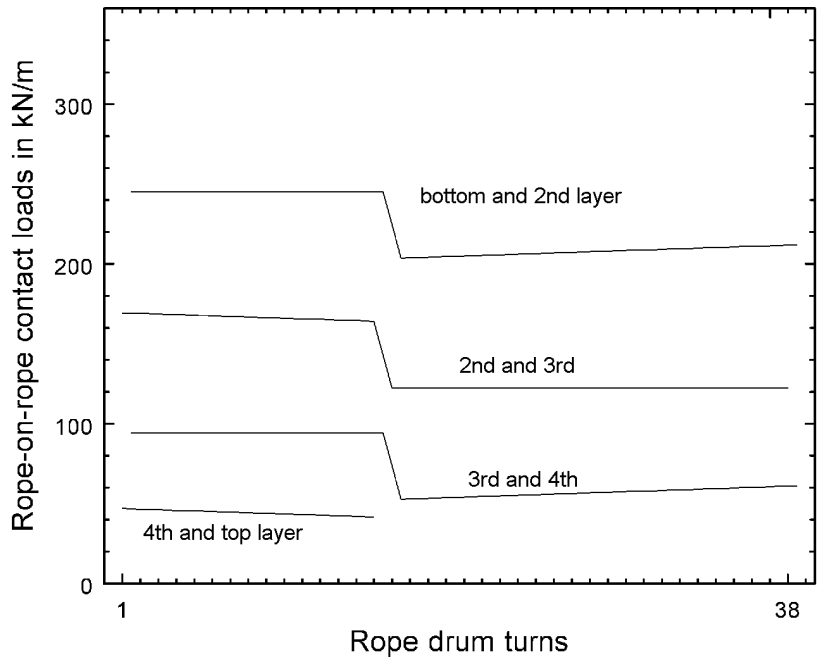

Figure D3.1: Rope-on-rope contact loads for the case winder.

Furthermore: For a headsheave and winder drum of the same diameter, the contact stresses between the rope and the headsheave groove will be orders of magnitude less than what will be experienced by the rope on the winder drum.

It is of interest that rope size has not yet entered the picture directly. A smaller rope size will reduce the rope mass and therefore reduce the radial rope loads. More turns of a smaller diameter rope can also be wound onto a drum of a given width. If the rope size is reduced substantially, it may even reduce the number of rope layers on the drum. It would therefore be of interest to analyse the Elandsrand experiments where the rope diameter was reduced from the original 52 mm to 48 mm, and then to 43 mm.

D4 Rope on rope contact

In the previous section the rope was considered as a cylinder with a smooth surface. Lengthwise contact between two smooth cylinders will be continuous. The effect of the actual rope surface is analysed in this section.

The outer wires of a new triangular strand rope are round. Contact between sections of a new rope on a winder drum should therefore only be at discreet points. With usage of the rope, the wires develop flat sections. The torque-tension characteristics of triangular strand ropes ensure that the flats appear right around the circumference of the rope.

The flats that develop on the outer wires of the rope are more a result of plastic deformation than of pure wear, because little material is actually removed. This fact alone demonstrates that the contact stresses are beyond the elastic limit of the wire material.

The plastic deformation of a drum winder rope is generally much more significant towards the back end of a rope. This should be the case because the contact loads experienced by the bottom layers on the drum are greater than the upper layers. The plastic deformation displayed by the rope surface increases with usage of the rope. This means that the contact area for rope-on-rope contact actually increases with usage of the rope, resulting in ever decreasing contact stresses.

It is therefore not unthinkable that, towards the end of the service life of a rope, the contact stresses for rope-on-rope contact on the drum could be much the same for the greater length of the rope.

D4.1 A well deformed rope

A picture of a triangular strand rope with a substantial amount of surface plastic deformation is shown in Fig. D4.1. The rope section shown was from the back end of a 38 mm rope that did rock hoisting for four years from a depth of 1 800 m. The valleys between the outer wires at the crowns of the strand were nearly "filled". It appears that the section of rope shown has reached its maximum deformation, or the limit of plastic deformation.

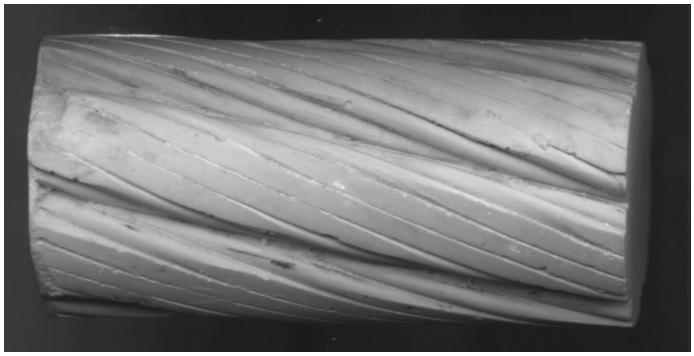

Figure D4.1: A well deformed triangular strand rope.

The rope laylength of the rope section shown above was 450 mm. The rope lengths between the strand valleys were therefore 90 mm. If the (very) small gaps between the flats of the crown wires are ignored, the length of the flat strand section was measured as 50 mm. From the actual winder data, the rope-to-rope contact load between the 2nd rope layer and the bottom rope layer was calculated as 125 kN/m for the rope section shown in Fig. D4.1.

Per length of rope, only 56% of the surface of this rope was available to make contact with other surfaces. Contact with a continuous surface (like a smooth drum surface) will produce actual

contact loads 1,8 times greater than the calculated values.

The situation for rope-on-rope contact if rather more complicated. If the section of rope shown In Fig. D4.1 was close to a layer crossover point on the drum, it can be imagined that the rope turns coiled onto this shown section would have much the same appearance and "flat length". The rope could be matched exactly, i.e. the 56% flat of one rope section could rest right on top of the 56% flat of the underlying layer, giving a contact length of 56% per length. However, the laylength of a triangular strand rope decreases towards the front end of the rope, and the coiling diameter on the drum increases with every additional rope layer. The perfect matched of flats will soon change to the 56% flat of the one rope section being positioned over the 44% gap of the rope section in contact, giving only 12% of contact length per length of rope. The actual loads at contact will then be of the order of ten times greater than the calculated rope-on-rope contact loads.

The situation becomes even more severe when the part of the strands with flats is shorter than 50% of the rope length from strand valley to strand valley. The rope strands of one rope section will then lie in the valleys between the strands of the rope section in contact, and actual contact could be on only one or two wires.

D4.2 A less deformed rope

A typical drum winder rope section is shown in Fig. D4.2. In this case the valleys between the wires at the crowns of the strands are still visible.

Figure 4.2: A typical deformed triangular strand rope

The total length of the flats of Fig. D4.2 is 35% of the rope length or 0,35 m per metre length of rope (called the contact length fraction), or 35% of the rope length between strand valleys. The rope section on the next rope layer in contact with the section shown in Fig. D4.2 could have a flat length of 20%.

To determine the actual contact between the rope section with 35% flats and one with 20% flats, the two rope sections were moved relative to one another with a computer simulation, and for every contact position, the actual contact length was determined. A specific contact situation will repeat itself in a length determined by the contact details and the rope laylength. It was therefore possible to establish the contact length per length of rope.

The actual process was as follows:

- Rope moulds were made on site of the in-service condition of a rope at various points along the length of the rope. Replicas could then be made of the rope sections from the moulds.

- A replica of a rope was then scanned at 600 dpi, and the position and lengths of the flats were then determined along the length of the rope. Each flat therefore had a length of a finite number of pixels.
- The contact between two rope sections were then determined by moving the two rope sections relative to one another, pixel for pixel. The number of pixels in contact determined the contact length between the two rope sections.
- Minimum, maximum and average contact lengths between two rope sections could be established in this way.
- Replicas of at least three sections of a rope were scanned (front, middle and back). A total of twelve ropes were scanned. A back end section was then moved relative to the rope section from midshaft, and the midshaft section was moved relative to the front end section. The length of a replica was increased by "repeating" a strand of a rope section. The complete process was time consuming.

For the 35%-flat in contact with the 20%-flat case mentioned above, the maximum contact length cannot be greater than 20% of the rope length. It was determined that this maximum of 20% will only be reached under exceptional circumstances and that it would not be the general case.

From the large number of rope-on-rope contact simulations it was established empirically that if a rope with a total contact length fraction of "*a*" made line contact with another rope section with a contact length fraction of "*b*", then the average contact length will be "$a \cdot b$". Therefore, for the mentioned 35% section in contact with a 20% section, the average contact length will be 7% per given length of rope. The actual contact loads on the rope will in this case be approximately 14 times the calculated rope-on-rope contact loads.

The calculation of the minimum contact lengths, which will give the greatest contact loads, was less clear. In some cases three consecutive strands did not make contact with opposing strands (the flats of the one rope were all opposite the gaps of the other rope). It can only be assumed that in such situations the rope has to deform more (maybe more oval) to establish some form of contact between the two rope sections. The actual contact loads would then most probably be far greater than the 14 times established from the average contact lengths.

Flats on the outer wires of a drum winder rope grow with usage. As the flats get bigger, the contact stresses will get lower. If the maximum flat length on a rope is of the order of 56% of the rope length, average actual contact loads will still be three times the calculated rope-on rope contact loads. For the 3 000 m case winder, the rope-on-rope contact load was calculated as 240 kN/m between the bottom rope layer on the drum and the 2nd rope layer. At best (that will be towards the end of the service life of a rope on such a winder), the actual line contact loads on the wires will still be around 720 kN/m for the rope turns and 1 200 kN/m at the drum turn crossover points (65% greater).

After a new rope has been installed, the flats will be small, and rope-on-rope contact will be restricted to discreet contact points. Even after small flats have developed, the actual contact loads on the rope wires will be orders of magnitude greater. The fact that flats develop and grow indicates that the contact stresses are beyond the elastic limit of the rope wire material.

D4.3 A counterweight rope

Two possible mechanisms for the outer wire degradation (plastic deformation) of drum winder ropes have been identified in the past: The contact stresses generated by multi-layer coiling on drums, and the rope slipback that occurs on the drum during unwinding of the rope after off-loading.

To be able to obtain a measure of the contribution of slipback to the generation of flats on the rope, a counterweight winder was added to the observed winders (see Appendix E). The attached load on the counterweight side of a counterweight winder remains the same. Although there will be some load variation during winder acceleration and deceleration, the larger part of the rope length will not be subjected to any slipback or forward-slip.

Figure D4.3 shows replicas of a counterweight rope of a counterweight winder. The shaft depth was 1 745 m. The replica on the left hand side of Fig. D4.3 was from the back end of the rope, and the replica on the right was from approximately 250 m from the back end of the rope.

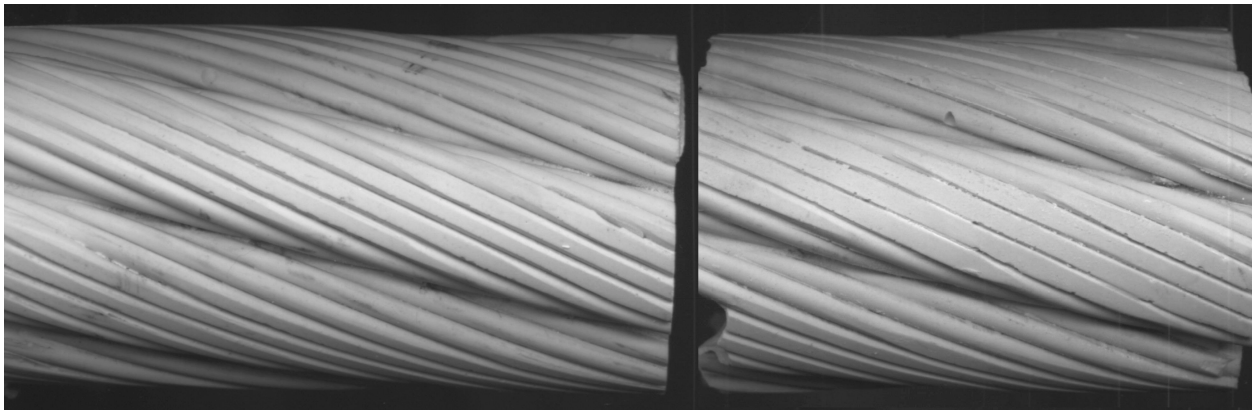

Figure D4.3 A counterweight drum winder rope

The length of the flats in line with the rope for the right hand side replica shown in Fig. D4.3 is 43% of the rope length. Slipback of the rope on the drum is therefore not a required ingredient for the degradation of the outer wires of a drum winder rope.

The only way in which the contribution of slipback can be evaluated is to compare the development of flats between the counterweight rope and that of a rock winder with the same drum parameters, depth, maximum attached load and rope construction and size.

D5 Summary

The rope-on-rope contact stresses generated during multi-layer coiling on a winder drum are larger than the elastic limit of the rope wire material. Flat sections are therefore created at the crowns of the rope strands.

As the flats on the rope grow larger with usage of the rope, the contact stresses will be reduced.

Rope-on-rope contact is far more severe than the contact between the rope and the drum surface or the contact between the rope and the headsheave.

The most severe contact is between the bottom rope layer on the drum and the second rope layer. The severity of the contact is determined by the total radial load on the second rope layer

when the rope is fully wound onto the drum.

Every turn of the second rope layer has two contact lines with the bottom layer, and two contact lines (at lower loads) with the third layer. The contact stresses between the bottom layer and a coiling sleeve is insignificant compared to rope-on-rope contact. For a winder drum with coiling sleeves, the contact stress degradation of the second rope layer should therefore be greater than any other rope layer. The greatest degradation of the second rope layer will depend on the distribution of the contact loads for that layer as shown in Fig. D3.1 (the line for *bottom and 2nd layer*).

The radial rope loads generated will be greater for smaller winder drums.

Drum coiling sleeves, with a drum turn crossover every 180°, are required to reduce contact stresses at the drum turn crossover points. For such sleeves the contact loads at turn crossovers will be about 65% greater than for the rest of the rope turn.

The contact loads and contact stresses between ropes and headsheaves are not even remotely comparable to that of the rope on the drum.

Slipback occurs when a rope is wound off the drum at a lower tension than during the winding up part. Slipback is not a necessary ingredient for the generation of plastic deformation on the outer rope wires.

Rope diameter never appeared directly in the estimations of contact stresses in this appendix.

D6 Limiting the effect of high contact stresses

Repeated generation of contact stresses beyond the elastic limit of the rope wire material will lead to fatigue and split wires. With such high contact stresses, cracks can be initiated after a relatively small number of loading cycles. Although the accumulation of winding cycles on a winder is relatively low (150 per day for a deep shaft winder), split wire problems have been experienced in the past.

The high contact stresses that are generated during multi-layer coiling on a drum are a reality, and cannot be eliminated. However, the number of loading cycles at the highest contact stresses experienced by any given section of rope (drum turn crossovers) can be reduced until flat sections are formed are lower stresses (at the rest of the drum turns).

Although the torque-tension characteristics of a triangular strand ropes will ensure that a rope is wound onto the drum at different rotational orientations with every winding cycle, the high loads will remain on the surface of the same section of rope. This situation is further intensified by the modern trend to use loadcells to determine the load discharged into skips. Drum turn crossover points will be at the same location on the drum if the same load is added to the skip for every winding cycle. This is even more the case for the bottom rope layer and the first part of the second layer for which small differences in load will have little effect.

There is merit in systems that load skips by volume instead of exact loads. Loading by volume will at least ensure that actual loads will be varied, and that drum turn crossover points will be shifted around on the winder drum. The same can of course be achieved with a loadcell system that varies the load deliberately form one winding cycle to the next.

The primary method of shifting the location of drum turn crossover points and drum layer crossover points, is by pulling in the back end of the rope at the winder drum. However, to date this has been done without giving much thought to the effect of pulling in back ends. Generally back ends are pulled in at intervals of three months or six months. There even have been reports

of increasing the frequency of doing back ends as ropes approached the end of their service lives.

Taking everything mentioned in this appendix into account, there is merit in adopting a new approach towards when back ends should be done. The following is proposed especially for deep winders:

> For the first month after installation, do back ends every week. For the next two months do back ends every fortnight. For the next four months, do back ends monthly. For the next year do back ends every three months. After this time in service, a rope will have evenly distributed surface deformation mostly produced at lower contact stresses. The frequency of doing back ends can then be increased to every six months.

D7 An interesting case

Between 1966 and 1970 a rock winder at Hartebeestfontein returned rope lives of 23 000, 28 000, 36 000, and 14 000 winding cycles[2] compared to a general average rope service life of 85 000 winding cycles.[3] In all cases the reason for discard was "numerous broken wires".

Purely from a contact stress viewpoint, everything was wrong with this drum winder: The shaft was relatively deep (2 060 m), the winder operated without coiling sleeves, the drum was relatively small (a *D/d* of 90), and the rope had to go onto a fifth layer on the drum. If the norm was to only do back ends every sixth months, one of the rope sets never had its back ends done, and all the other rope sets were discarded before the back ends could be done for a second time, or very shortly after the back ends were done for a second time.

Appendix E: Field studies: Rope degradation measured along the length of a rope

The observation and measurements on selected drum winders include taking moulds of the ropes at three to four points along the length of a rope. Plaster casts were made from these moulds to give replicas of the surface condition of the ropes.

Plastic deformation of the outer wires at the crowns of the strands are generated on all drum winder ropes. The plastic deformation cause flats to appear on the outer wires. The width of the flats on the wires could be measured from scans of sections cut from the rope replicas.

E1 A typical replica section

A typical section through a replica of a rope is shown in Fig. E1. The width of the flat section of a rope is shown in the figure. From scans such as the one shown in the figure, the total length of the rope flats around the rope section could be measured. This total length was then expressed as a percentage of the circumference of the rope at that point. The rope circumference was measured on site at the time that the rope mould was made.

Figure E1: A typical section of a replica of a rope.

The total width of the flats as a percentage of the rope circumference was then taken as a measure of the plastic deformation of the rope surface or as a measure of the degradation of the rope surface.

E2 Degradation along the length of a rope

For most of the winders observed, replicas were only available for the front ends, back ends, and somewhere along the rest of the rope.

For the BMR winder at East Driefontein, an additional section was chosen for a mould on each rope. For this BMR winder, the measurement of the surface degradation was much the same for all four ropes (of the same set) at the front and back ends. The positions of the other sections from which replicas were obtained along the length of the ropes were not the same for the two sides of the BMR. The surface degradation were in all cases much the same for the two ropes of the same side of the BMR for the same distance from the skip.

By combining the surface degradation values of all the ropes, a measure of the degradation along the length of a "single" rope could be obtained. Six points were obtained in this way for the BMR winder for every visit to the winder.

The same procedure was followed for the West Driefontein 4 shaft winder (four points) and for the winder at Premier (only three points).

The results obtained for the East Driefontein BMR are shown in Fig. E2. Two of the graphs are for measurements on the same set of ropes but approximately one year apart. The third graph was for a new rope set after six months in service. Measurements were not available for the front and back ends of the new rope set.

Some of the replicas were from points near or at layer crossover points on the drums. It was not possible to establish on which layer such a point started its service life and how its position changed with time, mainly because it was not considered to be very significant at the time that the field observations were done.

The results of the West Driefontein winder and the Premier winder are shown in Figs E2.1 and E2.2.

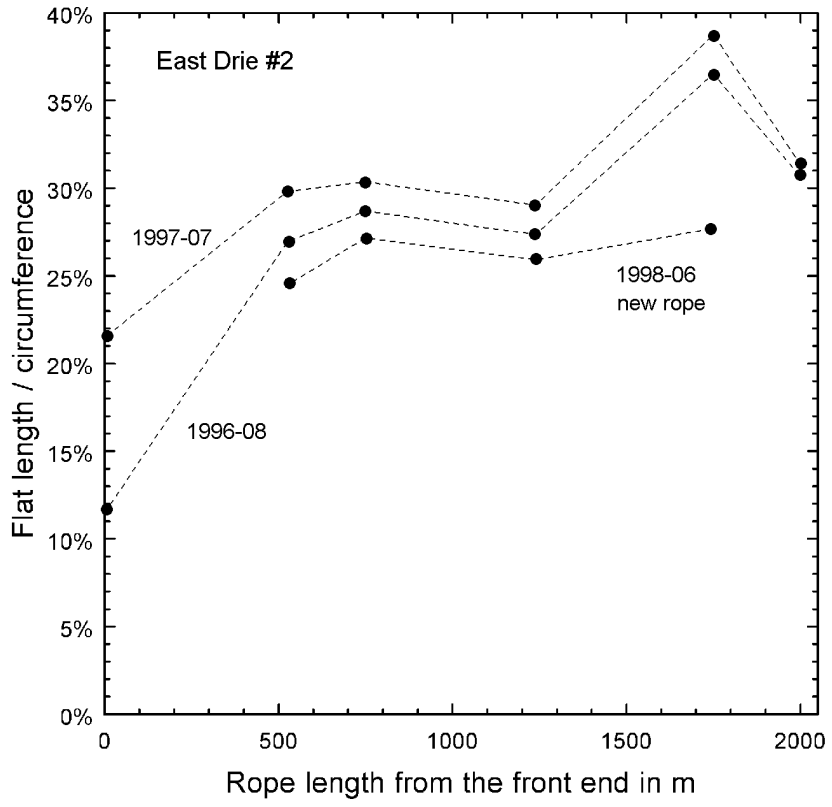

Figure E2: ***Surface degradation along the rope length of the BMR at East Driefontein #2.***

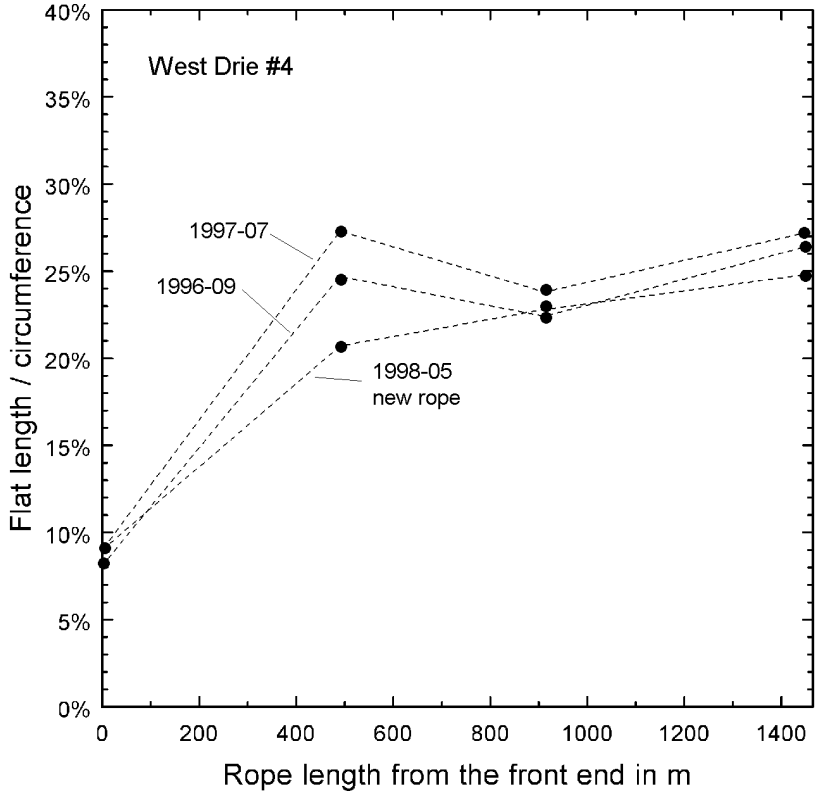

Figure E2.1: ***Surface degradation along the rope length of the West Driefontein #4 winder.***

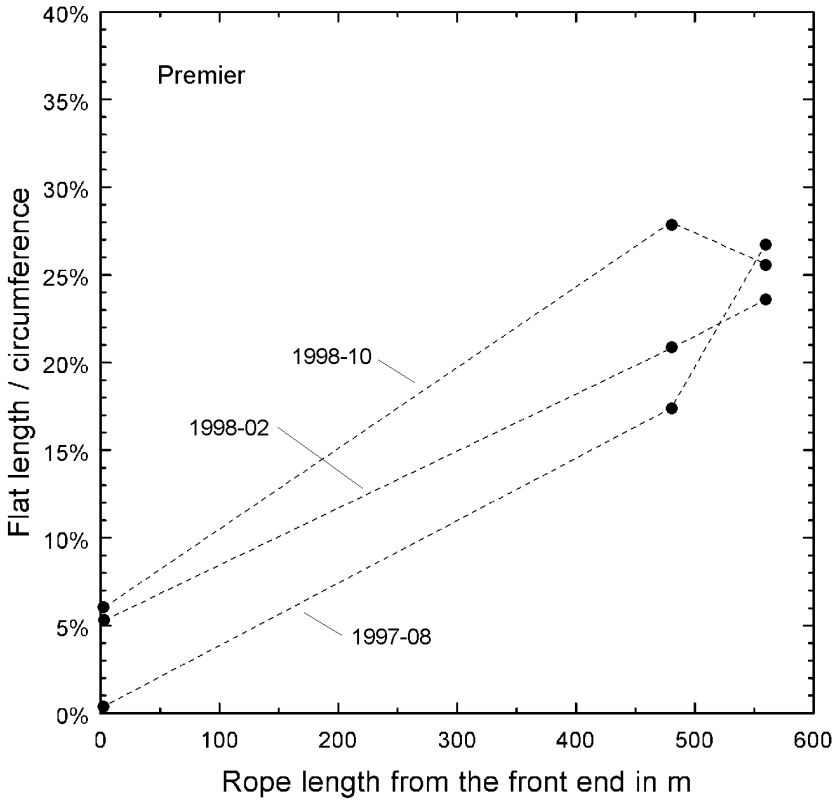

Figure E2.2: ***Surface degradation along the rope length of the Premier winder.***